



## **Shear Strength of Initially Unsaturated Soil**

Results measurement sites Westervoort and Oijen



## COLOFON

<b>Titel</b>	Shear Strength of Initially Unsaturated Soil
<b>Opdrachtgever</b>	HWBP De Innovatieversneller
<b>Auteur(s)</b>	Alexander van Duinen
<b>Foto omslag</b>	Alexander van Duinen
<b>Kenmerk</b>	2021-MACRO-002
<b>Inhoudelijke kwaliteitsborging</b>	Cor Zwanenburg
<b>Datum</b>	27-12-2021
<b>Status</b>	Definitief

## Shear Strength of Initially Unsaturated Soil

Results measurement sites Westervoort and Oijen




<b>Client</b>	Waterschap Rivierenland
<b>Contact</b>	Govert Heijn
<b>Reference</b>	2021061861/2021098199
<b>Keywords</b>	Slope stability, shear strength, unsaturated soil, suction, in situ tests, laboratory tests

### Document control

<b>Version</b>	1.0
<b>Date</b>	27-12-2021
<b>Project nr.</b>	11207253-002
<b>Document ID</b>	11207253-002-GEO-0001
<b>Pages</b>	101
<b>Classification</b>	
<b>Status</b>	final

### Author(s)

	Alexander van Duinen	

Doc. version	Author	Reviewer	Approver	Publish
1.0	Alexander van Duinen	Cor Zwanenburg	Goaitske de Vries	
				

# Summary

Commissioned by the Directorate-General for Public Works and Water Management and De Innovatieversneller (DIV), Deltares is working on a study of the shear strength of (initially) unsaturated soil in relation to the assessment and design of the slope stability of dykes. For this research field testing and sampling for laboratory testing take place at the IJsseldijk near Westervoort (dyke post Dp. 250 + 80) and at the Maasdijk near Oijen (dyke post Dp. 592 - 593). The approach for this research follows the results and recommendations of the research conducted in 2019 commissioned by Rijkswaterstaat (Deltares, 2019a).

Based on the collected data from the measurement sites the soil behaviour in the (initially) unsaturated soil is identified and quantified. In this research it is found that a substantial part of the soil above the normal daily phreatic surface can be permanently saturated (grey clay). On top of this permanently saturated zone lies a zone where degree of saturation and suction varies considerably (brown clay). From the shear strength measurements at Westervoort and Oijen it can be determined that the soil behaves undrained in the permanently saturated zone (grey clay). In the zone where degree of saturation and suction fluctuates (brown clay) the soil behaviour depends on degree of saturation. In this zone the drained shear strength depends on suction and degree of saturation and therefore also varies considerably. The soil behaves undrained from a certain threshold value in degree of saturation. In the shallow 1.0 m to 1.5 m where cracks and fissures can occur, the mobilized shear strength can be reduced, when slip surface can (partly) follow the pattern of the cracks and fissures. Dimensions of these three zones and magnitude of the shear strength within these zones depends on soil type and hydrological conditions.

This report has also been released under project number 11206817-015-GEO-0001 on behalf of Rijkswaterstaat.

# Contents

	<b>Summary</b>	<b>4</b>
<b>1</b>	<b>Introduction</b>	<b>7</b>
1.1	Background	7
1.2	Objective of the project	8
1.3	Approach	9
1.4	Outline	9
<b>2</b>	<b>Study areas</b>	<b>11</b>
2.1	IJsseldijk Westervoort	11
2.2	Maasdijk Oijen	11
<b>3</b>	<b>Methods</b>	<b>13</b>
3.1	Introduction	13
3.2	Model for drained shear strength	13
3.3	Model for unsaturated shear strength	14
3.4	Model for undrained shear strength	16
3.5	Site investigation	17
3.6	Volumetric water content measurements	20
3.7	Suction stress measurements	21
3.8	Pore water pressure measurements	23
3.9	Cone penetration tests (CPT)	24
3.10	Resistivity Cone Penetration Tests (RCPT)	27
3.11	Field vane tests (FVT)	28
3.12	Boreholes	31
3.13	Classification tests	31
3.14	Determination of shear strength in the laboratory	32
3.15	Proctor test	33
3.16	Determination of retention curves and shrinkage curves	33
3.17	Mercury intrusion porosimetry tests	34
<b>4</b>	<b>Results</b>	<b>35</b>
4.1	Introduction	35
4.2	Characterisation of the subsoil	35
4.3	Micro-structure of the soil	39
4.4	In situ water content, degree of saturation and suction stress	44

4.5	Correlation between CPT, FVT and laboratory tests	49
4.6	Relation between water content, suction and shear strength	57
4.7	Triaxial tests on reconstituted samples	63
4.8	Resistivity Cone Penetration Tests (RCPT)	68
<b>5</b>	<b>Discussion</b>	<b>70</b>
5.1	Introduction	70
5.2	Variations in water content, suction and degree of saturation	70
5.3	External factors and soil properties that affect the degree of saturation	72
5.4	Swelling and shrinkage and their influence on dynamics of cracks and fissures	72
5.5	Factors and soil properties that affect drainage conditions during shearing	73
5.6	Influence of water content and swelling and shrinkage behaviour on shear strength	74
5.7	Relationship between shear strength of aggregates and bulk shear strength of the soil	76
5.8	Application in slope stability analyses	76
<b>6</b>	<b>Conclusions</b>	<b>78</b>
<b>7</b>	<b>Recommendations for further research and optimization</b>	<b>80</b>
<b>8</b>	<b>References</b>	<b>81</b>
<b>A</b>	<b>Bore holes</b>	<b>85</b>
A.1	Introduction	85
A.2	Westervoort	85
A.3	Oijen	91
<b>B</b>	<b>Soil water retention curves</b>	<b>97</b>
B.1	Introduction	97
B.2	Westervoort	97
B.3	Oijen	98
B.4	Staring series	99

# 1 Introduction

## 1.1 Background

Commissioned by the Directorate-General for Public Works and Water Management and De Innovatieversneller (DIV), Deltares is working on a study of the shear strength of (initially) unsaturated soil in relation to the assessment and design of the slope stability of dykes. In practice the (initially) unsaturated soil means the zone above the normal daily phreatic surface. It has to be noted that the lower part of this zone, just above the phreatic surface, will be saturated. The purpose of this research is to prepare a guideline for the stability analysis of flood defence dykes, in which unsaturated conditions of low permeable soil layers play a role in determining the shear strength parameters. This report describes an analysis of the data which is collected at two measurement sites in the last two years.

The present guidelines and regulations for stability assessment of water retaining structures in the Netherlands (WBI 2017; I&M, 2021) assume fully saturated conditions during a high-water event for the different subsoil layers and the dyke body. For fully saturated low permeable soil layers the guidelines assume undrained soil behaviour. However, in practice some waterboards apply drained soil behaviour with the use of the friction angle  $\phi'$  for initially unsaturated soils, also for clayey soil layers.

A consequence analysis (Arcadis, 2020) shows that differences in modelling of the shear strength of the dike material can lead to differences in the calculated stability factor of up to a factor of 1.5. Expressed in terms of the probability of a slope instability occurring, this may be a decrease of this probability of failure by a factor of 10 to 10,000. It also follows from this analysis that it can make the difference between the need of a stability berm or not or a difference in the required length of the stability berm of up to 20 m. Based on the results of this research the consequence analysis will be updated.

In order to come to a clear approach, the development of a guideline for initially unsaturated soils is necessary. In the method, the shear strength should be interpreted on the basis of field and laboratory tests, taking into account the variations in moisture content and suction stress in the subsurface and the dyke material. From the normal daily unsaturated conditions, it is needed to make a translation to assessment and design conditions. This can be the fully saturated state or a state with a higher degree of saturation compared to normal daily conditions. The guideline should lead to more accurate analyses of the slope stability of dykes, both for assessment and design, which describe the soil behaviour well.

The research focusses on both, the unsaturated behaviour of the subsoil and the unsaturated behaviour of the dyke body itself. For eastern and south eastern part of the Netherlands, 'bovenrivierengebied', unsaturated conditions occur often. Here the Holocene layer is relatively thin with relatively low ground water tables. Questions were raised on the influence of the unsaturated soil behaviour in the strength development for these locations. The presence of an unsaturated zone in the dyke body is not typical for the conditions found in the eastern and south eastern part of the Netherlands. All around the country dyke bodies will have a partly saturated zone. However, for these areas, the influence of the shear strength of the unsaturated zone on slope stability is believed to be small in most cases, considering the total length of a possible sliding plane and the length of the part of the sliding plane that runs through the unsaturated soil. Note that for secondary failure mechanisms after an initial slope failure the behaviour of the unsaturated zone can also be important.

A complicating factor is the fluctuating water and groundwater tables near water retaining structures. Consequently, the degree of saturation of the cohesive soil in the embankment and in the upper part of the Holocene cover layer varies during the year. Due to moisturizing, evapotranspiration and seepage processes, this part of the soil can become fully saturated in the wet season, winter, and will be partially saturated in the dry season, summer. If the soil becomes partially saturated during the dry season, the shear strength will temporary increase along a certain height, because of capillary suction. Field work conducted for stability assessment is typically done in the summer, dry, period, while the results need to be applied for the winter, wet, period. This imposes questions on whether soil which is unsaturated in summer time becomes fully saturated in winter time and if cracks that are formed in the dry period, close during the wet period. Consequences of these seasonal effects are also found when interpreting cone penetration tests. The present guidelines prescribe an additional reduction of the net cone resistance of unsaturated soil with a factor 3, when relating it to saturated undrained soil strength. This method is however not underpinned very solidly. The WBI 2017 regulations finally prescribe that the favourable effect of suction stress on the shear strength above the phreatic level belonging to high water levels must be ignored and that a fully drained strength should directly be assumed.

## 1.2 Objective of the project

The ultimate goal of this study is to supply guidance on the characterization of the shear strength in cohesive soils in dykes and Holocene cover layers that is assumed to be fully saturated for assessment and design conditions, wet season, but not fully saturated during the dry season when parameter assessment takes place. This objective follows the research in 2019 commissioned by Rijkswaterstaat (Deltares, 2019a).

An important question to be answered in this research in order to achieve the objectives is whether an initially unsaturated soil becomes fully saturated during a high-water event. This is usually assumed for assessment and design of flood defence dykes, since it is expected to be a safe assumption, but this needs to be verified to obtain insight in the real behaviour of initially unsaturated soils. Next question is if an initially unsaturated soil due to infiltration, saturation and swelling, with a decrease of fissures, becomes as low permeable as required to behave undrained during a potential slope failure.

In order to reach the objectives and these two key questions, the following scientific questions were formulated:

1. What is the typical variation in water content of the cohesive soil in dykes and cover layers, if not constantly fully saturated?
2. For which hydraulic conditions and soil properties becomes the soil completely saturated during the wet season, when the precipitation and evaporation are given?
3. To what extend do the macro-pores in aggregated soil close at the saturated state, as a result of swelling of the aggregates? And which factors are of influence?
4. What are suitable criteria regarding texture, water content and aggregation to decide if the shear strength of saturated soil strength should be modelled drained or undrained, in case of stability analysis of primary flood defence dykes?
5. How does the water content and the coupled swelling and shrinkage behaviour affect the (drained or undrained) shear strength?
6. What is the relationship between the shear strength of the aggregates and the shear strength of the soil: to which extend can they be considered equal?



## 1.3 Approach

For this research field and laboratory tests take place at the IJsseldijk near Westervoort (dyke post Dp. 250 + 80) and at the Maasdijk near Oijen (dyke post Dp. 592 - 593). The approach for this research follows the results and recommendations of the research conducted in 2019 commissioned by Rijkswaterstaat (Deltares, 2019a). The approach is also described in the research proposals for Rijkswaterstaat (Deltares, 2019b) and the Projectoverstijgende Verkenning Macrostabieleit (Deltares, 2019c). At both locations suction pressure meters (tensiometers) and volumetric water content sensors are installed in the (initially) unsaturated zone. At the IJsseldijk location, piezometers are installed in the saturated zone of the low permeable cover layer and the top of the aquifer. The aim is to get a good picture of the development of the volumetric water content, suction stress and water pressure during the various seasons and under the influence of precipitation, evaporation and the river water level.

Close to the sensors, cone penetration tests (CPTs), field vane tests (FVTs) and mechanical drillings with undisturbed sampling are carried out. This part of the field research is carried out by Ingenieursbureau Wiertsema & Partners bv. The field tests are repeated with a certain regular interval during the entire period in which the measurements are made. This means that the tests are also conducted during the winter season (usually closed season for geotechnical investigations around dykes). These field tests are also continued in 2021. Classification tests and other laboratory tests are performed on the soil samples. The classification tests are carried out by Wiertsema & Partners. Laboratory tests are conducted by Deltares, TU Delft and Delft Solids Solutions.

For the site investigations it is desirable to use CPTs with measurement of the dielectric constant or permittivity. At present there is no cone available in the market that meets the desired specifications. Wiertsema & Partners has a CPT cone with the possibility to measure the dielectric constant. This cone is tested in the laboratory of Deltares and in the field at Westervoort and Oijen.

In this report the results of the analysis of the collected data of the last two years is described. In this analysis the data from the different sensors, in situ tests and laboratory tests is related to each other. Soil models for drained soil behaviour, unsaturated soil behaviour and undrained soil behaviour are applied to investigate the in-situ behaviour of the soil in the (initially) unsaturated zone.

## 1.4 Outline

Chapter 2 gives a short description of the two measurement sites IJsseldijk at Westervoort (Dp. 250 + 80) and Maasdijk at Oijen (Dp. 592 - 593). Chapter 3 describes the methods which are applied in the research. This report describes the methods and results of the monitoring of volumetric water content, suction stress and pore water pressure and the measurements of the in-situ shear strength with cone penetration tests and field vane tests and the results of the laboratory tests. The sensors which measure volumetric water content, suction stress and pore water pressure and the in-situ tests to measure shear strength are described. For both sites also boreholes are carried out. For the Westervoort and Oijen location classification tests and laboratory tests are carried out on samples from the boreholes. The methods used to perform the boreholes, classification tests and the laboratory tests are also described in Chapter 3. In Chapter 4 the results of the measurements with the various sensors and the results of the in-situ tests, boreholes, classification tests and laboratory tests are presented. In Chapter 5 the results of the analysis are discussed based on the scientific questions which are formulated for the research (see Paragraph 1.3).

Chapter 6 gives the conclusions of the report. Chapter 7 gives an overview of the recommendations based on the uncertainties which are encountered in the analysis.

Based on the results of this research, a report is made (Deltares, 2021a; in Dutch) for water boards and engineering contractors, aimed at application of the acquired knowledge in engineering practice. This report provides insight into the steps in investigations in the field and the laboratory and analysis which can be taken to improve the assessment or design of dykes in which the shear strength of the unsaturated zone plays an important role on slope stability.

This report has also been released under project number 11206817-015-GEO-0001 on behalf of Rijkswaterstaat.

## 2 Study areas

### 2.1 IJsseldijk Westervoort

The measurement site Westervoort is situated at the IJsseldijk (dyke post Dp. 250 + 80) north-westward of the village Westervoort (see Figure 2.1). The IJsseldijk is part of the administration of Waterboard Rijn en IJssel.

A floodplain lies between the dyke and the river IJssel. The width of the floodplain is about 250 m. A large pond is situated in the floodplain. A road is located on the crest of the dyke. At the inner site of the dyke is a berm with a grass-plot.

The in-situ measurements are carried out at the outer toe, crest, inner toe and on the inner berm. The sensors are installed at the outer toe, inner toe and on the inner berm. At the crest only one CPT is carried out. Details of the set-up of the in-situ measurements are given in Chapter 3.



Figure 2.1 Measurement location at the IJsseldijk at Westervoort

### 2.2 Maasdijk Oijen

At Oijen the measurement site is situated on the crest of the Maasdijk between the dyke posts Dp. 592 and Dp. 593 (see Figure 2.2). The official name of the dyke is Oijense Benedendijk. The Maasdijk is part of the administration of Waterboard Aa en Maas. The measurement site is located in the dyke section Ravenstein – Lith.

At this site also a floodplain is situated in front of the dyke. The width of the floodplain is about 380 m. Some channels and ponds are in the floodplain. The dyke is a relatively new construction, as the dyke was built in the 50s of the last century, according to the topographic maps, which are available on the website [www.topotijdreis.nl](http://www.topotijdreis.nl). The old dyke lies up to 100 m behind the new dyke. The topographic maps show a small pond just in front of the old dyke in

the period before 1890. This small pond may be filled with soil in later years and may be a reason for the settlement of the crest of the new dyke around the dyke posts Dp. 592 – 593. The area between the old dyke and the new dyke has been raised to the same height as the crest of the dykes.

The measurement location is on the crest of the dyke. At the crest of the dyke the sensors are installed and the CPTs and FVTs are performed. Details of the set-up of the in-situ measurements are given in Chapter 3.



Figure 2.2 Measurement location at the Maasdijk at Oijen

## 3 Methods

### 3.1 Introduction

As described in the approach of this research (see Paragraph 1.2) different geotechnical tests are performed in the field and in the laboratory. In this chapter the models which are used to interpret the field and laboratory measurements are explained first. These are the models which describe the shear strength of saturated drained soils, unsaturated soils and the undrained shear strength of saturated soils (assuming low permeability of fine grained soil). The parameters of these models have to be derived from the field and laboratory measurements. After the discussion of the models and their parameters, the applied field and laboratory tests, which are performed to derive the parameters, are described.

### 3.2 Model for drained shear strength

In case of limit equilibrium analysis (LEA), the shear strength of a saturated soil under drained shearing conditions is usually determined with the Mohr-Coulomb failure criterion (Craig, 2004):

$$\tau = c' + \sigma'_n \cdot \tan(\phi') \quad (3.1)$$

where:

$\tau$	[kPa]	The shear strength according to Mohr-Coulomb.
$c'$	[kPa]	The cohesion. When the soil is in the critical state, the cohesion is zero.
$\sigma'_n$	[kPa]	The effective stress normal to the shearing plane.
$\phi'$	[°]	The internal friction angle.

Following Critical State Soil Mechanics theory (Schofield & Wroth, 1968) cohesion is related to peak shear strength and the magnitude of cohesion depends on the overconsolidation ratio (*OCR*) of the soil. At large strains when the critical state of a soil is reached and for drained shearing conditions cohesion and overconsolidation play no role in the shear strength which can be mobilized by the soil.

Equation 3.1 implies associative soil behaviour. This means that Equation 3.1 describes soil behaviour accurately when the soil behaves dilative, such that the dilation angle is equal to the friction angle. Behaviour of soil samples in laboratory tests shows that dilation angle is much smaller than the friction angle. At the critical state the dilation angle becomes zero. To account for the effect of dilation on shear strength the non-associative failure criterion can be written as follows (Teunissen, 2016):

$$\tau = \frac{(c' \cos \phi' + \sigma'_n \sin \phi') \cos \Psi}{1 - \sin \Psi \sin \phi'} \quad (3.2)$$

where:

$\Psi$	[°]	The dilation angle.
--------	-----	---------------------

At the critical state cohesion becomes zero and dilation angle becomes zero too, as discussed before. Equation 3.2 then reduces to:

$$\tau = \sigma'_n \cdot \sin \phi' \quad (3.3)$$

This non-associative failure criterion is applied in the present guidelines and regulations for stability assessment of water retaining structures in the Netherlands (WBI 2017; I&M, 2021).

### 3.3 Model for unsaturated shear strength

An important aspect of unsaturated soils (or partially saturated soils) or soils above the phreatic surface where the soil still can be saturated (in the capillary zone) is the effect of capillary suction on effective stress and shear strength. There is however no unanimous consensus concerning the relationship to model the effect of partial saturation on the effective stress and on the shear strength of unsaturated soils (Baker & Frydman, 2009) (Vanapalli, 2010) (Alonso, Pereira, Vaunat, & Olivella, 2010) (Tarantino & El Mountassir, 2013) (Konrad & Lebeau, 2015) (Zhou, Huang, & Sheng, 2016).

Bishop (1959) was the first who came up with a formulation to calculate the effective stress for unsaturated soil conditions which accounts for the effect of capillary stresses. In this formulation an empirical soil parameter  $\chi$  adjust the effectiveness of suction for the degree of saturation. Unfortunately, the relationship between  $\chi$  and degree of saturation is far from unique and an extensive programme of laboratory tests is required to establish the  $\chi$  characteristics for each particular soil (Jardine, Gens, Hight, & Coop, 2004).

A number of authors use the effective degree of saturation  $S_e$  to relate the matric suction  $\psi_m$  to the effective suction (Han & Vanapalli, 2016). Fredlund, Rahardjo, & Fredlund (2012) show for three soil types that, for suction values up to 500 kPa, a good correspondence with experimental data can be found when applying a modified empirical equation by Goh, Rahardjo, & Leong (2010).

Romero & Vaunat (2000) and Tarantino & Tombolato (2005) and others use the dual porosity view to define the effective saturation as the macrostructural degree of saturation  $S_{rM}$ . The macrostructural degree of saturation describes the occupation of macro-pores by water, and is linked mainly to capillary effects. The additional microstructural degree of saturation concerns the water within the micro-pores. Water held in the latter part of the total pore space is attached to the solid by physico-chemical bonds and does not attribute to the shear strength because of the strong affinity of the clay platelets for water (Alonso, Pereira, Vaunat, & Olivella, 2010) (Alonso, Pinyol, & Gens, 2013). Only the water that partially fills the macro-pores will have a significant mechanical effect on the soil. The macrostructural degree of saturation  $S_{rM}$  is calculated with equation 3.4:

$$S_{rM} = \left( \frac{e_w - e_{wm}}{e - e_{wm}} \right) \quad (3.4)$$

where:

$e$	[-]	Void ratio
$e_w$	[-]	Water ratio
$e_{wm}$	[-]	Water ratio in the micropores

Applying the dual porosity view to define the effective saturation the definition of effective stress including the effect of suction  $s$  in partially saturated soils becomes:

$$\sigma_n = (\sigma_n + sS_{rM}) \quad (3.5)$$

Shear strength of partially saturated soils is then related to suction  $s$  weighted by the degree of saturation of the macropores  $S_{rM}$ , as long as drained conditions during shearing can be

assumed. According to the Mohr-Coulomb failure criterion (see equation 3.1) and accounting for the effect of suction failure of the soil can be calculated with equation 3.6.

$$\tau = c' + (\sigma_n + sS_{rM}) \cdot \tan(\phi') \quad (3.6)$$

For the critical state ( $c' = 0$  kPa) and assuming non-associative soil behaviour (see equation 3.3) the failure criterion is:

$$\tau = (\sigma_n + sS_{rM}) \cdot \sin(\phi') \quad (3.7)$$

Note that in equations 3.5, 3.6 and 3.7  $\sigma_n$  is used instead of  $\sigma'_n$ .  $\sigma_n$  is the total normal stress. The total normal stress is applied here, because in unsaturated soils no positive pore water pressures are active.

Tarantino & El Mountassir (2013) point out that different degrees of saturation may occur at the same suction, because of the effect of void ratio on the water retention curve. At the same suction, the degree of saturation is higher along a drying path than on a wetting path (hydraulic hysteresis) and this result in a higher shear stress contribution.

Figure 3.1 illustrates the effect of suction on shear strength. The figure presents the contribution of partial saturation to ultimate shear strength for reconstituted clayey silt samples (Boso, 2005; Tarantino & El Mountassir, 2013). Three different initial void ratios were used, causing also different water retention. The graph (a) at the left hand side shows that the critical state shear strength at a given matric suction differs significantly for the three cases. The graph (b) at the right hand side shows that these differences tend to disappear when the strength is plotted against the effective suction.

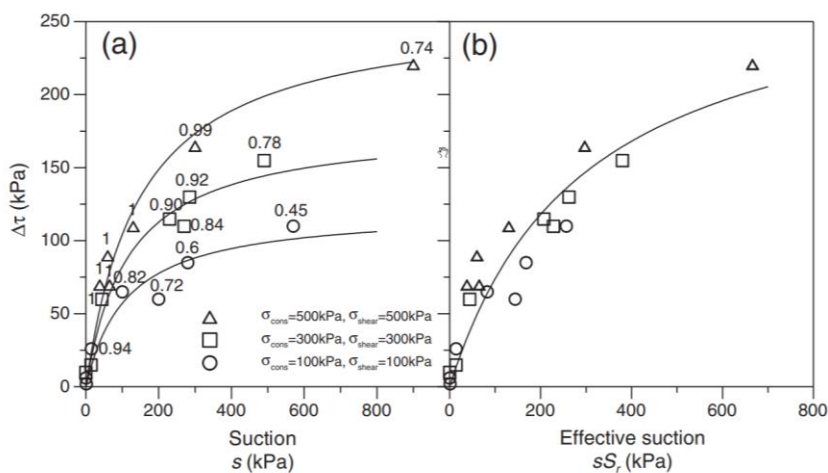


Figure 3.1 Critical state shear strength for total and effective suction for a reconstituted partially saturated clayey silt (Boso, 2005; Tarantino & El Mountassir, 2013).

Fredlund et al (Fredlund, Rahardjo, & Fredlund, 2012) also demonstrate that the shear stress has a curved envelope with increasing suction.

Tarantino et al (Tarantino & El Mountassir, 2013) show for 12 different clayey 'aggregated' soils that usage of equation 3.7 (and assuming associative soil behaviour) yields good correspondence with the actual shear strength as a linear function of effective suction  $sS_{rM}$ .

Tarantino et al suggest that conventional “constant water” laboratory tests can be used to fit the parameters  $e_{wm}$ .

A more elaborate discussion about the shear strength model for unsaturated soil can be found in the literature review (Deltares, 2019a).

### 3.4 Model for undrained shear strength

The operational shear strength of saturated soils depends on the drainage conditions during failure, stress level, stress history and the failure mode due to anisotropy of the undrained shear strength.

In soft low permeable soils excess pore water pressures are generated during shear failure. When the excess pore water pressure can dissipate drained shear strength is mobilized. The soil behaves undrained when the time to failure is relatively short compared to the dissipation of excess pore water pressures. The undrained shear strength  $s_u$  is mobilized when the excess pore water pressure cannot dissipate. In case of undrained behaviour, the excess pore water pressures influence the operational shear strength. The magnitude of the excess pore water pressures depends on the in-situ state (or stress history), which can be expressed as the yield stress  $\sigma'_{vy}$  or overconsolidation ratio  $OCR$ .

In geotechnical engineering undrained shear failure is assumed to be relevant in soft clay and peat for the assessments of the stability of slopes. In the interpretation of CPTs and FVTs in soft soils also undrained shear failure is assumed.

For the stability assessment of the Dutch primary flood defences Limit Equilibrium Analysis (LEA) are applied and saturated low permeable soil are assumed to behave undrained. The undrained shear strength has to be determined with the SHANSEP relationship between undrained strength, overconsolidation ratio and the vertical effective stress at the start of the undrained stage. The undrained shear strength field can be correlated to the net cone resistance from cone penetration tests (I&M, 2021).

According to the SHANSEP (Stress History And Normalized Soil Engineering Properties)-model (Ladd & Foot, 1974; Ladd, 1991) the undrained shear strength is determined with:

$$s_u = \sigma'_v \cdot S \cdot OCR^m \quad \text{with} \quad \sigma'_{vy} = \sigma'_{vi} \cdot OCR \quad \text{and} \quad \sigma'_{vy} = \sigma'_{vi} + POP \quad (3.8)$$

where:

$s_u$	Undrained shear strength (kPa).
$\sigma'_v$	Effective vertical stress (kPa).
$S$	Normally consolidated undrained shear strength ratio (-).
$OCR$	Overconsolidation ratio (-).
$m$	Strength gain exponent (-).
$\sigma'_{vy}$	Yield stress (kPa).
$POP$	Pre overburden pressure (kPa).

For variations of the effective vertical stress below the yield stress the undrained shear strength is more or less constant, following the SHANSEP-model, because the strength gain exponent is around 0.8.

Clayey soils with high soil unit weight above 17 to 18 kN/m<sup>3</sup> do not behave like the SHANSEP-model. These are soils with high silt and sand content. These soils are called Transitional soils, as they are in-between sand and clay. Due to their compact structure they behave dilative during undrained shear failure; negative excess pore water pressures give



the soil a temporary additional strength. For transitional soils the operational undrained shear strength depends on the initial void ratio of the soil (Coop, 2015). The operational undrained shear strength can be much higher than what could be expected based on the SHANSEP-model.

### 3.5 Site investigation

At the IJsseldijk location near Westervoort the research is carried out at the outer toe, crest, inner toe and inner berm. On the outer toe, crest, inner toe and on the inner berm, CPTus class 2 are carried out as a preliminary survey. At Westervoort some of the CPTus are applied with an additional magnetic module to trace potentially present explosives.

Suction stress sensors (tensiometers), volumetric water content sensors and pore water pressure sensors (piezometers) are installed at the outer toe, inner toe and at the inner berm. The tensiometers and the water content sensors are installed in the top of the clayey cover layer, between 1.0 and 2.5 m below surface level. The pore water pressure sensors are placed in the bottom of the clayey cover layer and in the top of the Pleistocene water-bearing sand layer (aquifer).

CPTs class 1 and FVTs to measure the shear strength of the soil are also carried out on the inner berm. The field investigation on the inner berm will be repeated with a regular interval during the entire measurement period. The goal of these measurements is to correlate volumetric water content, suction stress to shear strength to gain the understanding in the importance of the seasonal variation of volumetric water content and suction stress on the shear strength. Each time the CPTs and FVTs are performed double to be able to assess the heterogeneity of the shear strength. The class 1 CPTs and FVTs are conducted within a radius of about 7 meter around the sensors.

At the Maasdijk near Oijen a similar approach is followed. At the Maasdijk the research is carried out only on the crest of the dyke. Here also CPTus class 2 are performed as a preliminary survey. The volumetric water content sensors and tensiometers are installed at the crest of the dyke at 1.0 to 3.1 m below surface level. Similar to Westervoort CPTs class 1 and FVTs are conducted to measure the shear strength of the soil. Piezometers are not applied in Oijen. At Oijen the class 1 CPTs and FVTs are conducted within a radius of about 10 meter around the sensors.

At Westervoort and Oijen also mechanical drillings are performed. The samples of the boreholes are used to perform classification tests, triaxial tests, direct shear tests, direct simple shear tests, oedometer tests and mercury intrusion porosimetry (MIP) tests in the laboratory.

*Table 3.1* and *Table 3.2* give an overview of the CPTs, FVTs and boreholes which are performed at Westervoort and Oijen up to now. The set-up of the site investigations at Westervoort and Oijen is given in the factual report (Deltares, 2021b). Descriptions of the bore holes are in Appendix A.

Table 3.1 Performed CPTs, FVTs and boreholes at Westervoort

Date	CPT class 1 (DKM) or CPT class 1 with electric resistivity measurement (DKMG)	CPTu class 2 with magnetocone (DKM) or $u_2$ measurement (DKMP)	FVT	Borehole
23-10-2019		DKMP2003, DKMP2004, DKM2201, DKM2202, DKM2203		
24-10-2019		DKMP2001, DKMP2002, DKM2200		
31-10-2019	DKM2005, DKM2006		TV202	B201
	Start of the monitoring of volumetric water content, suction stress and pore water pressure.			
1-11-2019			TV201	
15-11-2019	DKM2007, DKM2008			
28-11-2019	DKM2009			
29-11-2019	DKM2010		TV203	
19-12-2019	DKM2011, DKM2012			
13-1-2020	DKM2013, DKM2014			
4-2-2020	DKM2015, DKM2016			
10-2-2020	DKM2017, DKM2018			
10-3-2019	DKM2019, DKM2020			
6-4-2020	DKM2021, DKM2022		TV206 test 1	
7-4-2020			TV206 test 2-7 TV205 test 1-2	
8-4-2020			TV205 test 3-7	
11-5-2020	DKM2023, DKM2024			
5-6-2020	DKM2025, DKM2026			
29-6-2020	DKM2027, DKM2028			
21-7-2020	DKM2029, DKM2030			
11-8-2020				B202, B203
24-8-2020	DKM2031, DKM2032			
7-9-2020	DKM2033, DKM2034			
8-9-2020			TV207	
9-9-2020			TV208	
30-9-2020	DKMG2045, DKMG2046			
29-10-2020	DKM2035, DKM2036			
3-12-2020	DKM2037, DKM2038			
30-9-2021	DKMG2042, DKMG2043			

Table 3.2 Performed CPTs, FVTs and boreholes at Oijen

Date	CPT class 1 (DKM) or CPT class 1 with electric resistivity measurement (DKMG)	CPTu class 2 with $u_2$ measurement	FVT	Borehole
17-9-2019		DKMP1001, DKMP1002, DKMP1003, DKMP1004		
18-9-2019	DKM1005, DKM1006			
25-9-2019				B001
3-10-2019	Start of the monitoring of volumetric water content and suction stress.			
11-10-2019	DKM1007, DKM1008			
23-10-2019			TV101 test 1-6	
24-10-2019	DKM1009, DKM1010		TV101 test 7-10 TV102 test 1	
25-10-2019			TV102 test 2-10	
31-10-2019 / 1-11-2019				B002
14-11-2019	DKM1011, DKM1012			
26-11-2019	DKM1013, DKM1014			
27-11-2019			TV103 test 1-9	
28-11-2019			TV103 test 10-11	
19-12-2019	DKM1015, DKM1016			
13-1-2020	DKM1017, DKM1018			
4-2-2020	DKM1019, DKM1020			
9-3-2020	DKM1021, DKM1022			
8-4-2020	DKM1023, DKM1024			
9-4-2020			TV105	
10-4-2020			TV104	
11-5-2020	DKM1025, DKM1026			
5-6-2020	DKM1027, DKM1028			
29-6-2020	DKM1029, DKM1030			
21-7-2020	DKM1031, DKM1032			
10-8-2020				B003
24-8-2020	DKM1033, DKM1034			
9-9-2020	DKM1035, DKM1036			
10-9-2020			TV107 test 1-12	
11-9-2020			TV107 test 13-18	
14-9-2020			TV106 test 1-11	
15-9-2020			TV106 test 12-18	
30-9-2020	DKMG1047, DKMG1048			
29-10-2020	DKM1037, DKM1038			
3-12-2020	DKM1039, DKM1040			
30-9-2021	DKMG1041, DKMG1042			

### 3.6 Volumetric water content measurements

Volumetric water content  $\theta$  is defined as the ratio of the volume of water  $V_w$  to the total volume of the soil  $V$ :  $\theta = \frac{V_w}{V}$ . Gravimetric water content  $w$ , which has been most commonly used in geotechnical engineering, is defined as the ratio of the mass of water  $M_w$  to the mass of soil solids  $M_s$ :  $w = \frac{M_w}{M_s}$ . Volumetric water content is related to gravimetric water content as follows:  $\theta = w \frac{\rho_d}{\rho_w}$ , in which  $\rho_d$  is the dry density of soil and  $\rho_w$  is the density of water. With the dry density of soil  $\rho_d$ , the density of water  $\rho_w$  and the relative soil density  $G_s (= \rho_s / \rho_w)$ , in which  $\rho_s$  is the solid density, the degree of saturation  $S_r$  can be calculated from volumetric water content  $\theta$  or gravimetric water content  $w$ , with:

$$S_r = \frac{\theta}{1 - \frac{\rho_d}{G_s \cdot \rho_w}} = \frac{w}{\frac{\rho_w}{\rho_d} \cdot \frac{1}{G_s}} \quad (3.9)$$

Water content reflectometers CS616 of Campbell Scientific are used to measure the in situ volumetric water content. Measuring water content using a water content reflectometer is an indirect measurement, which is sensitive to the dielectric permittivity of the material surrounding the 300 mm long probe rods. Since water is the only soil constituent that has a high value for dielectric permittivity and is the only component other than air that changes in concentration, a device sensitive to dielectric permittivity can be used to estimate volumetric water content (Campbell, 2016).

The water content reflectometer consists of two stainless steel rods which are connected to an electronic unit with a multivibrator. The applied signal from the multivibrator travels the length of the probe rods and is reflected from the rod ends traveling back to the probe head. When the reflection is detected the next pulse will be triggered. The travel time of the signal from the electronic multivibrator on the probe rods depends on the dielectric permittivity of the material surrounding the rods. The dielectric permittivity depends on the water content. Therefore, the oscillation frequency of the multivibrator depends on the water content of the media being measured. As water content increases, the propagation velocity of the signal decreases because polarization of water molecules takes time. The frequency of pulsing with the probe rods in free air is about 70 MHz. The probe output frequency or period is empirically related to volumetric water content using a calibration equation.

The water content reflectometer operation can be affected when the signal applied to the probe rods is attenuated. The probe will provide a well-behaved response to changing water content, even in attenuating soils, but the response may be different than described by the standard calibration. Consequently, a unique calibration is required. Changes in probe response can occur when soil bulk electrical conductivity is greater than  $0.5 \text{ dS m}^{-1}$ . The major contributor to soil electrical conductivity is the presence of free ions in solution from dissolution of soil salts. Soil organic matter and some clays can also attenuate the signal.

To derive the volumetric water content from the sensor output calibration factors which are slightly modified compared to the calibration factors for sandy clay loam from the instruction manual (Campbell, 2016) of the reflectometers are applied. The calibration factors are modified such that the degree of saturation  $S_r$  is 1.0 when the volumetric water content is relatively high and the adjacent tensiometer give positive pore water pressure.

The water content reflectometers are installed in the soil at depths between 1.0 m and 3.25 m below surface level. Details are presented in Table 3.3 and Table 3.4. The devices are installed in boreholes which are drilled with a hand auger. For each device a separate borehole is made. The devices are installed with the probe rods in vertical direction. The probe rods are pushed into the undisturbed soil at the bottom of the boreholes. The boreholes are filled with bentonite after installing the water content reflectometers to prevent

for leakage paths around the sensors. Mikolit 00 is used, which has a swelling capacity of 30-40% additional to the bulk volume of the Mikolit when enough water is available.

The measurements of the water content with the four sensors at the outer toe at Westervoort are interrupted from October 1, 2020 to October 15, 2020 due to damage to the cables.

Table 3.3 Volumetric water content devices at IJsseldijk Westervoort. The indicated depth of the sensors is halfway the probe rods

Sensor	Location	Surface level (m + NAP)	Depth of sensor below surface level (m)	Depth of sensor (m + NAP)
1	Outer toe	10.58	0.97	9.61
2	Outer toe	10.59	1.50	9.09
3	Outer toe	10.57	1.85	8.72
4	Outer toe	10.59	3.25	7.34
5	Inner toe	11.26	1.00	10.26
6	Inner toe	11.25	1.50	9.75
7	Inner toe	11.26	2.00	9.26
8	Inner toe	11.27	2.50	8.77
9	Inner berm	10.40	1.00	9.40
10	Inner berm	10.37	1.50	8.87
11	Inner berm	10.41	2.00	8.41
12	Inner berm	10.40	2.50	7.90

Table 3.4 Volumetric water content devices at Maasdijk Oijen. The indicated depth of the sensors is halfway the probe rods

Sensor	Location	Surface level (m + NAP)	Depth of sensor below surface level (m)	Depth of sensor (m + NAP)
1	Crest	9.30	1.00	8.30
2	Crest	9.28	1.70	7.58
3	Crest	9.35	2.40	6.95
4	Crest	9.29	3.10	6.19

### 3.7 Suction stress measurements

To measure the capillary suction (or matric potential) in the field conventional tensiometers are applied. The essential components of conventional tensiometers are a porous filter, a reservoir of liquid (usually water) and a means of measuring stress (Tarantino, Ridley, & Toll, 2008). Tensiometers work by allowing water to move between the water reservoir of the instrument and the soil until the water stress state in both is equal. When water is drawn out of the instrument into the soil tension is caused in the reservoir of liquid. The soil water tension is directly conducted to the pressure transducer which offers a continuous signal.

Conventional tensiometers only cover the range 0-80 kPa, which can be exceeded during the summer period. To date, tensiometers that can measure suction stress continuously over a relatively long period time have a suction range limited to ~80 kPa (Tarantino, Ridley, & Toll,

2008). If the soil dries out the tensiometer runs empty and must be refilled as soon as the soil is sufficiently moist again (Meter, 2018).

In this project the T5 tensiometer of Meter group is initially used. The measurement range is -100 (pressure) to 85 kPa (suction), with an accuracy of  $\pm 0.5$  kPa. So, this device can also be used for saturated conditions below the phreatic surface. The T5 tensiometer has a response time of only 5 seconds for a pressure change of 0 to 85 kPa. It reacts very fast to changing soil conditions because of its small water volume. The atmospheric reference pressure is provided through a membrane on the cable (Meter, 2018).

The tensiometers are installed in the soil at depths between 1.0 m and 3.1 m below surface level. Details are summarized in Table 3.5 and Table 3.6. The devices are installed in separate boreholes which are drilled with a hand auger. The ceramic tip of the tensiometers are pushed into the undisturbed soil at the bottom of the boreholes. After installing the tensiometers the boreholes are filled with bentonite to prevent for leakage paths around the sensors. Mikolit 00 is used, which has a swelling capacity of 30-40% additional to the bulk volume of the Mikolit when enough water is available.

During the dry summer period in 2020 four tensiometers became outside their measurement range. The porous filters of the sensors become unsaturated. Therefore, the measurements of these sensors are not reliable anymore. Three of these sensors are replaced by another type of tensiometer at March 12, 2021. These are UGT full range tensiometers with a measurement range of -100 (pressure) to 500 kPa (suction). The operating principle of the Full Range Tensiometer differs slightly from water filled tensiometers: the measurement volume in the sensor is filled with water that is bonded to a polymer. Due to the bonding of water to the polymer the physical measurement limit of approximately 80 kPa does not account for the Full Range Tensiometer (UGT, 2020). Therefore, the Full Range Tensiometer cannot run dry like conventional water filled tensiometers and is able to measure soil tensions up to 500 kPa.

The Full Range Tensiometers are installed in separate boreholes, which are made with a hand auger with a diameter of 4 cm. The boreholes are made somewhat deeper than the installation depth of the sensors. A thick slurry from drilled soil from the borehole and water is put at the bottom of the borehole and compacted. The tensiometers are pushed into this compacted slurry. After that the borehole is filled with drill grout (Cebo) to prevent for leakage through the borehole.

The measurements of suction with the four tensiometers at the outer toe at Westervoort are interrupted from October 1, 2020 to October 15, 2020 due to damage to the cables.

Table 3.5 Tensiometers at IJsseldijk Westervoort

Sensor	Location	Surface level (m + NAP)	Depth of sensor below surface level (m)	Depth of sensor (m + NAP)
1	Outer toe	10.60	1.00	9.60
2	Outer toe	10.62	1.50	9.12
3	Outer toe	10.60	2.00	8.60
4	Outer toe	10.60	3.00	7.60
5	Inner toe	11.21	1.00	10.21
6	Inner toe	11.17	1.50	9.67
7	Inner toe	11.19	2.00	9.19
8	Inner toe	11.21	2.40	8.81
9	Inner berm	10.35	1.00	9.35
9A (UGT)	Inner berm	10.43	1.00	9.43
10	Inner berm	10.36	1.50	8.86
11	Inner berm	10.37	2.00	8.37
12	Inner berm	10.43	2.55	7.88

Table 3.6 Tensiometers at Maasdijk Oijen

Sensor	Location	Surface level (m + NAP)	Depth of sensor below surface level (m)	Depth of sensor (m + NAP)
1	Crest	9.26	1.00	8.26
1A (UGT)	Crest	9,32	1.00	8.32
2	Crest	9.33	1.70	7.63
2A (UGT)	Crest	9,32	1.70	7.62
3	Crest	9.36	2.40	6.96
4	Crest	9.29	3.10	6.19

### 3.8 Pore water pressure measurements

At the IJsseldijk near Westervoort also piezometers are installed to measure changes in piezometric level in the aquifer and the saturated part of the Holocene clayey cover layer. The piezometer device uses a pressure sensitive diaphragm with a vibrating wire element attached to it (Geokon, 2019). A piezometer incorporates a porous filter stone ahead of the diaphragm, which allows water to pass through but prevents soil particles to act directly on the diaphragm. Standard porous filters are made from sintered stainless steel. Fluid pressures acting at the outer face of the diaphragm cause deflections of the diaphragm and changes in tension and frequency of the vibrating wire. The changes in frequency are sensed and transmitted to the readout device.

In this project Geokon piezometers 4500DP are applied. These piezometers have a pointed nose cone and therefore these devices can be pushed directly into soft ground with drill rods.

Table 3.7 presents the locations and depths of the piezometers at Westervoort.

Table 3.7 Pore water measurement devices at IJsseldijk Westervoort

Sensor	Location	Surface level (m + NAP)	Depth of sensor below surface level (m)	Depth of sensor (m + NAP)
1	Outer toe	10.57	3.62	6.96
2	Outer toe	10.59	4.14	6.45
3	Outer toe	10.61	4.61	6.00
4	Outer toe	10.63	5.62	5.01
5	Outer toe	10.62	6.14	4.48
6	Inner toe	11.08	3.12	7.96
7	Inner toe	11.10	3.64	7.46
8	Inner toe	11.08	4.10	6.98
9	Inner toe	11.08	6.12	4.96
10	Inner toe	11.09	7.13	3.96
11	Inner berm	10.39	3.14	7.25
12	Inner berm	10.39	3.65	6.74
13	Inner berm	10.31	4.12	6.19
14	Inner berm	10.32	4.64	5.69
15	Inner berm	10.32	5.10	5.22

The measurements of piezometric head with the five sensors at the outer toe at Westervoort are interrupted from October 1, 2020 to October 15, 2020 due to damage to the cables.

### 3.9 Cone penetration tests (CPT)

Cone penetration tests (CPT or CPT<sub>u</sub> when the pore water pressure  $u_2$  is measured) are relatively simple in situ tests. The CPT(u) gives more or less continuous readings of the cone penetration resistance  $q_c$ , sleeve friction  $f_s$  and excess pore water pressure  $u_2$  every 2 cm. The cone penetration test has a relatively small measurement error and high repeatability, depending on the applied accuracy class and the effort in preparation and maintenance of the cone. In the Netherlands CPTs are performed according to NEN-EN-ISO-22476-1. The surface area of the applied cone in this project is 10 cm<sup>2</sup>. The penetration rate is 2 cm per second. In soft low permeable soils this penetration rate induces undrained soil behaviour. Furthermore, this in situ test is very common in the Netherlands. So, there is a lot of experience with carrying out CPTs and using CPT results in geotechnical analyses.

In this project class 1 cones and class 2 cones are applied. CPT<sub>u</sub>s class 2 are carried out as a preliminary survey. CPTs class 1 are conducted to measure the shear strength of the soil. According to NEN-EN-ISO-22476-1 class 1 CPTs must be conducted including  $u_2$  measurements. As  $u_2$  readings are often unreliable in unsaturated soils the  $u_2$  measurements are not performed. According to NEN-EN-ISO-22476-1 the allowable minimum accuracy of the cone resistance is 35 kPa or 5% for class 1 cones and 100 kPa or 5% for class 2 cones. The zero drift after conducting the CPTs is reported by Wiertsema & Partners.

Table 3.1 and Table 3.2 give an overview of the CPTs which are performed at Westervoort and Oijen up to now.



### Derivation of the undrained shear strength

Derivation of the undrained shear strength  $s_u$  from the cone penetration resistance  $q_c$  is not straightforward due to the complex interaction between the soil and the cone. Commonly an empirical relationship between the undrained shear strength and cone penetration resistance is applied:

$$s_u = \frac{q_{net}}{N_{kt}} \quad (3.10)$$

with net cone resistance:

$$q_{net} = q_t - \sigma_{vi} \quad (3.11)$$

and corrected cone resistance:

$$q_t = q_c + u_2(1 - a) \quad (3.12)$$

where:

- $N_{kt}$  Empirical correlation factor (-).
- $q_t$  Corrected cone resistance for pore pressure effects (MPa).
- $\sigma_{vi}$  In situ total vertical stress (MPa).
- $\sigma'_{vi}$  In situ effective vertical stress (MPa).
- $q_{net}$  Net cone resistance corrected for pore pressure effects and in situ total vertical stress (MPa).
- $q_c$  Measured cone tip resistance (MPa).
- $u_2$  Pore water pressure measured just behind the cone during penetration (MPa).
- $a$  Area ratio (that area affected by the pore water pressure) (-).

Typical values of  $N_{kt}$  are between 10 and 20 (Ladd & DeGroot, 2004; Schnaid, 2009). It is important to note that  $N_{kt}$  depends on the reference strength as the undrained shear strength is not a unique soil parameter but a measure of the strength which depends on several factors. Based on finite element analyses Teh & Houlsby (1988) and Lu et al. (2004) pointed out that  $N_{kt}$  depends on the stiffness of the soil, horizontal stress and roughness of the cone and the shaft.

### Experience in unsaturated soils

Very little is known however on how to interpret the cone penetration test results when performed in unsaturated soils. Equation 3.13 was presented by (Pournaghiazar, Russell, & Khalili, 2013) to correlate changes in cone resistances in unsaturated sand to changes in effective isotropic stress, caused by different suction stress values. The correlation constant  $n$  was derived from a correlation between cone resistance and relative sand density, by assuming that the relative density remains constant for different mean effective stress values.

$$q_{c.2} \approx q_{c.1} \cdot \left( \frac{p'_2}{p'_1} \right)^n \quad (3.13)$$

where:

- $q_{c.i}$  cone resistance for different values of the mean isotropic stress (kPa).
- $p'_i$  mean isotropic effective stress:  $p'$  for different values of the effective suction(kPa).
- $n$  empirical correlation factor (-).

Regarding cone penetration tests in unsaturated clays, Blight (2013) refers to Powell & Quarterman (1988) who correlated cone penetration data with shear strength back-analysed from plate load test results obtained from various stiff clays and soft rock formations in the United Kingdom. Powell & Quarterman (1988) found a trend of the correlation factor  $N_k$  ( $s_u = \frac{q_c - \sigma_v}{N_k}$ ) to increase with plasticity index (Figure 3.). In their results was also a distinct influence of the spacing of the cracks and fissures in the clay in relation to the cone size. They distinguished between three classes of spacings: close spacing, intermediate spacing and wide spacing. With wide spacings,  $N_k$  values between 20 and 30 were obtained, whereas  $N_k$  values between 10 and 15 would be appropriate with close spacing.

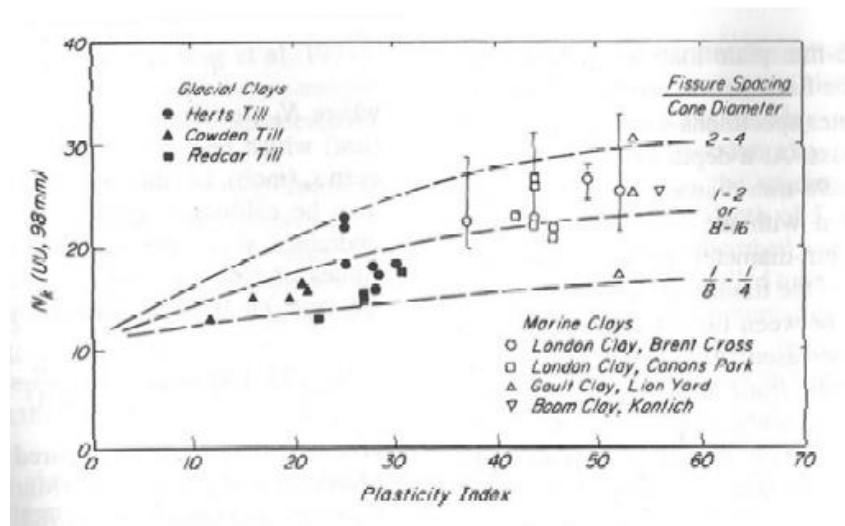


Figure 3.2 The cone resistance in unsaturated aggregated soil is overestimated in case of large distance between the cracks, and the  $N_k$  value should therefore increase (Powell & Quarterman, 1988)

Blight (2013) performed a series of comparative tests at two sites with the cone penetration test and the field vane test. Based on these tests Blight evaluated the correlation factor  $N_k$  for two stiff unsaturated clays in South Africa. Strengths of up to 500 kPa were measured. When relating cone penetration resistance to undisturbed vane shear strength (peak strength) the best average value for  $N_k$  appears to be 15. The data points were in a relatively narrow band.

The in situ measured effect of suction stress on the cone tip resistance for five different clayey soils at three measurement sites is shown in Figure 3., as reported by Miller et al. (2018). In this study the trend of the field data is fitted using bearing capacity theory, following Durgunoglu & Mitchell (1973). In this approach the Mohr-Coulomb failure criterion with effective stress parameters cohesion and friction angle are applied, assuming drained shearing conditions. Suction and degree of saturation are incorporated in the analysis by using the soil water retention curves as showed in the bottom part of the figure. The relations give large scatter, however there is a relatively consistent trend of increasing cone tip resistance with increasing suction stress as expected. According to Miller et al. (2015) the scatter can be attributed to other factors besides suction that influence the cone tip resistance, such as variations in soil type, density, degree of weathering, and stress history. The considerable scatter is therefore not surprising since the data represents a variable stratigraphy from zero to about 3 m of depth. Nevertheless, the data provide some insight into potential variations in tip resistance that may occur due to suction changes. Note that the cone tip resistances seem to tend to go to a certain minimum value, which corresponds with a cohesion of 40 kPa, when suction stress decreases.

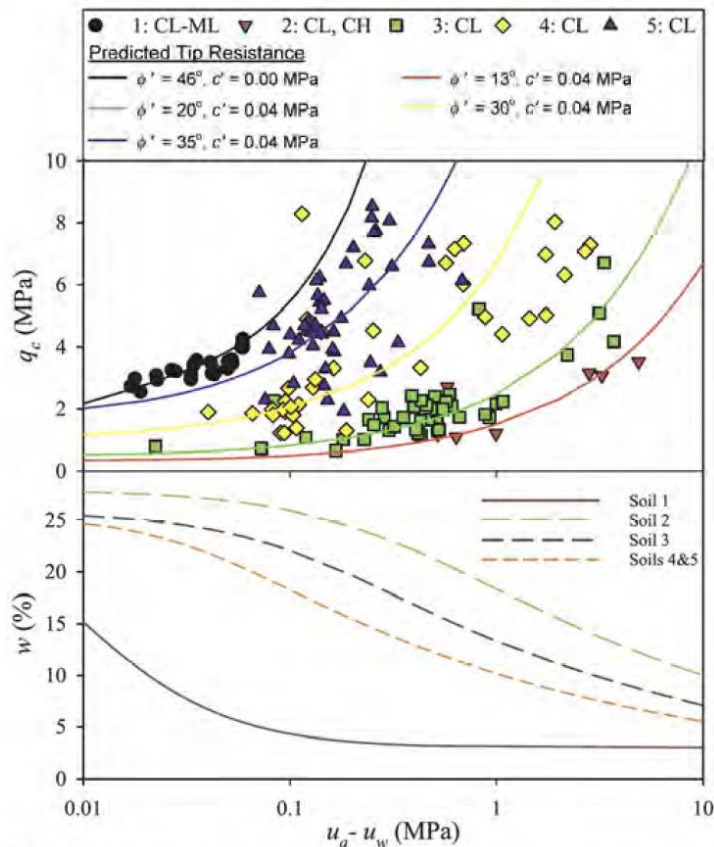


Figure 3.3 Effect of suction on cone tip resistance, for five clayey soils (Miller et al., 2018). The trend of the field data is fitted using bearing capacity theory

### 3.10 Resistivity Cone Penetration Tests (RCPT)

A CPT device can be equipped with various additional sensors. One of the possibilities is the addition of a module to measure the electrical resistivity (Mayne, 2007; Schnaid, 2009). The resistivity module is located directly behind the friction sleeve. The resistivity module consists of two or more electrodes separated by insulating material. The measurement operates within the principle that the potential drop across two adjacent pairs of electrodes, at a given electrical current, is proportional to the electrical resistivity of both soil and pore fluid. Comparable modules for dielectric measurements are also available. Whereas resistivity induces a direct electrical current into the ground, a similar approach can be provided using alternating current and thus established to obtain dielectric measurements (permittivity).

Measuring the resistivity, conductivity or dielectric constant of the soil during CPT testing would be helpful for the interpretation of CPT results in unsaturated soils. The resistivity, conductivity or dielectric constant are measures of the volumetric water content and via the volumetric water content suction stress can be estimated. In this way using a RCPT could make it possible to estimate suction stress and to interpret the measured cone penetration resistance considering the measured suction stress.

In this project a resistivity cone of Wiertsema & Partners is tested in the laboratory of Deltares and in the field at Westervoort and Oijen. This cone is made by GeoPoint some years ago and is able to measure electrical conductivity (range to 500 mS/m) and dielectric constant (range 1 – 80). The dielectric constant is converted in the CPT-software to the volumetric water content. Note that this cone is a special item. Currently none of the cone manufacturers in the Netherlands can supply a resistivity cone with the required specifications. Some of the

cones in the manufacturer's delivery programs do not have the required specifications. Other cones cannot be supplied because some of the required components are no longer available.

### 3.11 Field vane tests (FVT)

The field vane test (FVT) is applied to determine the in situ peak undrained shear strength and residual shear strength. *Table 3.1* and *Table 3.2* give an overview of the FVTs which are performed at Westervoort and Oijen up to now.

With a FVT a vane with four rectangular blades is rotated in the soil. It is assumed that a cylindrical shear plane is formed around the rotating vanes. The shear stress on this cylindrical shear plane can be determined based on the torque which is applied to rotate the vane. The failure mode of the FVT is thought to compare with the failure mode of a direct shear test (Chandler, 1988).

FVTs are usually applied to determine the in situ undrained shear strength of saturated soft soils. The undrained shear strength is calculated from the torque which is required to rotate the cylinder of soil within the four vane blades. When rotating the vane first the undisturbed or peak strength is measured and after five to ten rotations the remoulded vane shear strength is measured. Standards for FVT are ASTM D 2573-01 and FprEN 22476-9:2010.3.

There is a lot of experience with the application of these tests in saturated conditions. Empirical corrections based on plasticity index (Bjerrum, 1972; Chandler, 1988) or liquid limit (Larsson, Bergdahl & Eriksson, 1987) are used to derive the undrained shear strength from the measured torque. The empirical corrections are applied to account for the complex failure mode and rate of strain of the FVT. The corrections are based on back-analyses of failures of embankments and footings. So, these empirical corrections assure that the measured torque reflects the operational undrained shear strength of the investigated soft soils.

Drainage conditions of the FVT are a point of particular interest. To determine the in situ undrained shear strength the drainage conditions during performance of a FVT have to be fully undrained. In permeable soils this will not be the case when applying the standard rotation rate.

#### Interpretation

For standard vane dimensions with the height of the vane two times the diameter of the vane the undrained shear strength  $s_{u,FVT}$  of the soil can be determined with FprEN 22476-9:2010.3:

$$s_{u,FVT} = 0.273 \frac{T}{D^3} \quad (3.14)$$

where:

$T$  torque on the vane (kNm).

$D$  diameter of the vane (m).

To convert the FVT measurements to an accurate estimation of the operational shear strength there are several issues to be considered, such as friction along the rods, shear stress distribution on the vane blades, anisotropy of the soil, rate effects, and partial consolidation (Chandler, 1988; Schnaid, 2009). The friction along the rods plays no role in this project as a FVT device is applied with the motor just above the vane.

### Stress distribution and anisotropy

The shear stress distribution on the vane blades is uncertain. Several studies are conducted to determine the stress distribution on the vane blades. Anisotropy of the undrained shear strength due to the soil fabric developed during deposition and consolidation effects enhance the complexity of the shear stress distribution on the vane. When considering stress distribution and anisotropy a number of variations on equation 3.14 are possible (Schnaid, 2009). Equation 3.14 as proposed by FprEN 22476-9:2010.3 assumes isotropic soil conditions and uniform stress distribution on the vanes. Applying other assumptions, the calculated undrained shear strength may deviate substantially, at least when anisotropy is large. Bjerrum (1973) showed that the anisotropy of the undrained shear strength is low for soils with plasticity index above 40%. Assuming isotropic soil conditions and uniform stress distribution yields a low estimate of the undrained shear strength. As the stress distribution and anisotropy are very difficult to assess in practice equation 3.14 as proposed by FprEN 22476-9:2010.3 is commonly adopted (Schnaid, 2009). The resulting undrained shear strength is then corrected with empirical corrections which account for several aspects, such as strain rate, soil disturbance and anisotropy of the shear strength.

Becker et al. (1988) proposed that the FVT interpretation could be refined when the in situ horizontal effective stress and horizontal yield stress would be considered. As the common practice uses the vertical effective stress and empirical correlations are based on the vertical effective stress in the present research also the vertical effective stress will be used. It should be noted that for CPT interpretation the horizontal stress does play a role (see Paragraph 3.9), but for CPT interpretation also the vertical stress is commonly applied.

### Rate effects

Rate effects are important because the rotation of the vane is much faster than the rate of a slope failure. As the undrained shear strength exhibit rate dependency, correction for rate effects is required. This correction is generally incorporated in empirical corrections for the FVT. The empirical corrections are derived using a rotation rate of 6 degrees/minute. This rotation rate is also applied in this project.

### Empirical corrections

Bjerrum (1972) derived an empirical correction factor  $\mu$  to adjust the measured undrained shear strength from the FVT to the operational undrained shear strength in the field. This correction factor is related to the plasticity index  $I_p$  and accounts for effects of shear strength anisotropy and strain rate. Bjerrum obtained the correction factor from back calculated case histories. The correction factor decreases from 1.1 for  $I_p$  is 10% to 0.55 for  $I_p$  is 120%. The correction factor is applied as follows:

$$s_{u,field} = \mu s_{u,FVT} \quad (3.15)$$

Azzouz et al. (1983) also examined the required correction of the measured undrained shear strength from the FVT. These authors pointed out that Bjerrum (1972) ignored three-dimensional effects in the back-analyses of the case histories. Therefore, the correction factor proposed by Bjerrum can be reduced by some 10% for field conditions with a plane strain mode of failure (see Figure 3.4).

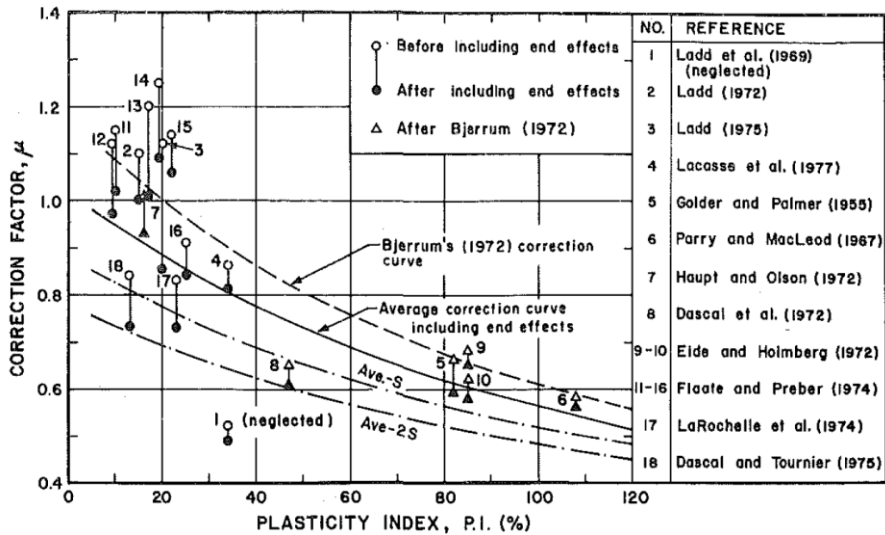


Figure 3.4 Correction factor to adjust FVT measurements (Azzouz et al., 1983). The correction factor is based on back-analyses of failures. Be aware of the considerable uncertainty of the correction factor

A widely used correction for the FVT measurements is suggested by Chandler (1988). This correction is also based on the plasticity index. The Chandler correction depends on the time to failure for the construction for which the correction factor is required (not the time to failure in the FVT). The Chandler (1988) correction corresponds with the correction of Azzouz et al. (1983) for the time to failure of  $10^4$  minutes. The Chandler correction is:

$$\mu_R = 1.05 - b (I_p)^{1/2} \quad \text{with } b = 0.015 + 0.0075 \log t_f \quad (3.16)$$

where:

$I_p$  Plasticity index (%).

$t_f$  Time to failure (min).

In Swedish practice the empirical correction for FVT as proposed by Larsson et al. (1987) and Larsson et al. (2005) is used. Instead of the plasticity index the liquid limit  $w_L$  is applied. The Larsson correction is largely based on high plastic soils, whereas the Bjerrum correction is mainly based on low- and medium plastic clays (Larsson et al., 1987). The lower limit of the Larsson correction is 0.5, which is based on Swedish experience with qualified laboratory investigations on organic soils with very high plasticity. For soils with overconsolidation ratio  $OCR$  larger than 1.3 an additional correction is applied. The FVT correction from Larsson et al. is the product of  $\mu$  and  $\mu_{OCR}$  as follows:

$$\mu = \left(\frac{0.43}{w_L}\right)^{0.45} \geq 0.5 \quad \text{and} \quad \mu_{OCR} = \left(\frac{OCR}{1.3}\right)^{-0.15} \quad (3.17)$$

where:

$w_L$  liquid limit (%).

### Experience in unsaturated soils

Blight (2013) mentions the FVT to determine the shear strength of unsaturated soils. This author presents some cases where the FVT is applied in residual weathered sandstone and mudstone and residual shales. The author states that the remoulded strength of the FVT approximates to the strength of the soil en masse in stiff jointed or fissured soils. Issues

related to the empirical corrections which are based on the experience with saturated soft soils are not mentioned by this author.

### 3.12 Boreholes

Mechanical drillings using the Ackermann sampling system are carried out in accordance with NEN-EN-ISO 22475-1 and BRL SIKB 2100, protocol 2101. The boreholes are carried out as a pulse bore system. Inside the casing samples have been taken each 0.5 m from surface level. The Ackermann sampling tubes are 0.4 m long. The sampling tubes have a diameter of 67 mm. The sampling tubes are pushed into the soil.

Table 3.1 and Table 3.2 give an overview of the boreholes which are performed at Westervoort and Oijen up to now.

### 3.13 Classification tests

The following classification tests are carried out in the laboratory:

- Determination of the bulk volume weight is carried out in accordance with NEN-EN-ISO 17892-2, Geotechnical investigation and testing - Laboratory testing of soil - Part 2: Determination of bulk density. The bulk volume weight of the complete samples from the sampling tubes is determined. The linear measurement method according to the aforementioned ISO standard is used.
- Determination of the gravimetric water content is carried out by drying samples in the oven according to NEN-EN-ISO 17892-1, Geotechnical investigation and testing - Laboratory testing of soil - Part 1: Determination of water content.
- Determination of the Atterberg limits is carried out according to NEN-EN-ISO 17892-12, Geotechnical investigation and testing - Laboratory testing of soil - Part 12: Determination of Atterberg limits. Only test samples consisting of fine soil (primary fraction of clay or silt) are tested. The determination of liquid limit is carried out with the fall cone; 4-point method.
- Determination of the grain size distribution is carried out in accordance with NEN-EN-ISO 17892-4, Geotechnical investigation and testing - Laboratory testing of soil - Part 4: Determination of particle size distribution. Only test samples consisting of fine soil (primary fraction of clay or silt) are tested using sieves from 0.002 mm to 2.0 mm.
- Determination of the specific gravity of the solid is carried out in accordance with NEN-EN-ISO 17892-3, Geotechnical investigation and testing - Laboratory testing of soil - Part 3: Determination of particle density. Only test samples consisting of fine soil (primary fraction of clay or silt) are tested. The liquid pycnometer method is used.
- Determination of the organic matter content is carried out according to NEN-EN-ISO 14688-2, Geotechnical investigation and testing - Identification and classification of soil - Part 2: Principles for a classification. Only test samples consisting of fine soil (primary fraction of clay or silt) are tested. The determination is carried out with hydrogen peroxide as described under NB.2 of NEN-EN-ISO 14688-2 starting from clay as the main soil type.
- Determination of specific surface using a surface area analyser with nitrogen gas (N<sub>2</sub>) as an adsorbate. The Brunauer, Emmett, and Teller (BET) gas adsorption theory (Brunauer et al, 1938) is applied to determine the volume of gas required to form a unimolecular layer of gas on adsorbents and to compute specific surface. Determination of the specific surface area is not covered in the ASTM and NEN-EN-ISO standards. The specific surface can be determined by various instruments and methodologies. To perform the N<sub>2</sub> BET tests the descriptions in Santamarina et al. (2002), Arnepalli et al. (2008) and Akin et al. (2014) are followed.

So far classification tests are conducted on samples of borehole B001 from Oijen and B201 from Westervoort. For each sample (0.4 m) these classification tests are carried out by

Wiertsema & Partners, resulting in profiles with depth of the concerning soil properties. Determination of specific surface is performed on samples of borehole B003 from Oijen and B203 from Westervoort by Delft Solids Solutions.

### 3.14 Determination of shear strength in the laboratory

In order to interpret the shear strength measurements in the field (CPTs and FVTs) different tests to measure shear strength are performed in the laboratory. These tests are conducted on intact samples and on reconstituted samples. Laboratory tests on intact samples are meant to investigate the relationship between water content, suction and shear strength and to verify the measured shear strength in the field. For this goal unconsolidated undrained (UU) triaxial compression tests, direct shear tests and direct simple shear tests are conducted. Other UU triaxial compression tests are performed at TU Delft. The aim of these tests was to determine the relationship between water content, suction and shear strength. This concerns the tests on samples from bore hole B202 (Westervoort) and bore hole B002 (Oijen). The results of the individual tests are given in the factual report (Deltares, 2021b).

The aim of the tests on reconstituted samples is to investigate the causes of the relatively high shear strength which is found by the CPTs and FVTs in the field during winter period when suction is negligible (see Paragraph 4.5). Reconstituted samples are tested with isotropic consolidated undrained (CIU) triaxial compression tests. Reconstituted samples are prepared from a slurry and from moist material. The slurry is made applying a water content corresponding to 1.25 times the liquid limit  $w_L$ . The slurry samples are dried in the air to simulate the effect of ripening of clay, which occurs in nature after sedimentation of clayey material due to interaction with the atmosphere. The slurry samples are dried to different target water contents. After drying the samples are saturated, consolidated and sheared in a triaxial apparatus to simulate saturated conditions like winter conditions in the field. Moist samples are compacted with a Proctor mould and a Proctor hammer according to ASTM D 698 with applying a different number of blows and different water content to get different samples with a range of densities. These moist compacted samples are intended to investigate the effect of compaction on shear strength of dike material when building a dike. After compaction the samples are saturated, consolidated and sheared in a triaxial apparatus to test the samples at saturated conditions like winter conditions in the field.

The reconstituted samples are based on material from borehole B203 from Westervoort, samples 1, 3 and 5, and borehole B003 from Oijen, samples 1, 4, 6, 7, 9 and 10.

#### Triaxial tests

Unconsolidated undrained (UU) triaxial compression tests and isotropic consolidated undrained (CIU) triaxial compression tests are conducted according to NEN-ISO 17892-8 and NEN-ISO 17892-9 respectively. The protocol (Deltares, 2016) is also applied.

UU triaxial tests are performed on intact samples with 67 mm diameter. To test the samples in their intact state the samples are not saturated and not consolidated. With the used triaxial apparatus suction in the samples cannot be measured. Therefore, the influence of suction on measured shear strength with these UU tests have to be interpreted by applying the relationship between water content and suction (retention curve; see Paragraph 3.16). The samples are sheared to 25% axial strain.

CIU triaxial tests are conducted on reconstituted samples. These samples are prepared in the laboratory and are saturated and consolidated in a triaxial apparatus as mentioned above. For the moist compacted tests 67 mm samples are applied. For the tests on the slurry samples 50 mm diameter samples are used to save time with drying and consolidation of the samples.



### **Direct simple shear tests**

Direct simple shear tests are performed according to ASTM D 6528-07 and the Deltares protocol (2016). Direct simple shear tests are performed with constant vertical load, to be able to determine the dilatancy angle.

The samples are tested in their intact state, without saturation and consolidation. Similar to the UU triaxial tests the results of the direct simple shear tests have to be interpreted by using the relationship between water content and suction from the retention curves. The samples are sheared to 40% shear strain.

The intact samples are prepared carefully to place them on the end plates with pins. Because some of the intact samples were very stiff, they could not be prepared to place the sample on the end plates with the pins or the ridges. Therefore, direct shear tests are performed for the very stiff intact samples.

### **Direct shear tests**

Direct shear tests are conducted according to ASTM D 3080. Direct shear tests are performed with constant vertical load, in order to determine the dilatancy angle. Direct shear tests are executed on very stiff samples which could not be tested in the direct simple shear apparatus. Furthermore, the test procedure of the direct shear test is similar to the procedure of the direct simple shear test.

### **Oedometer tests**

Oedometer tests are performed according to NEN-EN-ISO 17892-5 and the Deltares protocol (2016). Oedometer tests are conducted on intact samples and reconstituted samples (slurry). The results of these tests are helpful for the interpretation of the soil behaviour and for the interpretation of the results of the shear strength tests.

## **3.15 Proctor test**

A standard Proctor test is conducted to get insight in the relationship between water content and dry unit weight. The dry unit weight is a measure of the density of the sample which can be achieved given the amount of water in the sample. Water content in the sample has a relationship with suction when the samples become unsaturated and a relationship with shear strength.

The standard Proctor test is performed according to the Dutch code RAW 2015 test 9.0. The Proctor tests are carried out on a mixed sample based on borehole B001 from Oijen, samples 21 - 27 (6,7 kg), and borehole B201 from Westervoort, samples 15 - 19 (5,3 kg). According to the classification tests as reported in Paragraph 4.8 these samples have comparable soil properties. A series of triaxial tests is conducted on reconstituted samples, which are derived from a mixed sample, which is composed in the same way from samples of boreholes B003 and B203. The Proctor test is performed by the laboratory of Wiertsema & Partners.

## **3.16 Determination of retention curves and shrinkage curves**

For unsaturated soils the relationship between water content and suction, the soil water retention curve, is relevant to understand soil behaviour. The retention properties of a series of samples have been investigated with the Hyprop device (Meter Group). The HYPROP consists of a main sensor unit comprising two tensiometers of different lengths. An 80 mm stainless steel ring with a 50 mm height is used for containing the soil sample that is placed on the sensor unit. The entire setup sits on top of a weighing scale to measure the increase or decrease of water content. The air-entry value of the ceramic tips is 880 kPa, but as the

water in shaft cavitates earlier, the maximum suction that can be measured is approximately 100 kPa.

The HYPROP data allows inferring the response of the soil (e.g. with a van Genuchten's model) for both drying and wetting events, which will facilitate the interpretation of the shear strength data, beyond their dependence on the water content.

The HYPROP tests are performed by the geotechnical laboratory of TU Delft. The graphs of the soil water retention curves are in Appendix B.

As the volume of a soil sample changes during drying or wetting the degree of saturation also changes. This behaviour is measured in shrinkage tests. In a shrinkage test the relationship between water content and void ratio is measured. These shrinkage tests are performed by the geotechnical laboratory of TU Delft.

### 3.17 Mercury intrusion porosimetry tests

The pore size distribution (PSD) of 12 samples is determined using mercury intrusion porosimetry (MIP). This technique gives a useful quantitative characterization of microstructure of a soil sample. In the MIP test a sample is immersed in mercury and a pressure is applied to the mercury such that the mercury enters the pores. To perform a MIP test the water that occupies the pores has to be removed because the water will prevent the entry of mercury. Drying the samples is performed with the freeze-drying technique. With the MIP test the entrance diameters of the pores can be detected as the entrance pore diameter, contact angle between mercury and the pore walls and the surface tension of mercury determines the required mercury pressure.

The MIP test is described in ISO 15901-1:2016 and ASTM D 4404-18. The procedures to prepare the samples with freeze drying technique and to perform the MIP tests is derived from Mitchell et al. (2005), Romero et al. (2008), Koliji et al. (2010) and Liu et al. (2015). The MIP tests are performed by Delft Solids Solutions.

Integration on PSD data of the pore volume between the minimum detectable pore size (0.006  $\mu\text{m}$ ) and the delimiting pore size, normalised by solid volume gives the microstructural void ratio. The delimiting pore size is the pore size at the boundary of the PSD function between the region where the macro pores are dominant and where the micro pores are dominant. These void ratios of the macro pores and the micro pores will be used to determine the effective degree of saturation as only the capillary suction in the macro pores contribute to the shear strength.

## 4 Results

### 4.1 Introduction

In this chapter the results of the interpretation of the field and laboratory measurements of the measurement locations Westervoort and Oijen are presented. First a characterisation of the subsoil is given, based on the descriptions of the boreholes, the cone penetration tests and the classification tests. After that the results of the monitoring of volumetric water content, suction and pore water pressure are presented. This data gives insight in the fluctuations of water content, suction and pore water pressure. Based on this data the degree of saturation  $S_r$  is derived. The results of the interpretation of the shear strength measurements in the field and on intact samples in the laboratory are also presented. Suction and degree of saturation are important parameters to explain the shear strength measurements of the intact soil. The results of shear strength measurements on reconstituted samples are also used to explain the results of the shear strength measurements of the intact soil.

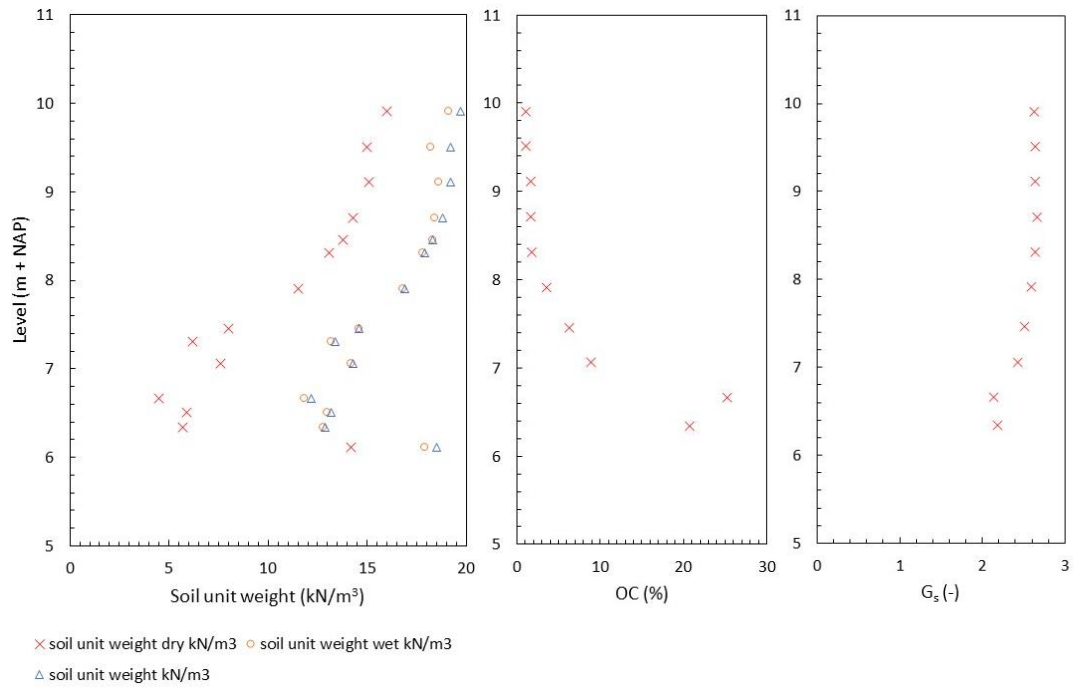
### 4.2 Characterisation of the subsoil

Based on the boreholes with soil descriptions, photos of the samples from the boreholes and the cone penetration tests the stratigraphy of the subsoil is derived. The subsoil at the IJsseldijk at Westervoort consist of about 4.0 m thick Holocene clayey layers and sandy clay layers. These clayey layers lie on top of the Pleistocene sand layer (at NAP +6.30 m). The results of the particle size distributions show that the Holocene cover layer get less clayey from the bottom to the top. The silt and sand content increases from the bottom to the top of this layer. This compares with the trends of the soil unit weight and Atterberg limits. The first meter at the bottom of the cover layer is much more organic than the overlying soil.

The gravimetric water content  $w$  at the bottom part of the cover layer is close to the liquid limit  $w_L$ , while the gravimetric water content at the top of the cover layer is close to the plastic limit  $w_P$ . This means that the soil at the top of the cover layer is relatively dry. This compares with the brown color of the top clay layer at the photos of the boreholes, which indicates oxidation of this clay.

The descriptions of the boreholes are presented in Appendix A for the location Westervoort and the location Oijen. More results of the site investigations are given in the factual report (Deltares, 2021b).

The results of the classification tests as performed on the samples from borehole B201 at Westervoort are summarized in Figure 4.1 - Figure 4.3.



(a) (b) (c)  
 Figure 4.1 Profiles of (a) soil unit weight, (b) organic content (OC) and (c) specific gravity of the soil particles ( $G_s$ ) against depth from borehole B201 at Westervoort

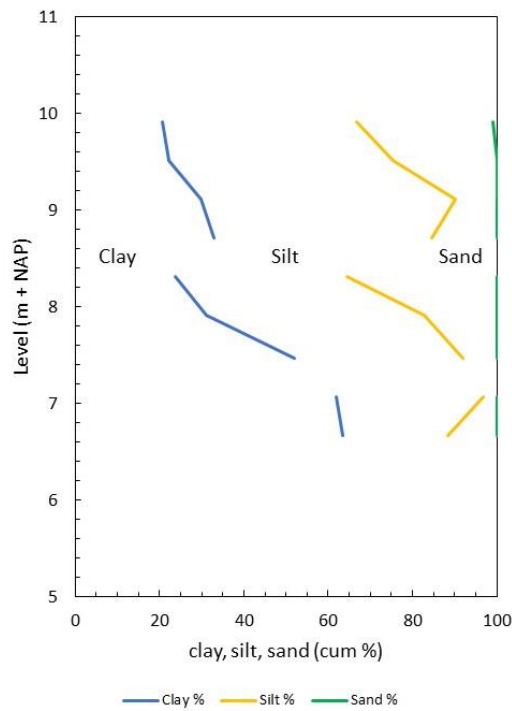
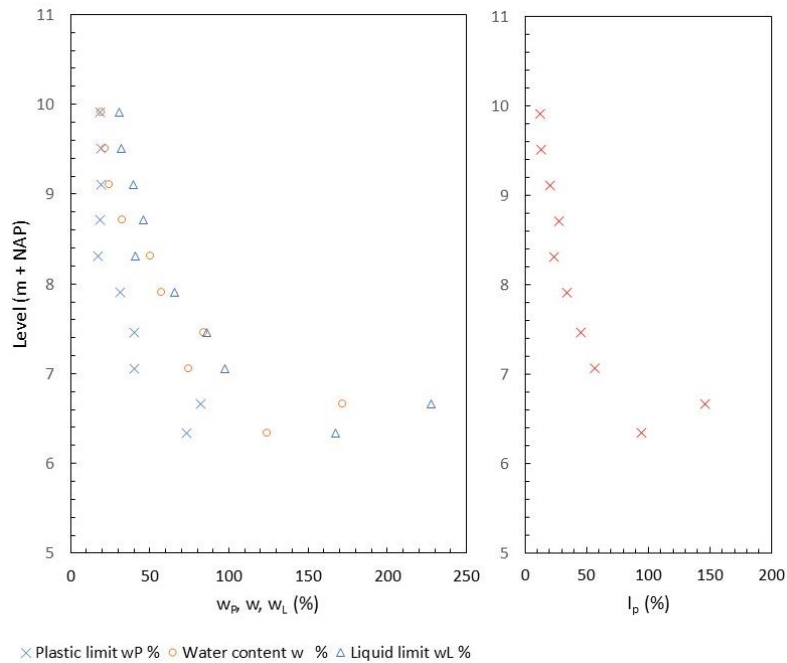


Figure 4.2 Profile of clay, silt and sand content against depth from borehole B201 at Westervoort



(a) (b)  
 Figure 4.3 Profiles of (a) plastic limit  $w_P$ , liquid limit  $w_L$  and gravimetric water content  $w$  and (b) plasticity index  $I_p$  against depth from borehole B201 at Westervoort

The subsoil at the Maasdijk at Oijen consist of 1.7 to 5.8 m thick Holocene clay layers and sandy clay layers on top of the Pleistocene sand layer. The top of the Pleistocene sand layer varies between NAP -0.70 m to NAP -4.80 m, within the measurement site. This variation of the top of the Pleistocene sand layer and the thickness of the Holocene clay layers will be related to the pond, as discussed in Paragraph 2.2. The top of the Holocene cover layer may be around NAP +3.0 m or NAP +4.0 m. The new dyke is built from clay and sandy clay. Between NAP +3.90m and NAP +5.65 m some sandy layers or sandy inclusions are observed in bore holes B001 and B003. The particle size distribution show that the clay, silt and sand content vary randomly in the dyke material. This variation is confirmed by the soil unit weights and the Atterberg limits.

From NAP +5.5 m and upwards the gravimetric water content moves towards the plastic limit, indicating that the soil becomes dryer towards the surface level. The photo of the samples of the borehole show brown clay from NAP +6.5 m.

The results of the classification tests as performed on the samples from borehole B001 at Oijen are summarized in Figure 4.4 – Figure 4.6.

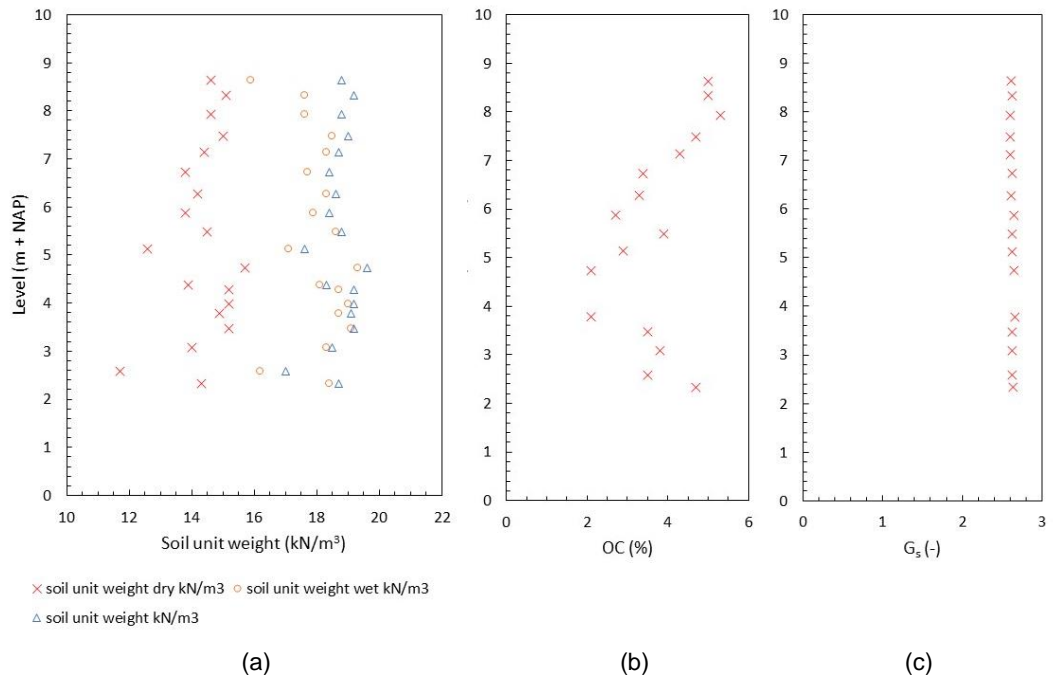


Figure 4.4 Profiles of (a) soil unit weight, (b) organic content (OC) and (c) specific gravity of the soil particles (G<sub>s</sub>) against depth from borehole B001 at Oijen

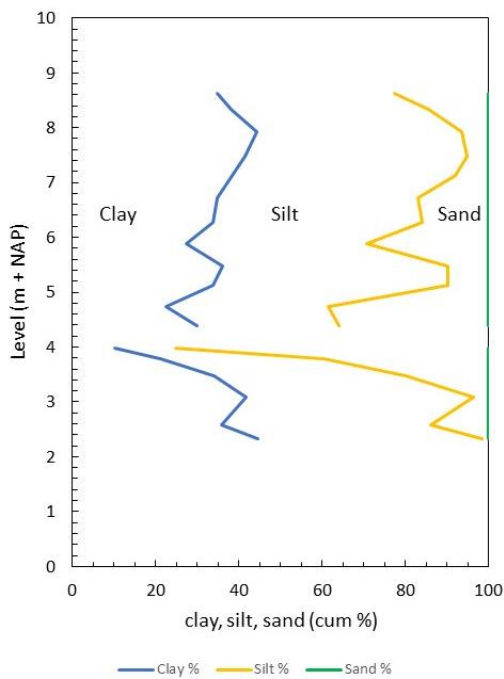


Figure 4.5 Profile of clay, silt and sand content against depth from borehole B001 at Oijen

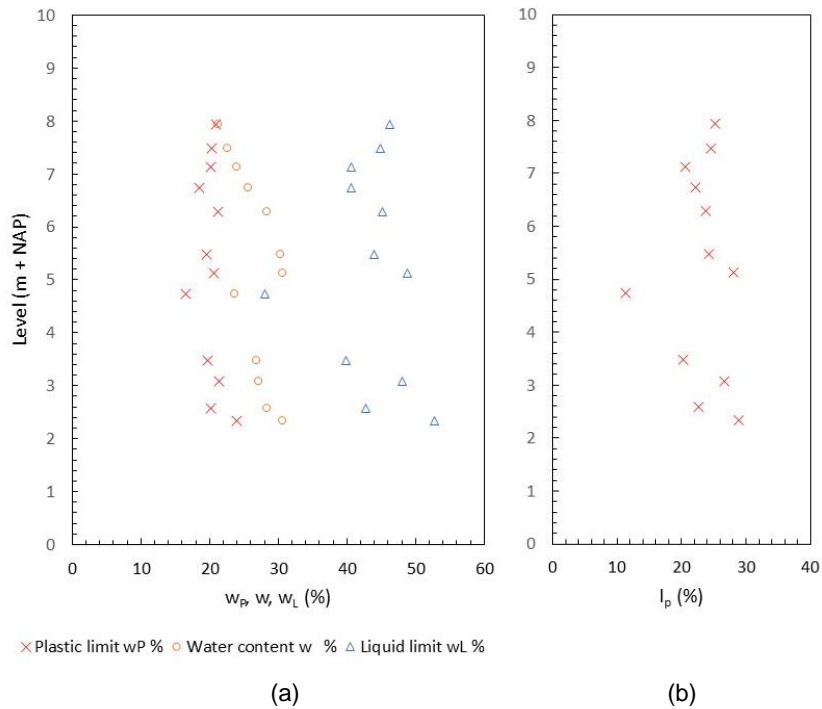


Figure 4.6 Profiles of (a) plastic limit  $w_P$ , liquid limit  $w_L$  and gravimetric water content  $w$  and (b) plasticity index  $I_p$  against depth from borehole B001 at Oijen

### 4.3 Micro-structure of the soil

Specific surface of six intact clay samples and six reconstituted clay samples is determined using the  $N_2$  BET method (determination of specific surface using nitrogen gas ( $N_2$ ) following Brunauer, Emmett, and Teller (BET) gas adsorption theory; see Paragraph 3.13). The results of these tests are presented in Table 4.1 and Table 4.2. On the same samples the pore size distribution (PSD) is determined using mercury intrusion porosimetry (MIP). The PSD's give the volume of pores for a range of pore diameters in the samples. The PSD's are used to derive the microstructural void ratio  $e_m$ , which is used to calculate the effective degree of saturation  $S_{rM}$ . The PSD's are given in Figure 4.7 to Figure 4.10. More results of the laboratory tests are given in the factual report (Deltares, 2021b).

Table 4.1 Specific surface of intact samples determined with  $N_2$  BET method

Location	Borehole	Sample	Level (NAP + m)	$\rho_{i,dry}$ (kg/m <sup>3</sup> )	Water content $w_i$ (-)	Specific surface $S$ (m <sup>2</sup> /g)
Wester-voort	B203	15	9.79 – 9.66	1606	0.170	7.13
	B203	17	8.98 – 8.85	1541	0.264	22.10
	B203	21	7.82 – 7.64	999	0.619	19.90
Oijen	B003	3	8.38 – 8.26	1644	0.156	23.60
	B003	5	7.52 – 7.39	1534	0.254	20.80
	B003	11	4.97 – 4.85	1544	0.277	17.10

Table 4.2 Specific surface of reconstituted samples determined with N<sub>2</sub> BET method

Sample	$\rho_{i,dry}$ (kg/m <sup>3</sup> )	Water content $w_i$ (-)	Water content $w_e$ (-)	Specific surface S (m <sup>2</sup> /g)
1	1533	0.250	0.234	10.8
3	1490	0.280	0.254	13.0
5	1589	0.200	0.238	14.5
8	1783	0.170	0.206	10.8
9	1472	0.300	0.298	11.3
11	1690	0.200	0.223	13.1

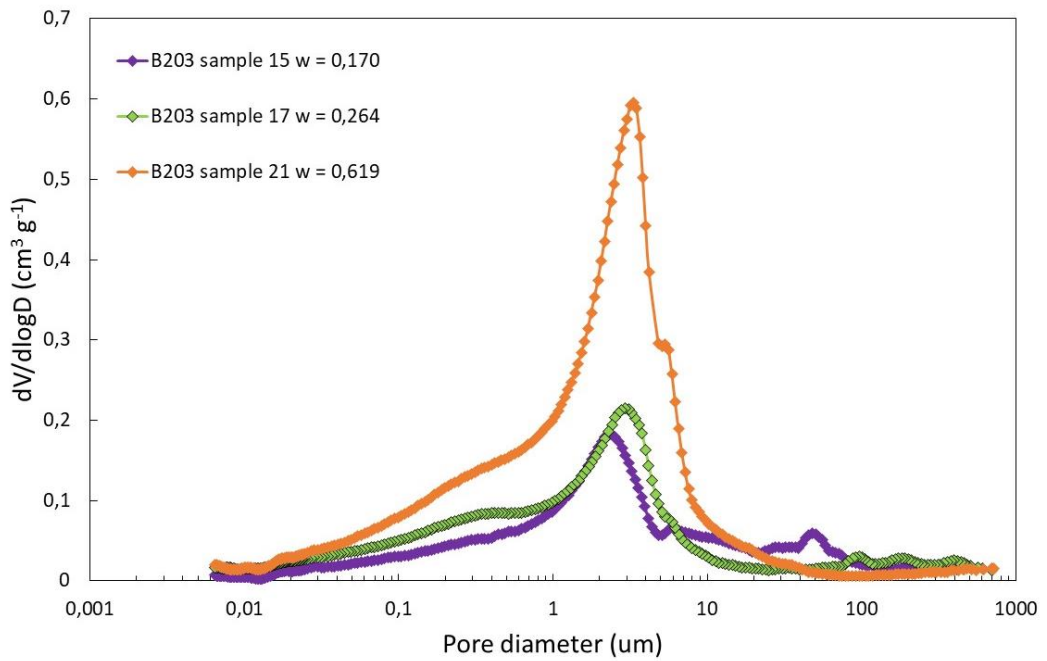


Figure 4.7 Pore size distributions of three samples from Westervoort (bore hole B203). The water content of the samples is given in the legend. The discriminating pore size between the micro pores and macro pores is chosen at 0.6  $\mu\text{m}$



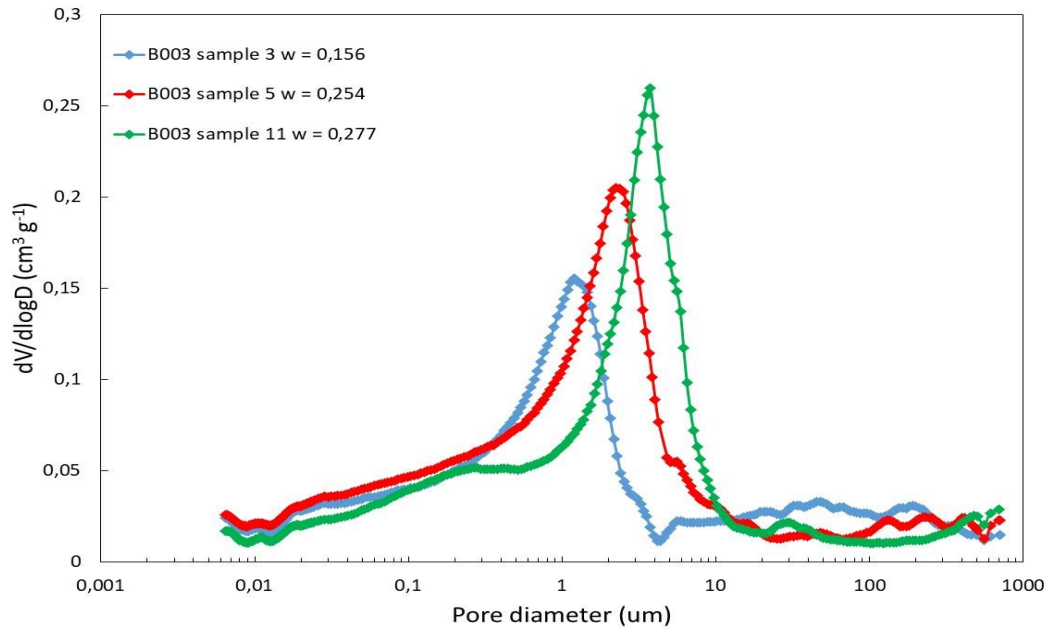


Figure 4.8 Pore size distributions of three samples from Oijen (bore hole B003). The water content of the samples is given in the legend. The discriminating pore size between the micro pores and macro pores of the samples 3, 5 and 11 is chosen at 0.25, 0.4 and 0.6  $\mu\text{m}$  respectively

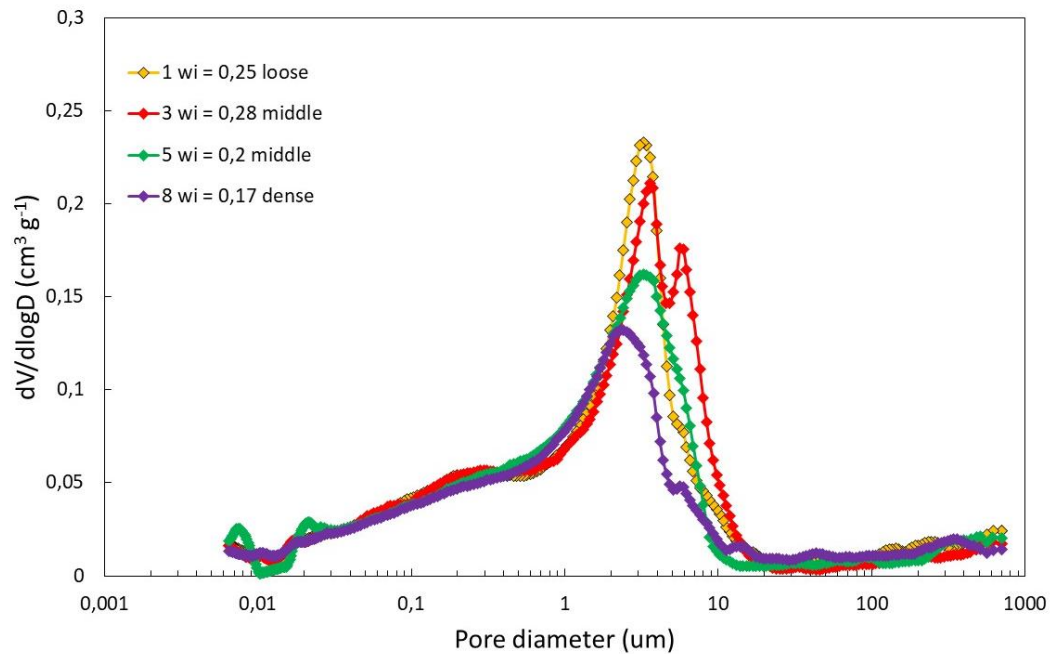


Figure 4.9 Pore size distributions of four reconstituted samples, which are prepared with different water contents and compacted with the Proctor hammer with different amount of energy. The water content of the samples is given in the legend. The discriminating pore size between the micro pores and macro pores is chosen at 0.5  $\mu\text{m}$

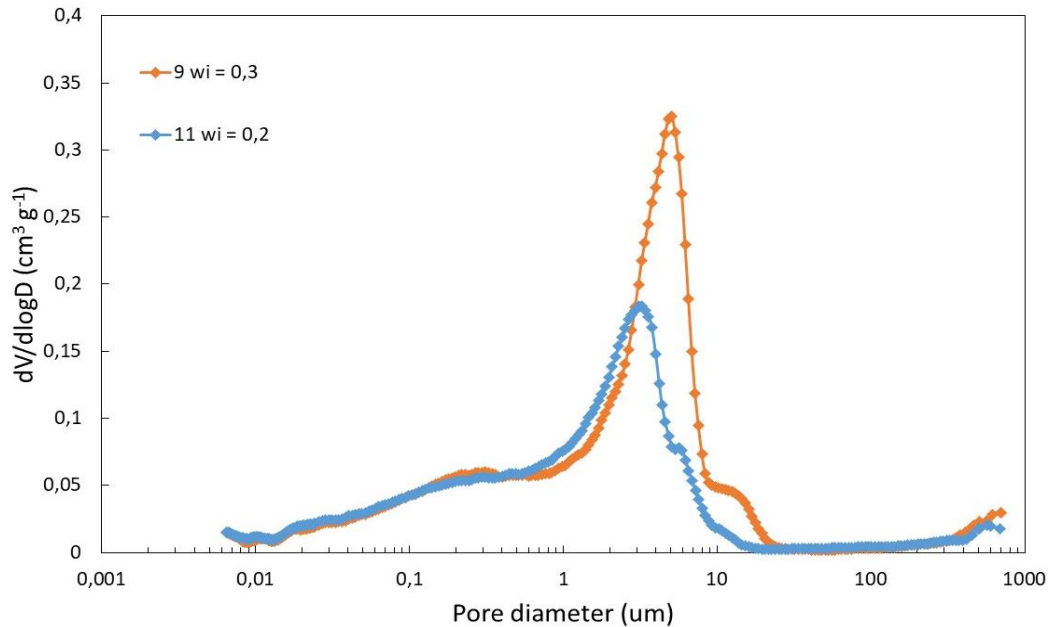


Figure 4.10 Pore size distributions of two reconstituted samples, which are prepared as a slurry and are dried in the air to different water contents. The water content of the samples is given in the legend. The discriminating pore size between the micro pores and macro pores of the samples 9 and 11 is chosen at 0.9 and 0.6  $\mu\text{m}$  respectively

All samples in Figure 4.7 to Figure 4.10 show a predominant contribution of pores between approximately 0.3  $\mu\text{m}$  and 20  $\mu\text{m}$ , but the smaller pore diameters are also relatively well represented. All samples also still show a small contribution at 0.006  $\mu\text{m}$  indicating that smaller pores are present in the samples. These smaller pores can not be detected in a MIP test. Pores with a diameter larger than about 20  $\mu\text{m}$  are not much present. As can be seen in Figure 4.7 to Figure 4.10 the size and shape of the peak in the PSD's changes dependent on water content and compaction of the samples.

To determine the microstructural void ratio  $e_m$  the PSD's are integrated. As a discriminating pore size between the micro pores and the macro pores the pore size at the toe at the left-hand side of the peak in the PSD's is chosen. Integration of the PSD's between the minimum measured pore sizes and the discriminating pore sizes, normalized by the solid volumes gives the microstructural void ratios of the samples (Romero et al., 2011). In Figure 4.11 and Figure 4.12 the microstructural void ratio  $e_m$  and total void ratio  $e$  of the intact samples and reconstituted samples as derived from the PSD's are plotted against water ratio  $e_w$ .

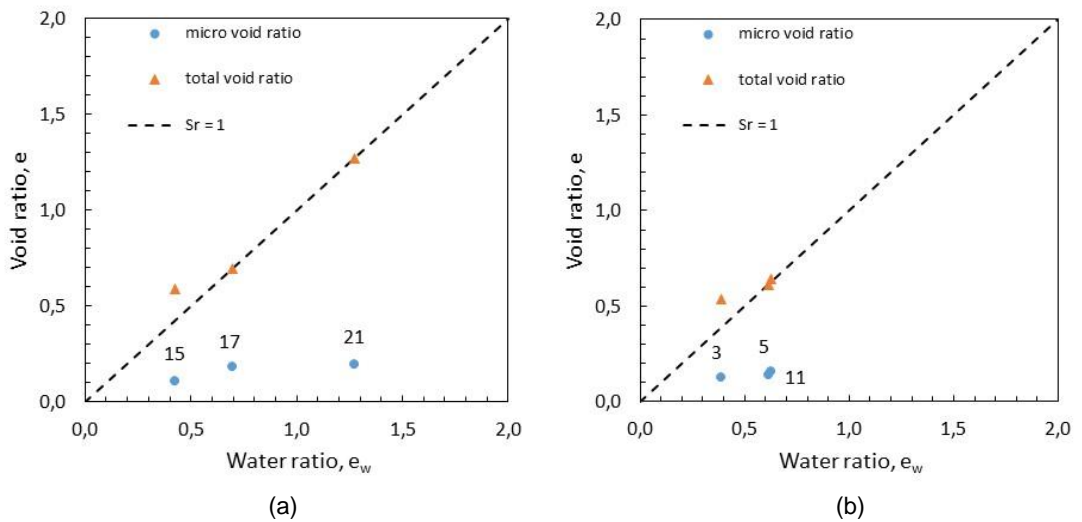


Figure 4.11 Microstructural void ratio  $e_m$  and total void ratio  $e$  against water ratio  $e_w$  of (a) Westervoort (B203) and (b) Oijen (B003). The sample numbers are mentioned beside the derived values

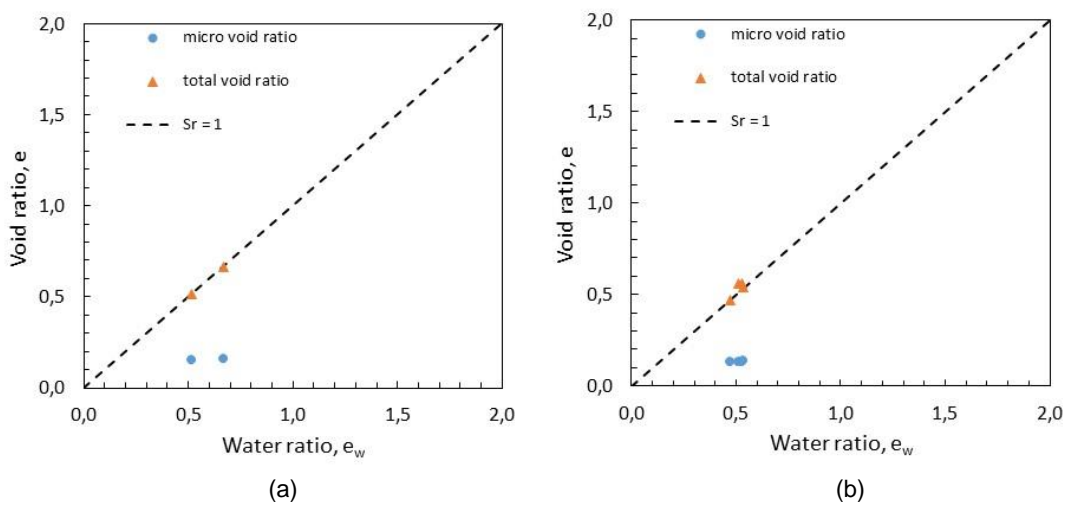


Figure 4.12 Microstructural void ratio  $e_m$  and total void ratio  $e$  against water ratio  $e_w$  of (a) air dried slurry samples and (b) dry compacted samples

Figure 4.11 and Figure 4.12 show a more or less constant microstructural void ratio  $e_m$  independent of the water ratio  $e_w$ . Romero et al. (2011) investigated different soils and found a decreasing microstructural void ratio  $e_m$  when water ratio  $e_w$  decreases. The value of the water ratio  $e_w$  at the intersection of the microstructural void ratio  $e_m$  with the  $S_r = 1$  line is the water ratio at which all micro pores are fully saturated and all macro pores are empty. This value of the water ratio is called the microstructural water ratio  $e_{wm}$  (Tarantino et al., 2013). Assuming a microstructural void ratio  $e_m$  independent of the water ratio  $e_w$  the microstructural water ratio  $e_{wm}$  is found as follows:

- Oijen: 0.14.
- Westervoort below NAP +9.0 m: 0.19.
- Westervoort above NAP +9.0 m: 0.10.

For Westervoort the microstructural water ratio  $e_{wm}$  is differentiated, because above NAP +9.0 m the clay has relatively high soil unit weights and low plasticity index compared to the soil layers below NAP +9.0 m (see Paragraph 4.2).

In Figure 4.13 the microstructural water ratio  $e_{wm}$  is plotted against the specific surface  $S_{BET}$  of the intact samples from Westervoort and Oijen and the air dried slurry samples and the dry compacted samples. The results are compared with the upper bound and lower bound of the correlation as given by Romero et al. (2011). The comparison shows that the results for Westervoort and Oijen are relatively low compared to the correlation of Romero et al.

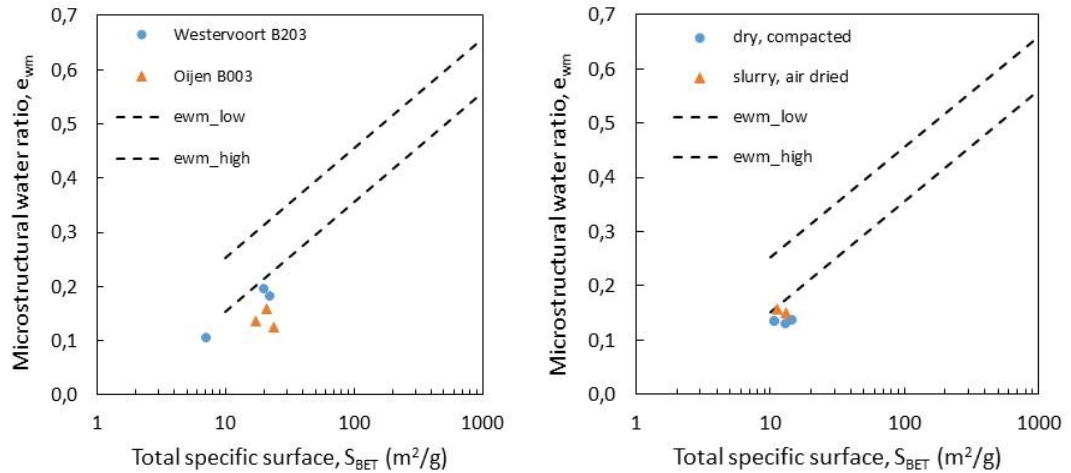


Figure 4.13 Microstructural void ratio  $e_m$  plotted against total specific surface  $S_{BET}$  of (a) the intact samples from Westervoort and Oijen and (b) the air dried slurry samples and the dry compacted samples. The dashed lines are the upper and lower bound as found by Romero et al. (2011).

#### 4.4 In situ water content, degree of saturation and suction stress

Volumetric water content  $\theta$  is measured at the locations Westervoort and Oijen. The type of the applied sensors and the locations of the sensors are described in Paragraph 3.6. From the volumetric water content the gravimetric water content  $w$  and degree of saturation  $S_r$  are calculated, using the soil unit weight  $\gamma$  and specific gravity  $G_s$  as discussed in Paragraph 4.2. As described in Paragraph 3.7 suction stress  $s$  is also measured at the measurement sites. The type of the applied sensors and the locations of the sensors are described in Paragraph 3.7.

Figure 4.14 and Figure 4.15 present the gravimetric water content, degree of saturation and suction stress at Westervoort and Oijen. The values between brackets in the legends are the positions of the sensors below surface level. During the dry summer period in 2020 four tensiometers became outside their measurement range (suction > 80 kPa). The porous filters of the sensors then become unsaturated. Therefore, the measurements of these sensors are not reliable anymore and are therefore not presented for the period August 2020 to April 2021.

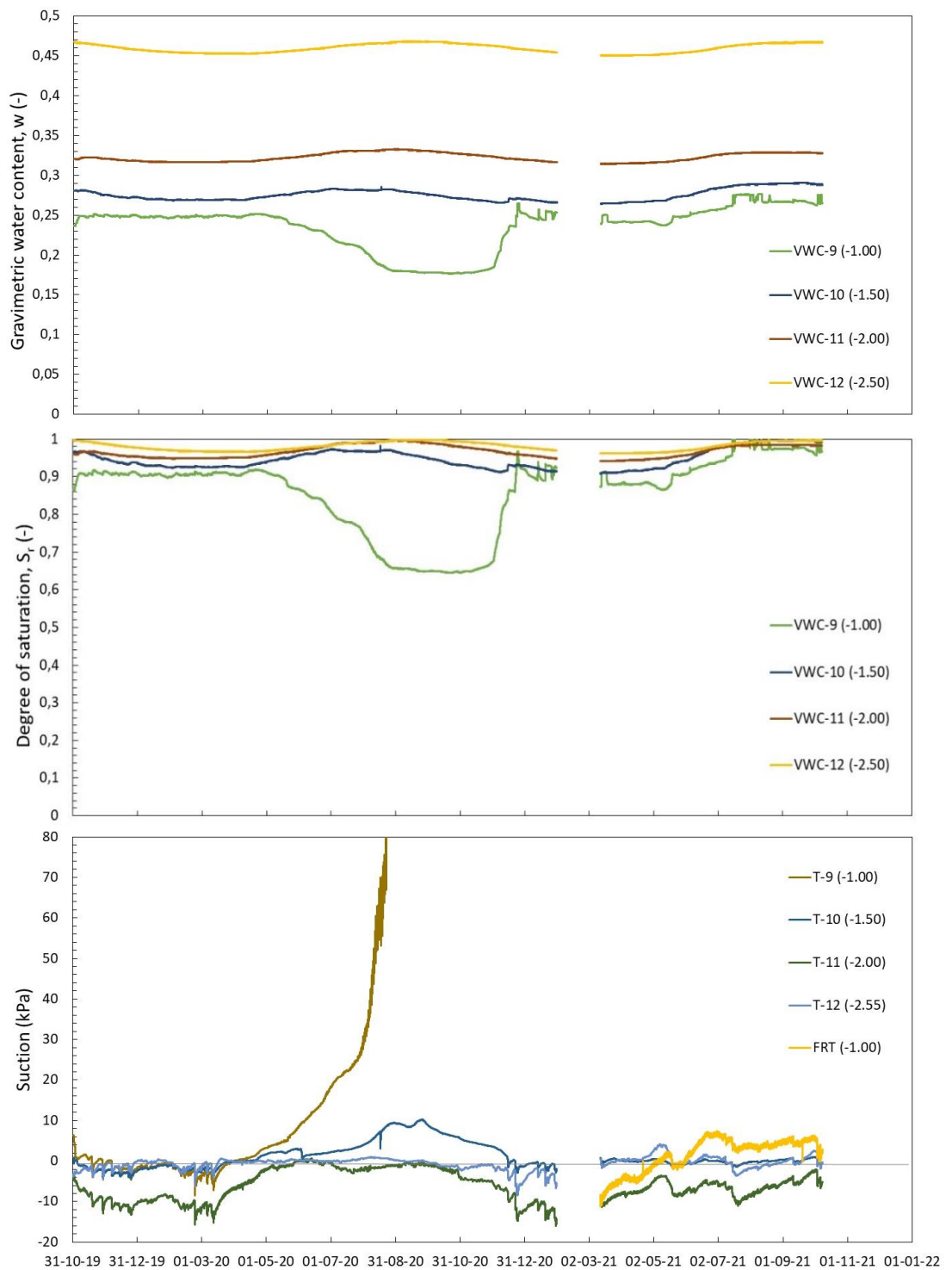


Figure 4.14 Gravimetric water content  $w$ , degree of saturation  $S_r$  and suction stress  $s$  at Westervoort at the inner berm

VWC-9 and T-9 in Figure 4.14, which are the shallowest sensors at 1.0 m below surface level, show the largest fluctuations of water content, degree of saturation and suction. During summer of 2020 water content decreases and suction increases. The minimum and maximum values respectively are reached at the end of the summer and beginning of the autumn, which will reflect the interaction with the atmosphere. During summer period 2020

the shallowest sensors reach suction values from 30 kPa and beyond 80 kPa. The sensors at 1.5 m depth reach suction values between 10 and 40 kPa. In 2021 the effect of evaporation in summer is much less than in 2020. For all suction sensors at Westervoort suction has become negative in winter period in Figure 4.14 implying positive pore water pressures. So, the level of the phreatic surface is in winter period above the sensors. The results of the measurements of the deeper sensors at Westervoort show overall a relatively constant water content, degree of saturation and suction. Interestingly during a large part of 2020 the deeper sensors show the maximum water content and degree of saturation when the shallow sensors have their minimum values.

The water content sensors VWC-1, VWC-2 and VWC-3 at Oijen in Figure 4.15 show some fluctuations in the first two weeks after installation of the sensors. These fluctuations can at least partly be attributed to installation effects, due to adding water to the bentonite by which the boreholes are filled after installation of the sensors. At October 11, 2019 again water is added to the bentonite in the boreholes. The sensors respond to that action. It seems that the measurement results are reliable from the end of October 2019. The shallow sensor VWC-1 shows the same behaviour as the shallow sensors at Westervoort, with decreasing water content during summer and reaching the minimum values at the end of the summer and beginning of the autumn. VWC-1 and VWC-2, which are the shallowest sensors, also show fluctuations from November and December 2019 and beyond. From February 2020 similar fluctuations are present for the deeper sensor VWC-3. In this period the sensors show an increasing trend. Likely these fluctuations are induced by precipitation. During the second part of the winter and in spring 2020 VWC-4 measured a clearly higher water content compared to the rest of the year. Sensor VWC-3 at 2.4 m below surface level gives degrees of saturation close to 1.0 over the whole measurement period. Sensor VWC-4 at 3.1 m below surface level gives remarkably more variations than VWC-3. This is possibly caused by sandy layers or sandy inclusions in the dyke (see also the explanation of Figure 4.17). In 2021 there were fewer fluctuations than in 2020.

Just as the water content sensors the suction sensors T-2 and T-3 at Oijen in Figure 4.15 show firm fluctuations in the first two weeks after installation of the sensors and after adding water at October 11, 2019. During October 2019 the sensors T-2, T-3 and T-4 show a continuous increase of suction stress. In this period the sensors move towards an equilibrium with the surrounding soil. It seems that the measurement results of the sensors T-2, T-3 and T-4 are reliable from the end of November 2019, as the increase of the previous period has stopped, and the sensors seem to respond to precipitation. Sensor T-1 show a rapid drop to negative suction in the last part of November and in December 2019. This means that fully saturation and positive water pressure is reached. This implies a phreatic surface in de top of the dyke. In December 2019 and January and February 2020 the suction of the other sensors also declined to lower values, but these values are still positive (suction 1-4 kPa). For sensors T-2 and T-4 this declination of suction also occurred rapidly. Only a few days in March 2020 all sensors show negative suction values (pressure) and thereafter suction starts to increase again in spring 2020. The shallow sensor T-1 shows a very rapid increase of suction in the end of May 2020 and exceeds the measurement range of 80 kPa. Sensor T-2 exceeds the measurement range in August 2020. Suction in the other two sensors stays below 10 kPa. The suction values in 2021 are very low compared to 2020.

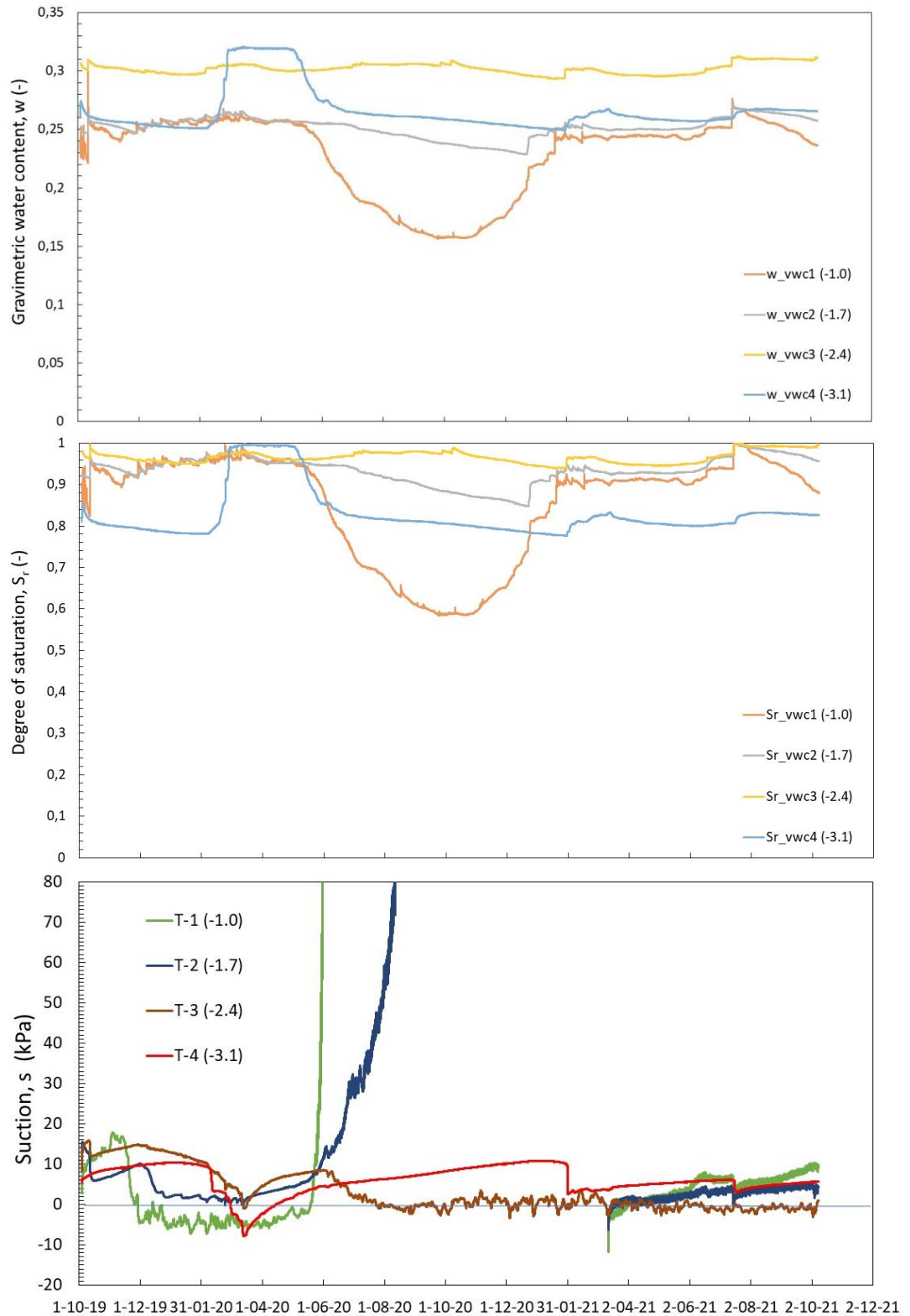


Figure 4.15 Gravimetric water content  $w$ , degree of saturation  $S_r$  and suction stress  $s$  at Oijen

Figure 4.16 and Figure 4.17 give an overview of degree of saturation, suction and pore water pressure against depth. The degree of saturation is based on the measurements in the field with the four water content sensors at six time steps (plotted with solid lines in the figures). These six time steps are distinctive points in the time series in Figure 4.14. Additionally two series of determinations of degree of saturation in the laboratory from two time steps are

plotted (plotted with markers in the figures). These values are derived from samples from two bore holes at both measurement sites, which are conducted at different moments. Profiles of suction and pore water pressure are presented for the same time steps as the degree of saturation. Descriptions of the bore holes with the markers for the lowest, highest and actual phreatic surface are also given. Figure 4.16 gives the data of Westervoort and Figure 4.17 gives the data of Oijen.

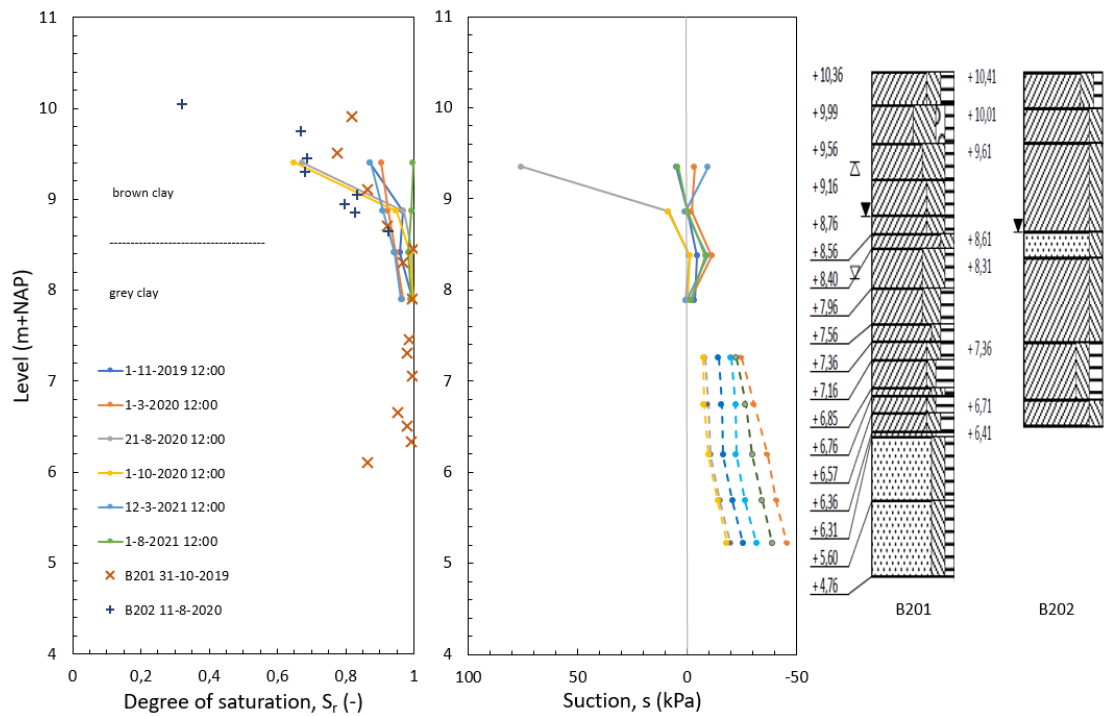


Figure 4.16 Profiles of degree of saturation  $S_r$  and suction stress  $s$  (pore water pressure in the saturated zone when  $s$  is negative) at Westervoort at the inner berm. The description of the subsoil based on two bore holes is also given

The profiles of degree of saturation and suction show in summer and autumn 2020 a remarkable gradient towards the surface. Below NAP +8.50 m degree of saturation is close to 1.0. Above NAP +8.50 m degree of saturation fluctuates in time. The in-situ measurements of degree of saturation (lines) and laboratory measurements of degree of saturation (crosses) in Figure 4.16 compare with each other. The boundary of NAP +8.50 m coincides with the boundary between brown oxidized clay and grey clay as observed in the bore holes. When degree of saturation is low in the shallowest sensor at NAP +9.40 m suction is high. When degree of saturation is high in the shallowest sensor suction is somewhat noisy. The suction sensors at NAP +8.87 m and NAP +7.90 m show relatively little fluctuations. The fluctuations in the suction sensor at NAP +8.41 m however seem to follow the fluctuations of the pore water pressure in the deeper part of the Holocene subsoil and the aquifer (below NAP +6.40 m). Possibly the sandy layer at NAP +8.50 m influences suction at NAP +8.41 m.



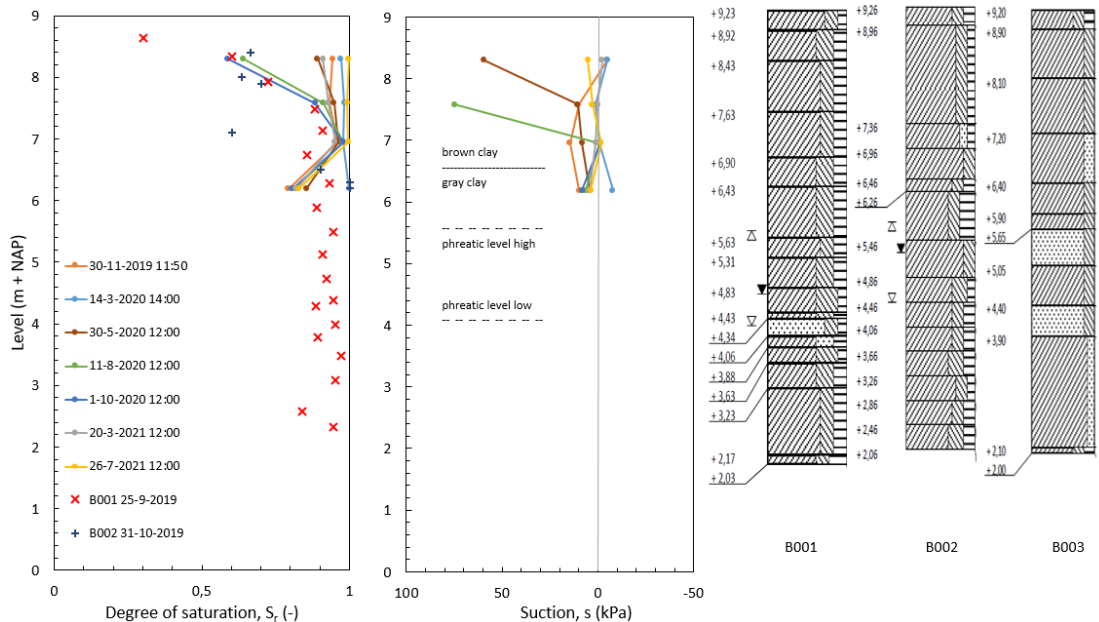


Figure 4.17 Profiles of degree of saturation  $S_r$  and suction stress  $s$  (pore water pressure when  $s$  is negative) at Oijen. The description of the subsoil based on three bore holes is also given

At Oijen the degree of saturation and suction also show a strong gradient towards the surface. At NAP +7.0 m degree of saturation shows only small variations close to 1.0. Suction at NAP +7.0 m reached values up to 20 kPa, suggesting that degree of saturation could have been lower than 0.95. The description of the subsoil from the bore holes shows differences in soil profile. This heterogeneity may explain the differences between the measurements at the sensors. The water content sensor at NAP +6.19 m show larger variations in degree of saturation than the sensor at NAP +6.95 m. This is possibly caused by sandy layers or sandy inclusions in the dyke. The overall trend of the data suggest that influence of precipitation and evaporation will reach a depth up to 2.5 m below the surface. At this level the soil descriptions and photo from the bore holes give a boundary between brown and grey clay. However, at larger depths also brown coloration is observed, possibly due to the sandy layers.

#### 4.5 Correlation between CPT, FVT and laboratory tests

Cone penetration tests (CPT), field vane tests (FVT), unconsolidated undrained (UU) triaxial tests, direct shear tests (DS) and direct simple shear tests (DSS) are conducted to determine the in-situ shear strength. Backgrounds of these tests can be found in Chapter 3. As described in Paragraph 3.5 CPTs class 2 are performed for a first investigation of the sites. CPTs class 1 are executed to measure the in-situ shear strength. Results of UU and CU triaxial compression tests on intact samples are presented in Table 4.3. Results of DSS and DS tests on intact samples are presented in Table 4.4. More results of the laboratory tests are given in the factual report (Deltares, 2021b).

Table 4.3 Results of UU and CU triaxial compression tests on intact samples

Location	Bore-hole	Sample	Level (NAP + m)	$\rho_{i,dry}$ (kg/m <sup>3</sup> )	Water content $w_i$ (-)	$\sigma_v$ (kPa)	$\tau_{max}$ (kPa)	$\tau_{ult}$ (kPa)
Westervoort	B202	1	10.05	--	0.077	10	335.0	195.0
	B202	2	9.75	--	0.130	10	260.0	165.0
	B202	3-1 (CU)	9.45	--	0.267	10	45.5	44.0
	B202	3-2	9.30	--	0.188	10	105.0	105.0
	B202	4-1 (CU)	8.85	--	0.278	10	48.0	46.5
	B202	4-2	8.95	--	0.164	10	280.0	165.0
	B202	4-3	9.05	--	0.238	10	75.0	75.0
	B202	5	8.65	--	0.202	10	97.5	97.5
	B203	15	9.79 – 9.66	1606	0.170	11.0	99.3	73.0
	B203	17	8.98 – 8.85	1541	0.264	25.7	56.3	56.0
	B203	21	7.82 – 7.64	999	0.619	45.2	20.4	17.0
	Oijen	B002	1	9.10	--	0.145	15	237.5
B002		3	8.40	--	0.127	15	330.0	207.5
B002		4-1	8.00	--	0.186	15	130.0	130.0
B002		4-2 (CU)	7.90	--	0.263	15	82.5	82.5
B002		6	7.10	--	0.184	40	87.5	87.5
B002		7	6.50	--	0.208	40	157.5	155.0
B002		8-1	6.20	--	0.357	40	35.0	35.0
B002		8-2	6.30	--	0.335	40	60.0	60.0
B003		3	8.38 – 8.26	1644	0.156	15.0	131.5	110.0
B003		5	7.52 – 7.39	1534	0.254	31.1	86.7	80.0
B003		11	4.97 – 4.85	1544	0.277	73.0	73.8	73.8

Table 4.4 Results of direct simple shear (DSS) tests and direct shear (DS) tests on intact samples

Location	Bore-hole	Sample	Level (NAP + m)	$\rho_i$ (kg/m <sup>3</sup> )	Water content $w_i$ (-)	$\sigma_v$ (kPa)	$\tau_{max}$ (kPa)	$\tau_{ult}$ (kPa)
Westervoort	B203	14 (DS)	9.70 – 9.65	1790	0.132	11.0	68.9	19.0
	B203	16	8.85 – 8.80	1928	0.266	26.0	22.8	20.0
	B203	20	7.70 – 7.65	1650	0.607	44.1	25.5	25.3
Oijen	B003	2 (DS)	8.50 – 8.45	1608	0.137	9.0	102.1	77.3
	B003	4	7.25 – 7.20	1860	0.245	29.1	31.2	29.0
	B003	8	6.10 – 6.05	1940	0.256	51.1	34.3	33.0
	B003	10	5.02 – 5.00	1950	0.274	73.2	46.5	46.3

Figure 4.18 - Figure 4.21 present the results of the FVT, CPT (class 1) and laboratory tests of the location Westervoort. The FVT corrections using the Chandler (1988) correction with plasticity index  $I_p$  and the Larsson et al (1987, 2005) correction with liquid limit  $w_L$  are applied as presented in Paragraph 3.11. For the Chandler correction a time to failure  $t_f$  of 360 min is applied. The Atterberg limits which are used for the FVT corrections are presented in Paragraph 4.2. The shear strength is derived from the CPTs using ( $s_u = \frac{q_c - \sigma_v}{N_k}$ ). The pore water pressure  $u_2$  is not incorporated in this analysis, as  $u_2$  is not measured with the class 1 CPTs, because the reliability of the  $u_2$  measurements in the unsaturated zone is questionable. For the CPT interpretation an average soil unit weight of 18.0 kN/m<sup>3</sup> is assumed. A  $N_k$  value of 11.0 is used to fit the CPT data to the FVT results when using the Chandler correction. In combination with the Larsson et al correction a  $N_k$  value of 12.0 is found (see Figure 4.18). For each FVT at the four specific testing moments this single  $N_k$  values on average agree well with the CPTs, independent of the height of the shear strength and the actual suction. Regarding the UU triaxial tests the  $N_k$  value seem to fit better with the peak shear strength than with the ultimate shear strength (25% axial strain), at least for the very high shear strength in the top layer (Figure 4.19).

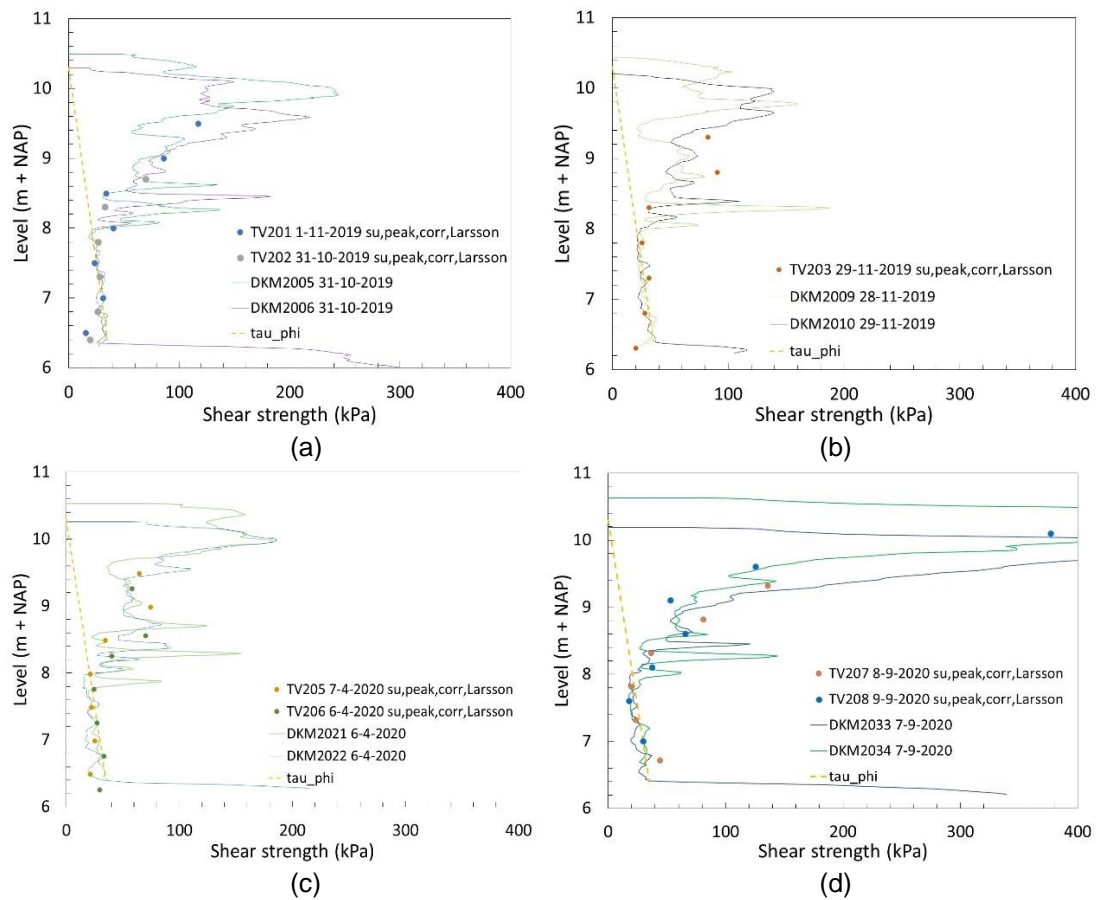


Figure 4.18 Comparison between FVT and CPT (class 1) results of location Westervoort at four testing moments during the measurement period

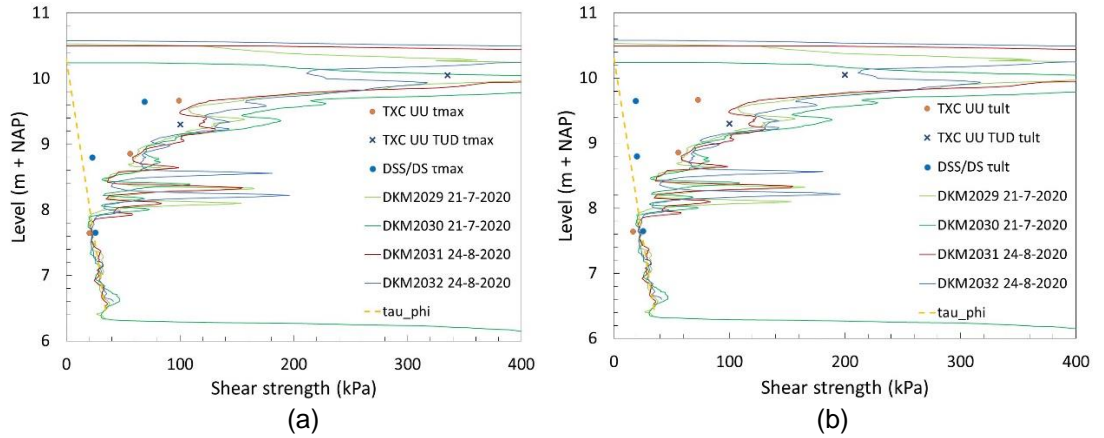


Figure 4.19 Comparison between shear strength derived from UU triaxial tests, direct shear tests and direct simple shear tests with shear strength derived from CPT's at location Westervoort: (a) for peak deviator stress and (b) for deviator stress at ultimate state (25% axial strain and 40% shear strain)

Using the  $N_k$  value of 12.0 Figure 4.20 and Figure 4.21 shows the derived shear strength from the CPTs. Because of the large number of CPTs to be presented and because of the fact that the CPTs are conducted in duplo each time the even numbers of the CPTs are presented in Figure 4.20 and the odd numbers are presented in Figure 4.21.

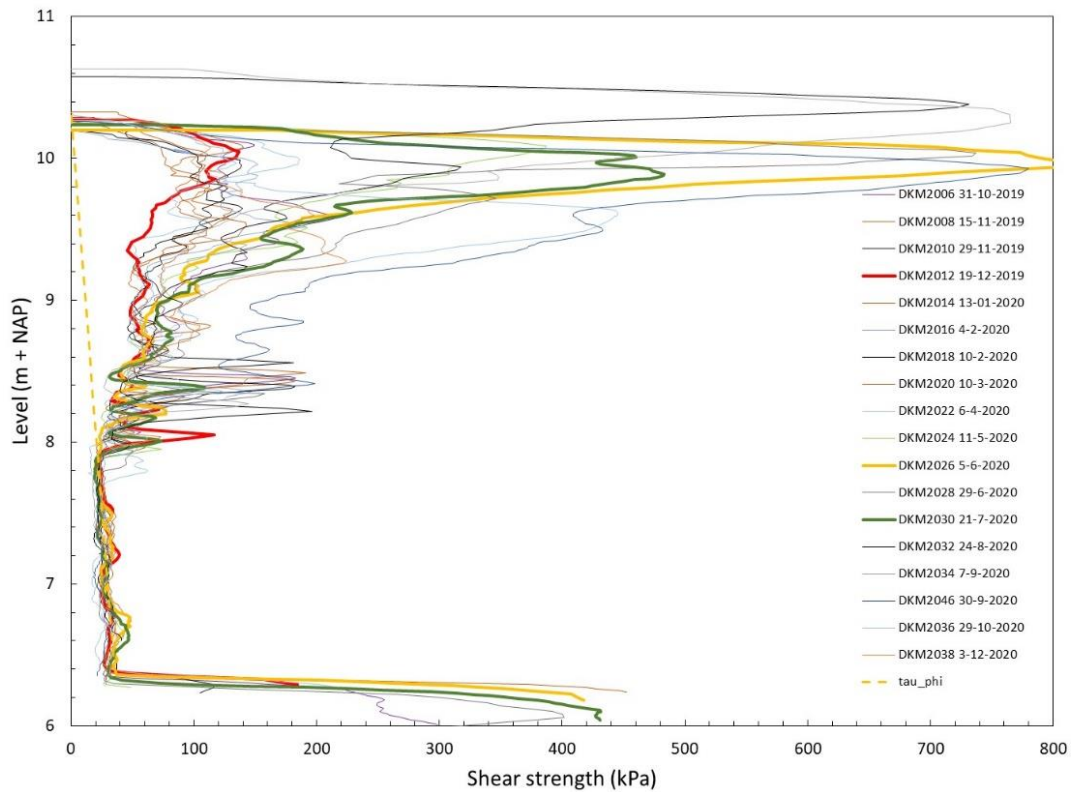


Figure 4.20 CPT (class 1, even numbers) results of location Westervoort

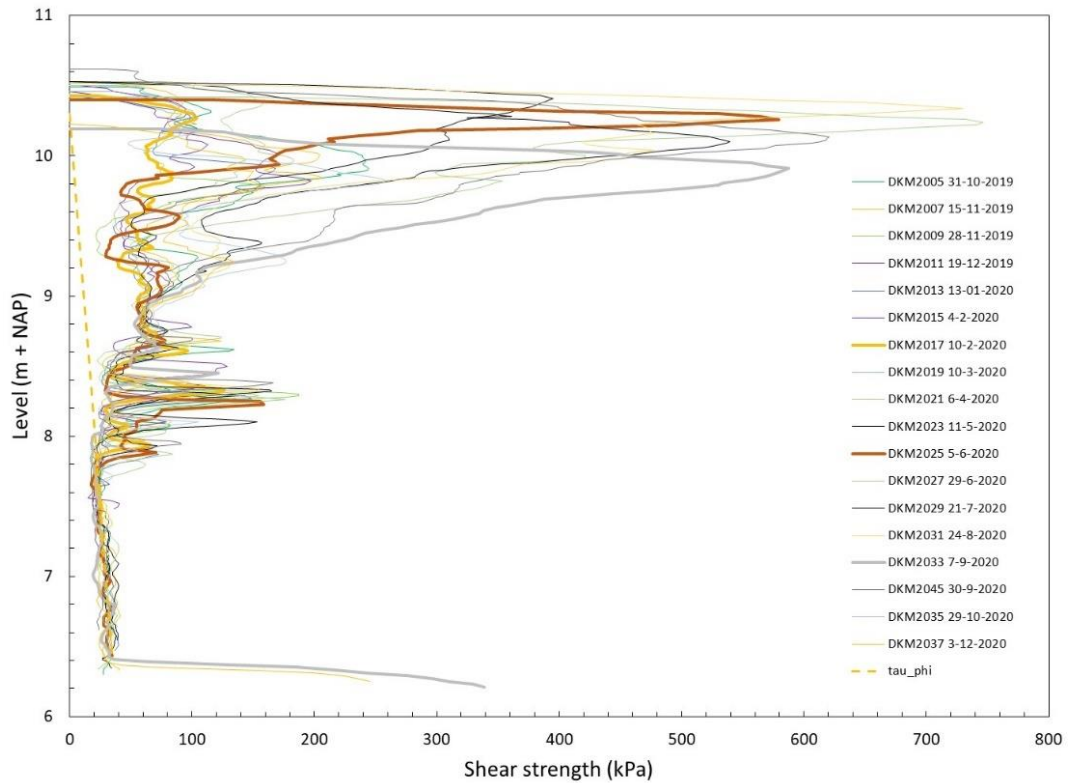


Figure 4.21 CPT (class 1, odd numbers) results of location Westervoort

The transition between the stable pattern of the shear strength profile below NAP +8.5 m and the scatter of the shear strength above NAP +8.5 m at Westervoort in Figure 4.20 and Figure 4.21 coincide with the boundary between brown oxidized clay and grey clay, as discussed in Paragraph 4.4. The shear strength above NAP +8.5 m generally varies with time, but the natural variability of the shear strength gives much scatter. Around NAP +8.5 m also a small sandy layer is present, which also gives some scatter in the shear strength (see also Paragraph 4.4). To highlight the effect of the seasonal variation of the shear strength some of the CPTs are plotted with bold lines. Figure 4.20 and Figure 4.21 generally give the same pattern. It can be seen that shear strength is relatively low in the second part of the winter. In spring shear strength increases. High shear strength values are measured at shallow depth. In summer the shear strength also increases at larger depth, but due to precipitation the shear strength near surface level can be lower compared to spring. Note that the shear strength as derived from FVTs and CPTs is substantially larger than the drained shear strength based on friction angle (yellow dashed line) even when suction is reduced to very low values during February and March 2020 as discussed in Paragraph 4.4.

The results of the FVT, CPT (class 1) and laboratory tests of the location Oijen are presented in Figure 4.22 - Figure 4.25. The FVT results are corrected again using the Chandler (1988) correction with  $I_p$  and the Larsson et al (1987, 2005) correction with  $w_L$  as presented in Paragraph 3.11. For the Chandler correction again a time to failure  $t_f$  of 360 min is applied. The tests are performed each 0.5 m in the dyke and the top of the Holocene clay layers. A  $N_k$  value of 17.0 is applied to fit the CPT data to the FVT results with the Chandler correction. When the Larsson correction is used the  $N_k$  value is 15.0. Here again these single  $N_k$  values give on average a good agreement for each FVT with the accompanying CPTs at the different testing moments; see Figure 4.22. The relationship between FVT and CPT results seems not to be sensitive for the effect of suction in the top layers. Note that with use of the Larsson et al correction the  $N_k$  values for the Westervoort and Oijen sites are closer together. In Figure 4.23 a comparison is made between CPT results and triaxial tests, direct simple

shear tests and a direct shear test. The results are split into two testing moments because the bore holes to retrieve the samples for the laboratory tests are conducted at two times and the laboratory tests are conducted at the natural water contents at the times when the bore holes are carried out. The figures show that the results of the UU triaxial tests, both for peak shear strength and ultimate state shear strength, fit with the CPT results. For Oijen the triaxial test results fit with the CPT results for high shear strength in the top layer as well.

Using the  $N_k$  value of 15.0 from the Larsson et al correction Figure 4.24 and Figure 4.25 show the derived shear strength from the CPTs. In Figure 4.24 the odd numbers of the CPTs are presented and in Figure 4.25 the even numbers are presented.

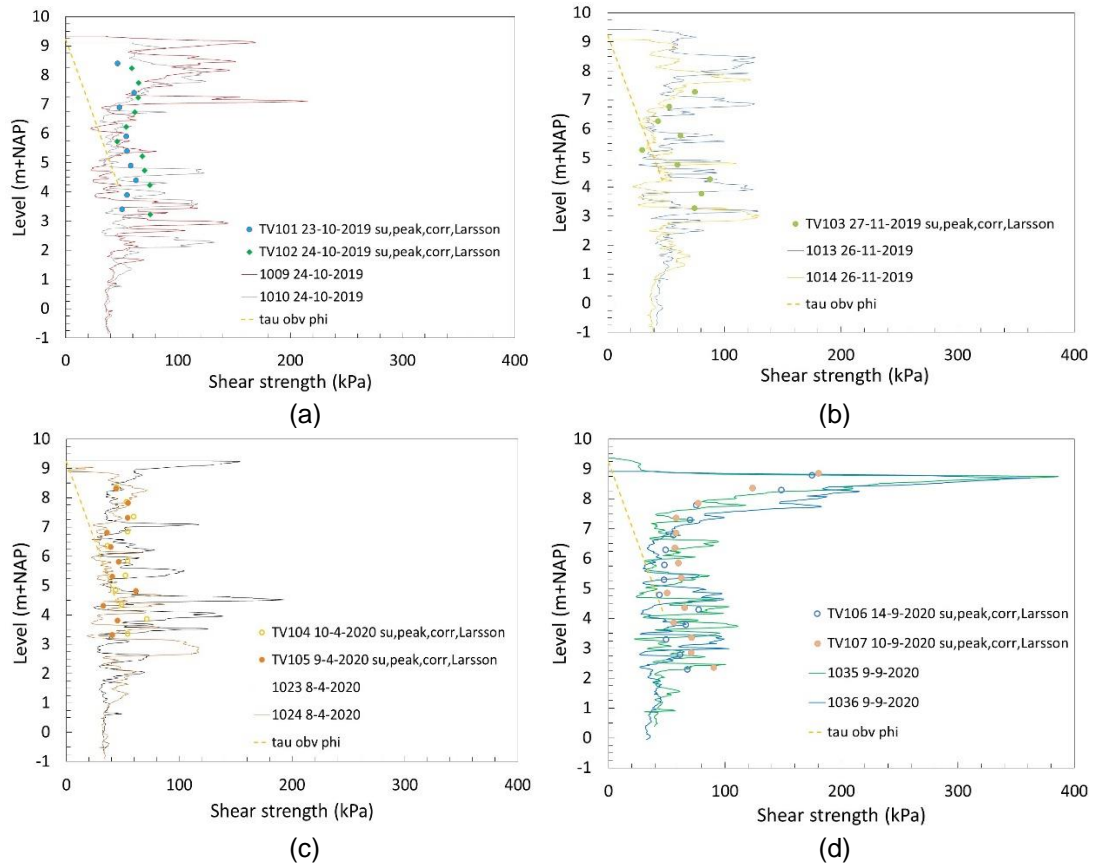


Figure 4.22 Comparison between FVT and CPT (class 1) results of location Oijen

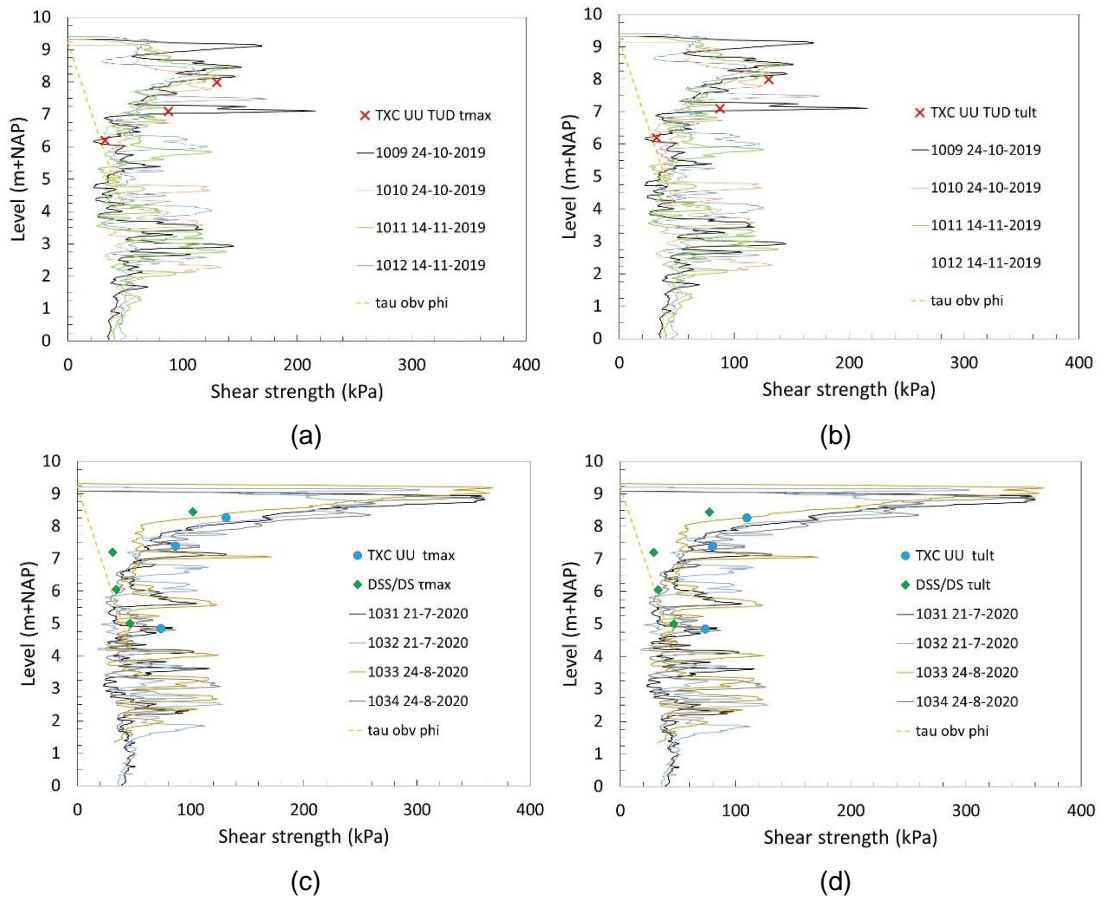


Figure 4.23 Comparison between shear strength derived from UU triaxial tests, direct shear tests and direct simple shear tests with shear strength derived from CPT's at location Oijen: (a) and (c) for peak deviator stress and (b) and (d) for deviator stress at ultimate state (25% axial strain and 40% shear strain)

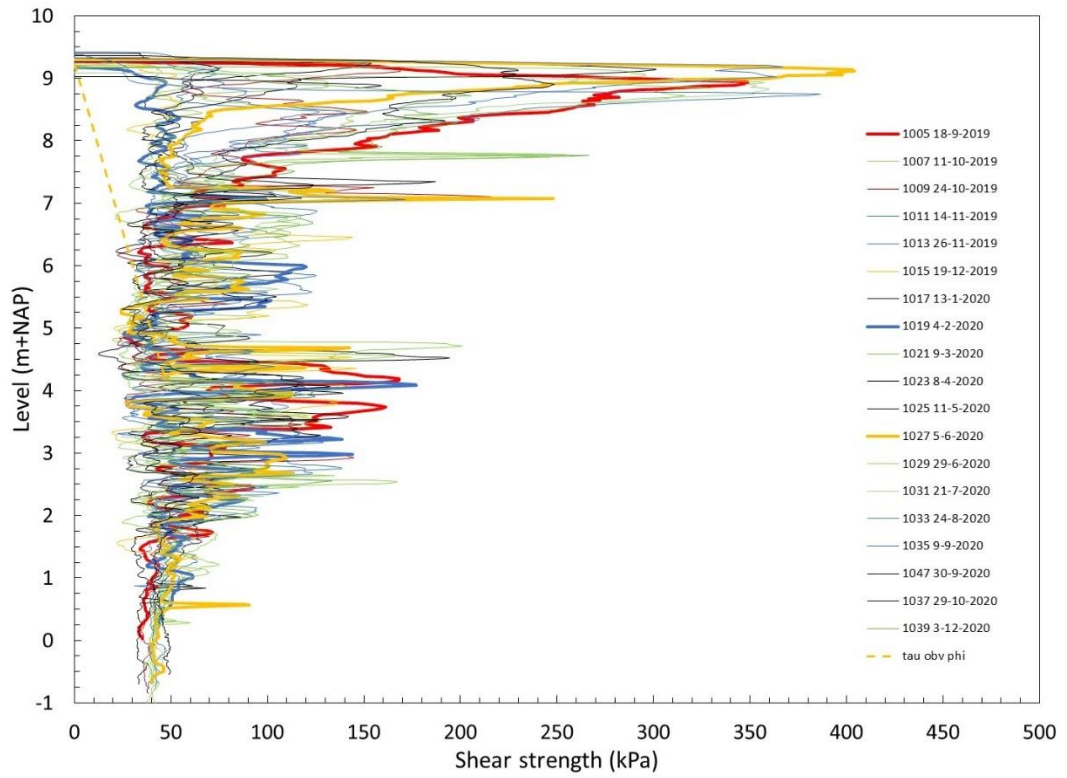


Figure 4.24 CPT (class 1 odd numbers) results of location Oijen

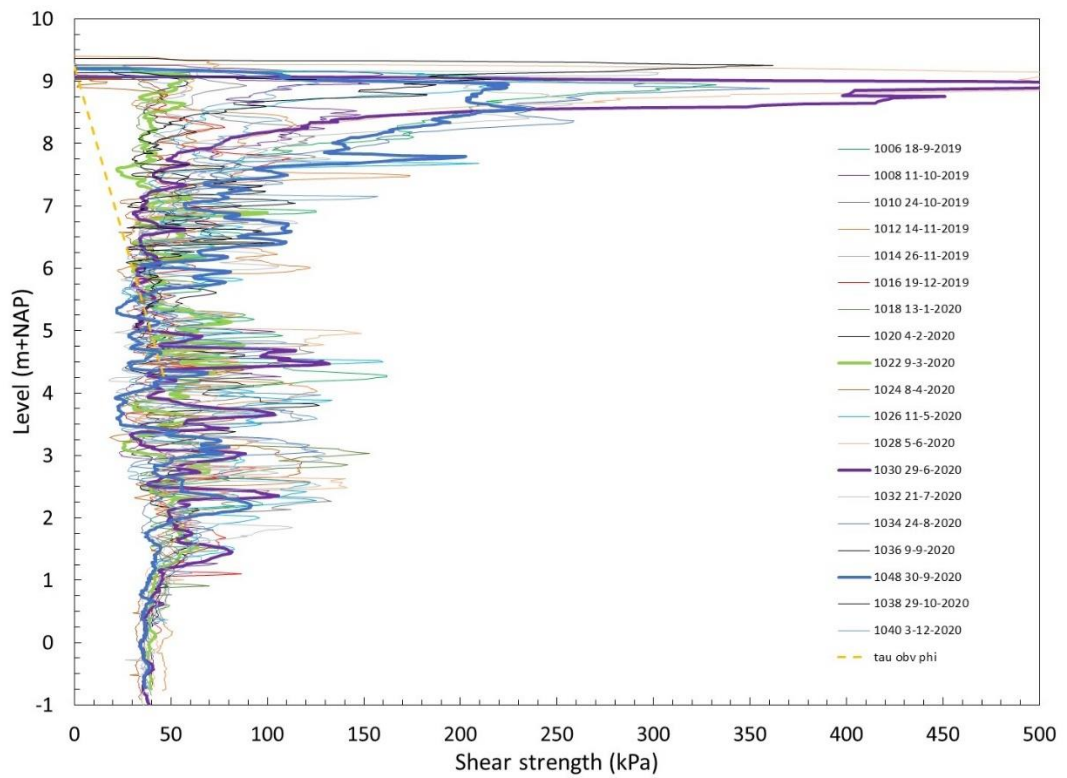


Figure 4.25 CPT (class 1 even numbers) results of location Oijen



The shear strength derived from the cone penetration resistance at Oijen shows the same seasonal pattern as the shear strength at Westervoort. In Figure 4.24 and Figure 4.25 this is highlighted with the bold lines. At Oijen the influence of the interaction of the subsoil with the atmosphere reaches a depth of about 2.5 m. Similar to the results at Westervoort the shear strength as derived from FVTs and CPTs is substantially higher than the drained shear strength based on friction angle (yellow dashed line in Figure 4.24 and Figure 4.25). Variability of the shear strength of the top of the Holocene clay layer and the dyke is also remarkably at Oijen. In the deeper part of the Holocene clay layer the variability of the shear strength is low. Note that the first two CPTs at Oijen are carried out in mid-September 2019, but the monitoring of water content and suction stress at Oijen started at the beginning of October 2019. Therefore, the high cone resistances of the first two CPTs in September 2019 cannot be correlated to measurements of suction stress and water content.

## 4.6 Relation between water content, suction and shear strength

In Paragraph 4.4 the in situ water content, degree of saturation and suction is discussed and in Paragraph 4.5 the in situ shear strength is determined based on the in situ tests and laboratory tests. In this paragraph the data from the previous paragraphs is combined and the relation between suction, degree of saturation and shear strength is presented.

Figure 4.26 and Figure 4.27 give an overview of the development over time of suction  $s$ , water content  $w$ , degree of saturation  $S_r$ , cone penetration resistance  $q_t$  and undrained shear strength  $s_u$ . Cone penetration resistance  $q_t$  and undrained shear strength  $s_u$  are averaged values over a height of 0.3 m around the levels where the water content sensors and suction sensors are installed. Figure 4.26 gives the results from Westervoort. Figure 4.27 gives the results from Oijen. Both figures show that cone penetration resistance  $q_t$  and undrained shear strength  $s_u$  around the shallowest sensors follow the development of suction  $s$ , water content  $w$  and degree of saturation  $S_r$ . For Westervoort this concerns only the shallowest sensor. For Oijen the cone penetration resistance  $q_t$  and undrained shear strength  $s_u$  around the second sensor at NAP +7.63 follows somewhat the development of suction  $s$ , water content  $w$  and degree of saturation  $S_r$ . (the levels of the sensors are mentioned in the legend of Figure 4.26 and Figure 4.27).

In Figure 4.28 and Figure 4.29 undrained shear strength  $s_u$  is plotted against total stress  $\sigma + sS_{rM}$  and water content  $w$ . In Figure 4.28 results of Westervoort are plotted and in Figure 4.29 results of Oijen are given. Note that in these figures the y-axis of the figures with total stress  $\sigma + sS_{rM}$  have a smaller range compared to the figures with water content  $w$ , as the suction sensors failed in summer 2020 and for a part of the undrained shear strength  $s_u$  the corresponding total stress  $\sigma + sS_{rM}$  is not known. In both figures the variation of water content and suction at the deepest sensors is relatively small. However, for small fluctuations of water content the fluctuations in suction are not to be neglected, which can also be seen in the soil water retention curves with their logarithmic scale for the suction. The large variation of the undrained shear strength  $s_u$  around the deepest sensor can be attributed to the heterogeneity of the soil. At the shallow sensors water content and total stress vary during the measurement period. The variations of water content and total stress affect the undrained shear strength. However, when total stress is low the minimum value of the undrained shear strength is substantial. This holds not only for the undrained shear strength around the shallowest sensors but also for the undrained shear strength around the deeper sensors.

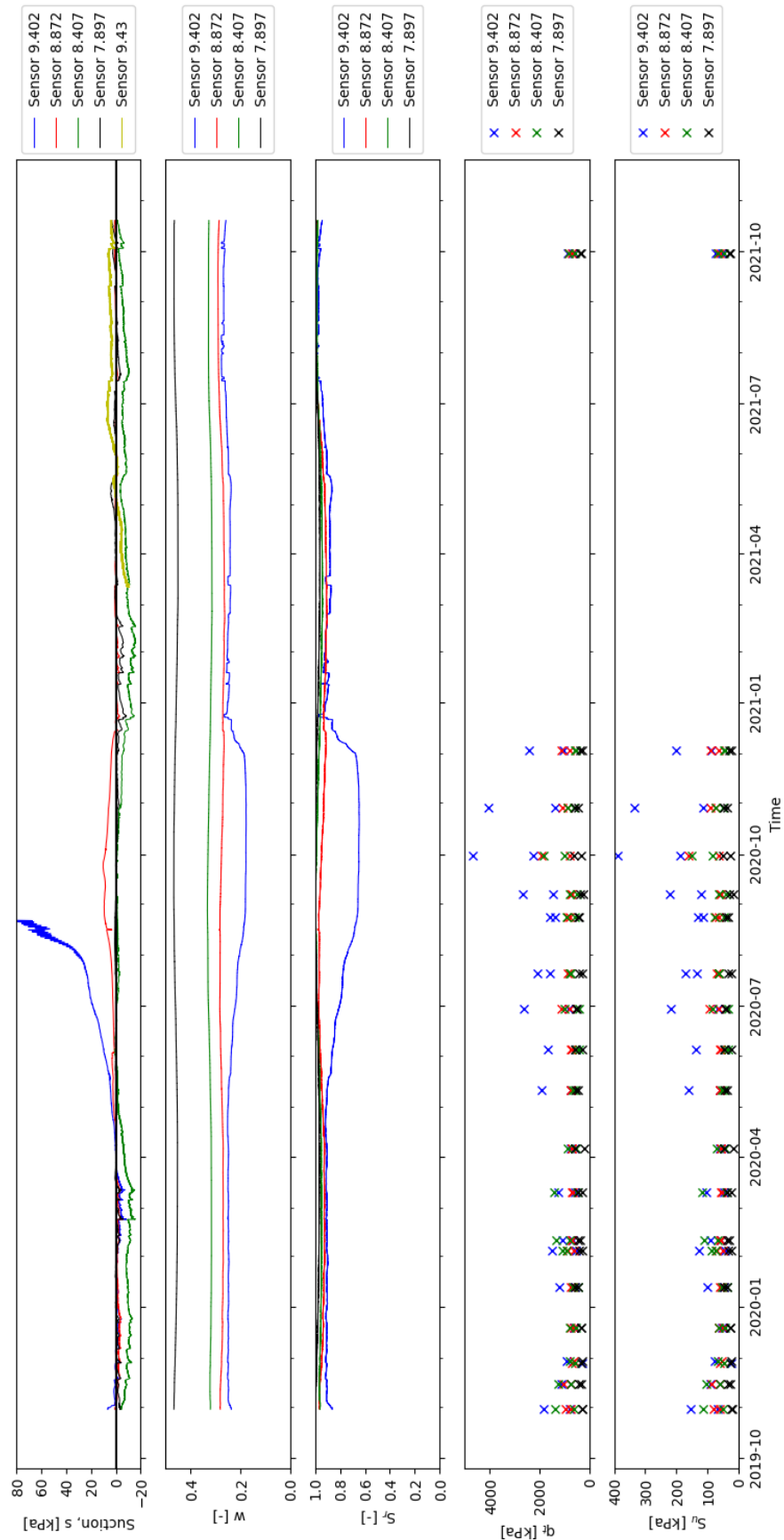


Figure 4.26 Development over time of suction  $s$ , water content  $w$ , degree of saturation  $S_r$ , cone penetration resistance  $q_t$  and undrained shear strength  $s_u$  at Westervoort

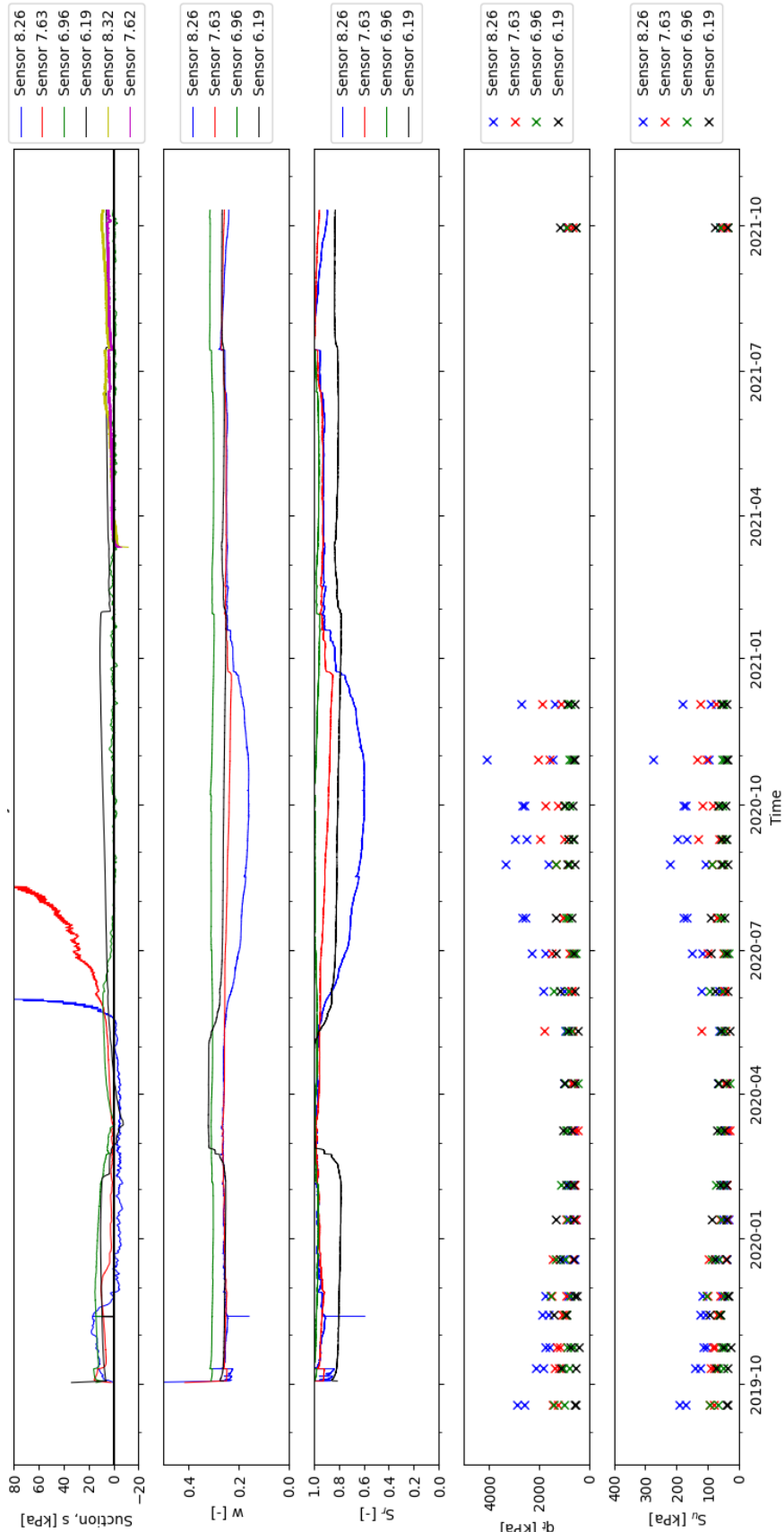


Figure 4.27 Development over time of suction  $s$ , water content  $w$ , degree of saturation  $S_r$ , cone penetration resistance  $q_t$  and undrained shear strength  $s_u$  at Oijen

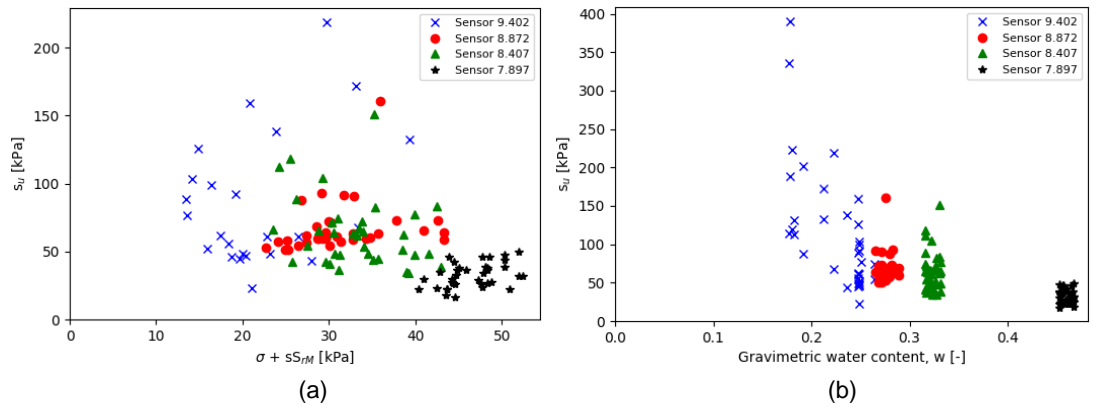


Figure 4.28 Undrained shear strength  $s_u$  plotted against (a) total stress  $\sigma + sS_{rM}$  and (b) water content  $w$  for location Westervoort

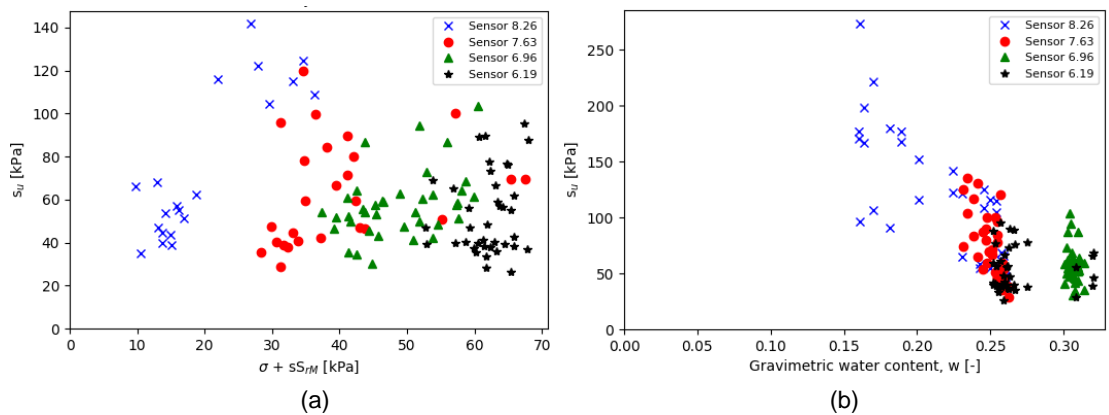


Figure 4.29 Undrained shear strength  $s_u$  plotted against (a) total stress  $\sigma + sS_{rM}$  and (b) water content  $w$  for location Oijen

To get more insight in the soil behaviour when performing CPTs and FVTs the relation between suction  $s$ , water content  $w$ , degree of saturation  $S_r$ , cone penetration resistance  $q_t$  and undrained shear strength  $s_u$  is investigated further. Therefore, three shear strength models as discussed in Chapter 3 are applied to fit the shear strength data from the field. These models are the drained shear strength model (Paragraph 3.2), unsaturated shear strength model (Paragraph 3.3) and undrained shear strength model (SHANSEP-model) (Paragraph 3.4). The drained shear strength model concerns the Mohr-Coulomb failure criterion, with cohesion  $c'$  is 0 kPa, following CSSM-theory for the ultimate state. For the drained shear strength model and the unsaturated shear strength model non-associative behaviour is applied, with a friction angle  $\varphi'$  of 32°. For the SHANSEP-model an undrained shear strength ratio  $S$  of 0.35 and a strength gain exponent  $m$  of 0.9 is chosen. Note that  $S$  and  $m$  are not determined in this research. The choice of  $S$  is based on Deltares (2020) where in situ tests and laboratory tests on sandy clay are performed. The choice for  $m$  is an expert guess. The overconsolidation ratio OCR is based on the oedometer tests, which are performed in the laboratory for this project. The results of the oedometer tests are summarized in Table 4.5. The SHANSEP-model is to be used for saturated conditions. Only the samples 19 (Westervoort), 7 and 7A (Oijen) concern samples with saturated conditions. Regarding sample 19 this is a sample which belongs to the soft deposit below the firm crust. To estimate the undrained shear strength only the results from the samples 7 and 7A are used for Oijen as well as for Westervoort. Because of the trend of the undrained shear strength as derived from the in situ tests, with a more or less constant shear strength with depth for Oijen and a decreasing shear strength with depth for Westervoort a constant yield

stress  $\sigma'_{vy}$  of 145 kPa is assumed. The overconsolidation ratio OCR is calculated based in this value of the yield stress. To fit these shear strength models to the shear strength data two moments are chosen, which are representative for a wet and a dry situation in the field. Suction  $s$ , water content  $w$  and degree of saturation  $S_r$  are derived from the sensor data for the testing moments at which the CPTs are performed. Missing suction data from the shallow suction sensors is estimated from the soil water retention curves, which are determined in this project. The estimation of suction is based on the measured water content. For suction values above 80 kPa the Staring series (soil types O10 and O11) are applied. The graphs of the soil water retention curves are in Appendix B. Figure 4.30 and Figure 4.31 show the results for Westervoort and Figure 4.32 and Figure 4.33 show the results for Oijen.

Table 4.5 Results of oedometer tests on intact samples

Location	Bore-hole	Sample	Level (NAP + m)	$\gamma_{i,bulk}$ (kN/m <sup>3</sup> )	$\gamma_{i,dry}$ (kN/m <sup>3</sup> )	Water content $w_i$ (-)	Yield stress (kPa)	POP (kPa)
Westervoort	B203	13	9.65 – 9.60	17.6	15.6	0.128	350	339
	B203	19	7.65 – 7.60	16.2	10.2	0.586	49	5
Oijen	B003	1A	8.26 – 8.23	13.8	11.5	0.207	332	317
	B003	7	6.05 – 6.00	19.2	15.5	0.237	139	88
	B003	7A	6.05 – 6.00	18.4	14.9	0.237	150	99

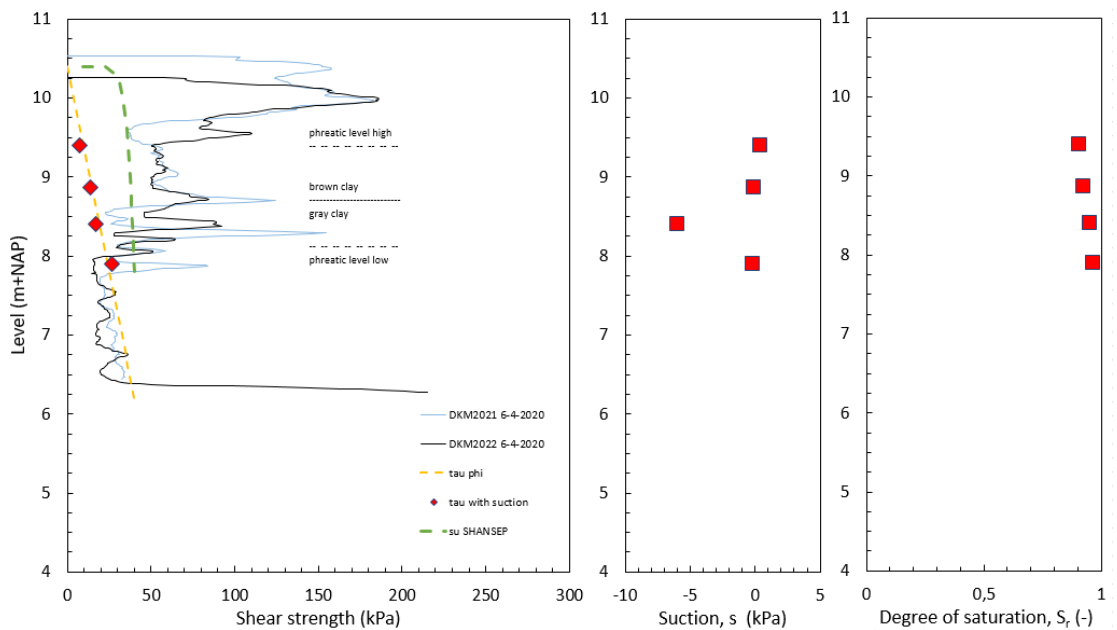


Figure 4.30 Comparison between in situ shear strength at April 6, 2020 (end of the wet season) at Westervoort and three shear strength models. Measured suction and degree of saturation are also given

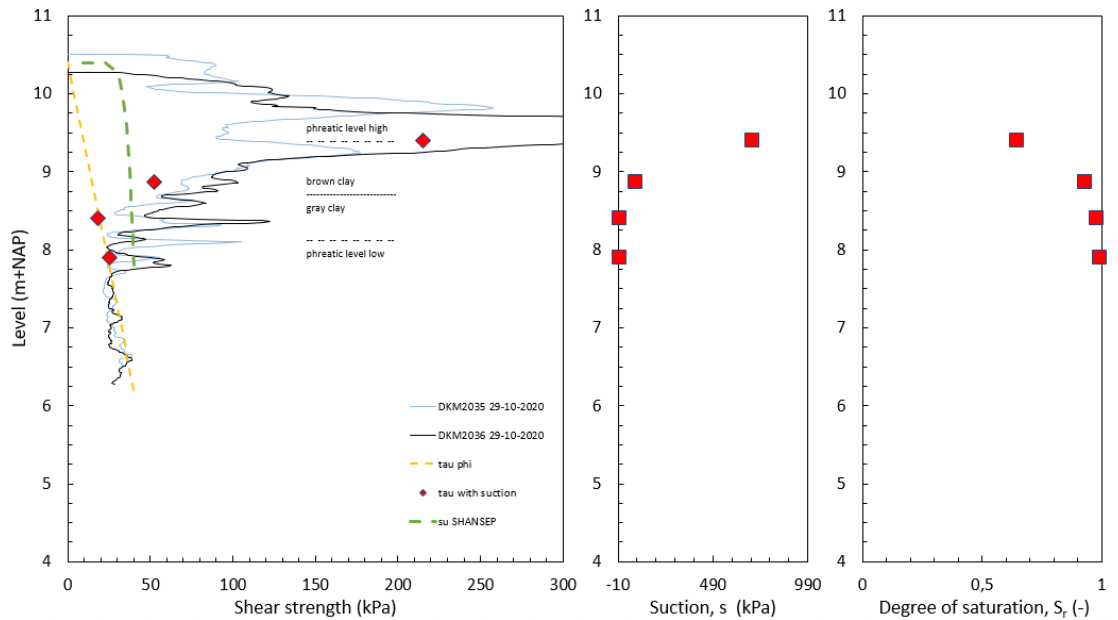


Figure 4.31 Comparison between in situ shear strength at October 29, 2020 (end of the dry season) at Westervoort and three shear strength models. Measured suction and degree of saturation are also given

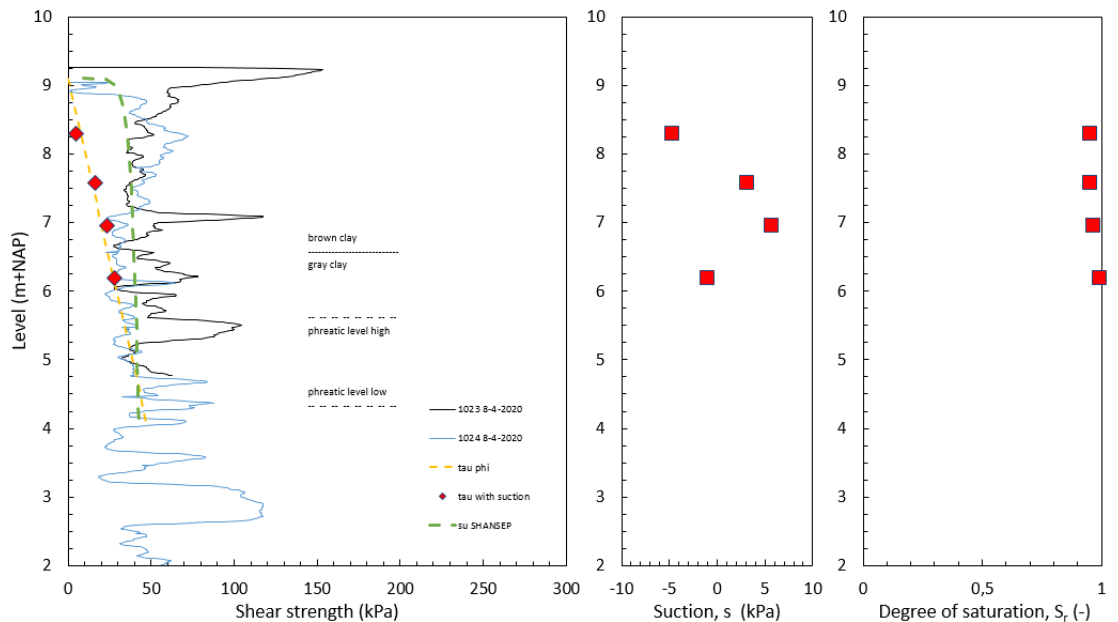


Figure 4.32 Comparison between in situ shear strength at April 8, 2020 (end of the wet season) at Oijen and three shear strength models. Measured suction and degree of saturation are also given

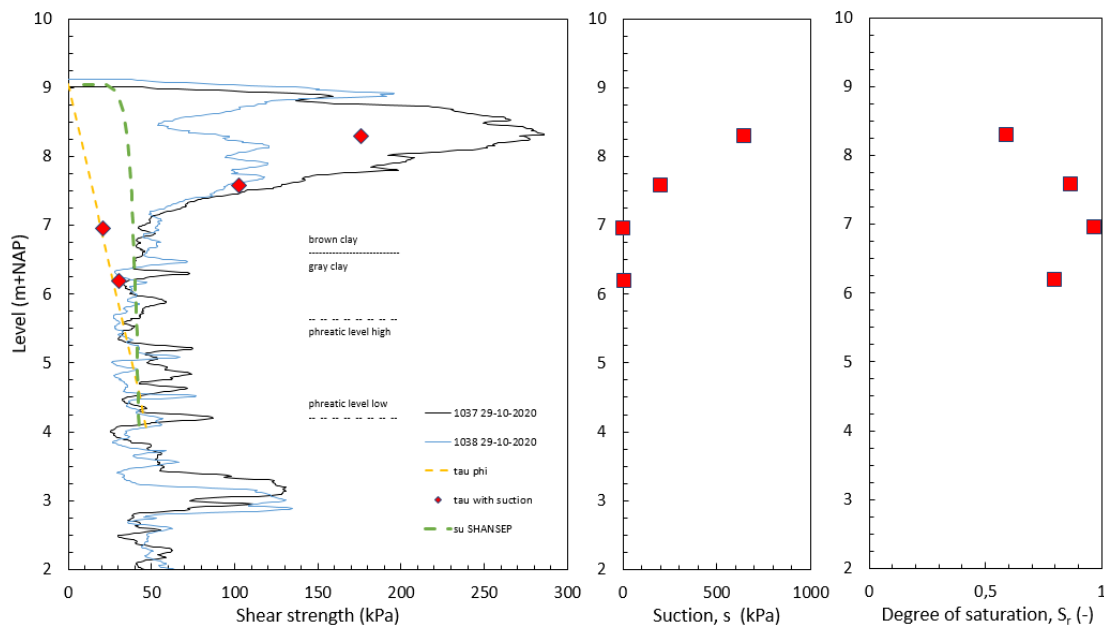


Figure 4.33 Comparison between in situ shear strength at October 29, 2020 (end of the dry season) at Oijen and three shear strength models. Measured suction and degree of saturation are also given

Regarding the drained shear strength model (yellow dashed lines) Figure 4.30 - Figure 4.33 show that this model underestimates the measured shear strength of the initially unsaturated soil for all cases. The unsaturated shear strength model (red points) gives a good approximation of the measured shear strength in the shallow layers for the dry season, when suction is high. For the wet season and for the deeper layers, when degree of saturation is high and suction is low, the unsaturated shear strength model and the drained shear strength model converge. So, when suction is low the unsaturated shear strength model also underestimates the measured shear strength. The undrained SHANSEP-model (dashed green lines) compares with the measured shear strength when degree of saturation is high and suction is low, both for the shallow and the deeper soil layers. This is at least the case for Oijen. For Westervoort the chosen yield stress is possibly too low for the firm top layer. For dry conditions with high suction in the shallow layers the turning point were the unsaturated shear strength model and the undrained SHANSEP model describe the measured shear strength good lies around the boundary between grey clay and brown oxidized clay.

## 4.7 Triaxial tests on reconstituted samples

As the shear strength as discussed in the previous paragraph can be much higher than the Mohr-Coulomb criterion despite (nearly) saturated conditions, also at relatively low effective stresses, the possible backgrounds of this high shear strength is investigated. Therefore, the undrained shear strength of reconstituted samples is determined in the laboratory as described in Paragraph 3.14. Two series of tests are conducted: compacted samples and air-dried samples. More results of the laboratory tests are given in the factual report (Deltares, 2021b).

### Moist compacted samples

As described in Paragraph 3.14 reconstituted samples are prepared in the laboratory and the shear strength of these samples is measured with CIU triaxial compression test. Table 4.6 gives the results of a series of tests on moist compacted samples. The samples are compacted using a standard Proctor hammer and Proctor mould according to ASTM D 698. The density "middle" with 25 blows per soil layer of 39 mm thickness corresponds to standard compaction effort following ASTM D 698. For the series "loose" and "dense" ten blows less and more are applied respectively. 67 mm diameter samples are used. After preparation the

samples are saturated and consolidated to a vertical stress of 50 kPa. An undrained shearing phase is applied. As a reference for these triaxial tests a Proctor test is conducted. This test is performed on the same mixed material. The samples are retrieved from bore hole B001 (samples M021 - M027) and B201 (samples M015 - M019). The results of the Proctor test are given in Figure 4.34. The optimum water content in the Proctor test is 0.206. The triaxial tests are performed with water contents above and below this optimum water content.

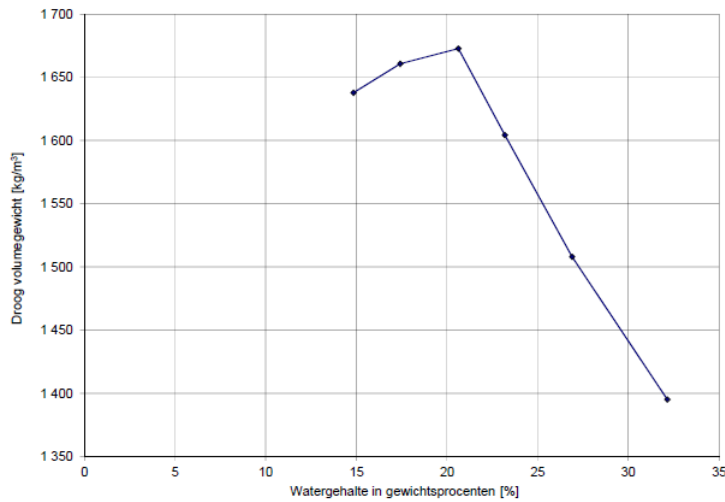


Figure 4.34 Results of the Proctor test

Table 4.6 Results of CIU triaxial compression tests on reconstituted samples which are moist compacted using a Proctor hammer and Proctor mould with different compaction effort

Sample	Material preparation and compaction at water content $w_i$ (-)	Material compaction effort	$\rho_{i,bulk}$ (kg/m <sup>3</sup> )	$\rho_{i,dry}$ (kg/m <sup>3</sup> )	Water content $w_c$ (-)	$t_{max}$ (kPa)	$t_{ult}$ (kPa)
1	0.25	Loose (15 blows per soil layer of 39 mm thick)	1918	1533	0.234	50.4	50.4
2	0.17	Loose (idem)	1887	1617	0.252	47.3	47.3
3	0.28	Middle (25 blows per soil layer of 39 mm thick)	1902	1490	0.254	38.4	38.3
4	0.25	Middle (idem)	1919	1532	0.250	48.8	48.8
5	0.20	Middle (idem)	1906	1589	0.238	112.5	112.4
5A	0.19	Middle (idem)	2012	1685	0.211	87.9	87.9
6	0.15	Middle (idem)	2009	1749	0.141	70.8	70.8
6A	0.14	Middle (idem)	1979	1732	0.206	78.7	78.7
7	0.26	Dense (35 blows per soil layer of 39 mm thick)	1947	1551	0.232	51.5	51.5
8	0.17	Dense (idem)	2079	1783	0.206	194.9	194.9



Figure 4.35 and Figure 4.36 show the results of the CIU triaxial tests on moist compacted samples. The stress paths in Figure 4.35 show the dilative behaviour of the compacted samples. The shear strength  $t$  can be very high compared to the mean stress  $s'$ . The graph of the normalized shear strength  $t/s'$  versus axial strain  $\epsilon_a$  (Figure 4.36) show a peak value of  $t/s'$  between 2% and 6% axial strain. Towards the ultimate state the ratio  $t/s'$  converges.

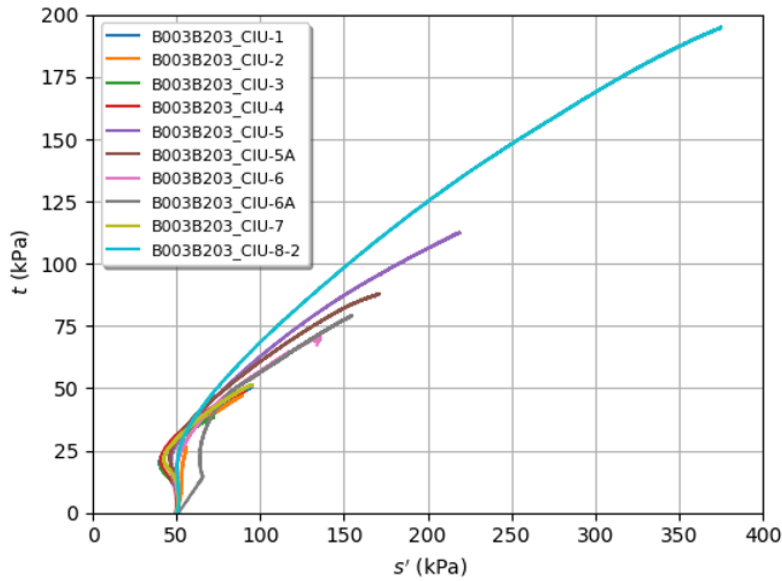


Figure 4.35 Stress paths of CIU triaxial tests on reconstituted moist compacted samples

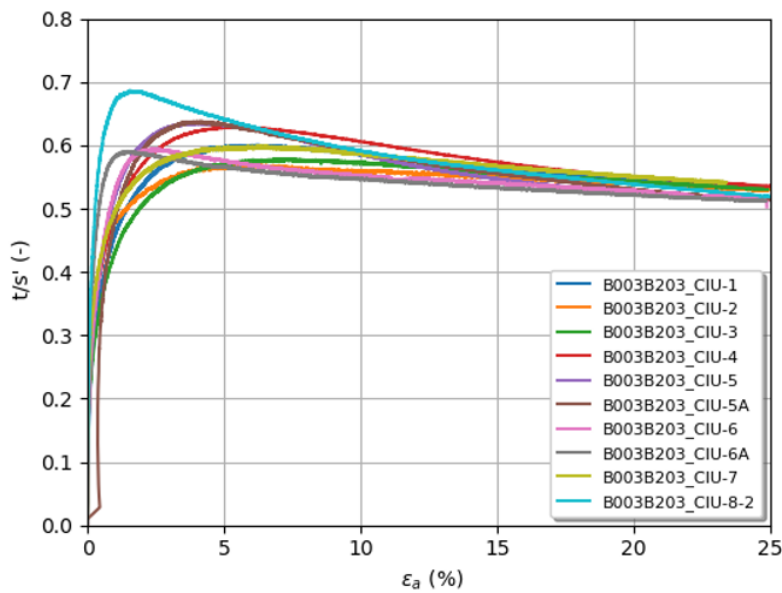


Figure 4.36 Normalized shear strength  $t/s'$  versus axial strain  $\epsilon_a$  of CIU triaxial tests on reconstituted moist compacted samples

The effect of the compaction of the samples on the shear strength is further investigated in Figure 4.37. This figure illustrate that the shear strength is affected by the compaction effort and the initial water content at which the samples are compacted. As can be seen from the Proctor test (Figure 4.34) the initial density at which a sample is compacted influences the dry soil unit weight. A high density of a sample on his turn results in a high shear strength.

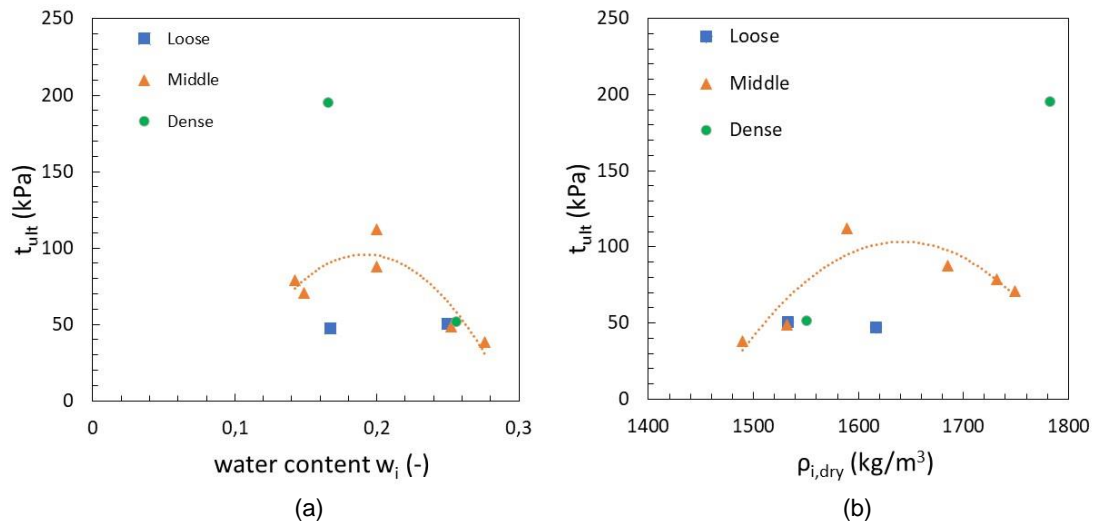


Figure 4.37 Shear strength  $t$  versus (a) initial water content  $w_i$  and (b) initial dry unit weight  $\rho_{i,dry}$

### Air dried samples

A second series of reconstituted samples is prepared using the slurry method. The slurry is made applying a water content corresponding to 1.25 times the liquid limit  $w_L$ . The liquid limit of the intact samples which are used to prepare the reconstituted samples is between 0.3 and 0.5. The slurry samples are dried in the air to achieve different target water contents. 50 mm diameter samples are used to ensure that the time required for drying the samples became not too long. After preparation the samples are saturated and consolidated to 50 kPa. An undrained shearing phase is applied. In this shearing phase no suction was present in the samples. Results of these tests are presented in Table 4.7.

Table 4.7 Results of CIU triaxial compression tests on reconstituted samples which are made from a slurry and dried to different target water contents

Sample	Material dried in the air to target water content $w_i$ (-)	$\rho_{i,bulk}$ (kg/m <sup>3</sup> )	$\rho_{i,dry}$ (kg/m <sup>3</sup> )	Water content $w_c$ (-)	$t_{max}$ (kPa)	$t_{ult}$ (kPa)
9	0.30	1912	1472	0.298	16.6	16.0
10	0.15	1949	1697	0.234	90.3	87.0
11	0.20	2019	1690	0.223	79.3	77.0
12	0.07	1876	1754	0.220	111.4	109.0
13	0.22	2010	1653	0.215	51.1	49.0

Figure 4.38 and Figure 4.39 show the results of the CIU triaxial tests on air dried samples. The stress paths in Figure 4.38 show again a dilative behaviour of the samples. The shear strength  $t$  can be high compared to the mean stress  $s'$ . The graph of the normalized shear strength  $t/s'$  versus axial strain  $\epsilon_a$  (Figure 4.39) show a peak value of  $t/s'$  between 2% and 15% axial strain. After the peak the ratio  $t/s'$  converges.

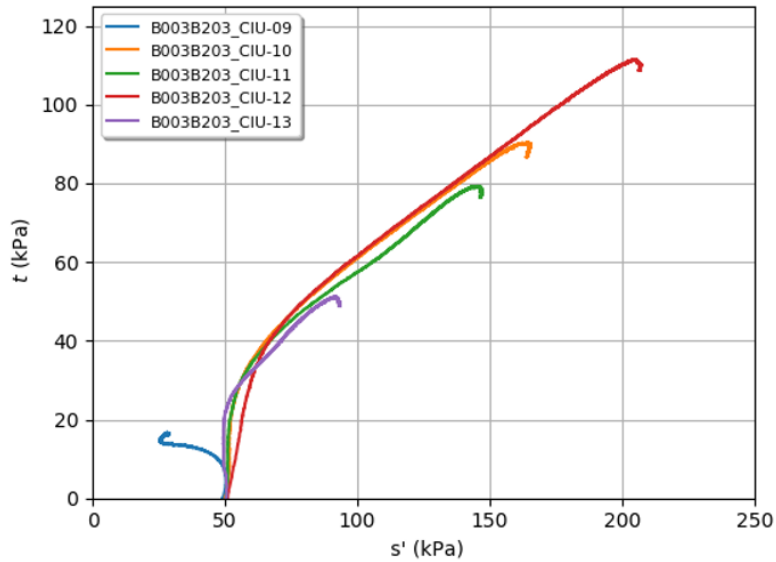


Figure 4.38 Stress paths of CIU triaxial tests on reconstituted air dried samples

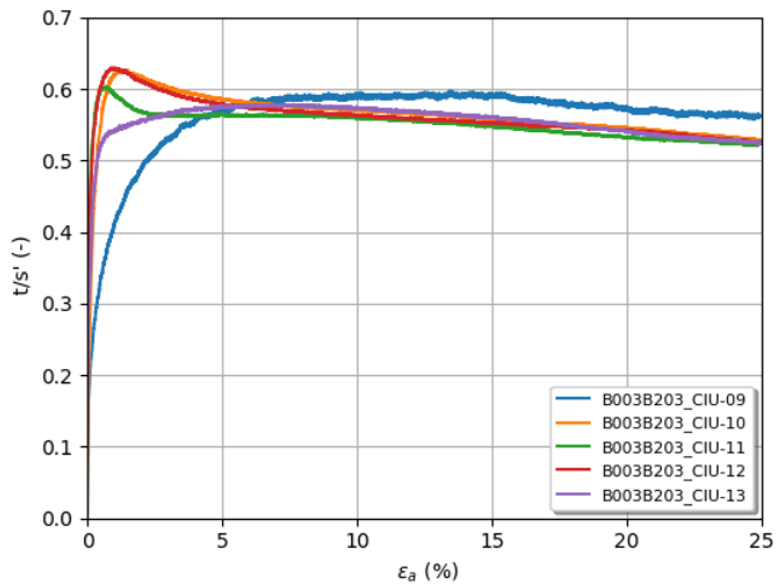


Figure 4.39 Normalized shear strength  $t/s'$  versus axial strain  $\epsilon_a$  of CIU triaxial tests on reconstituted moist compacted samples

In Figure 4.40 the shear strength  $t$  is plotted against water content  $w$  and unit weight  $\rho_i$ . Regarding the target water content  $w_i$  at which the samples are dried in the air it can be seen that there is a relation between the shear strength and this target water content. Concerning the water content  $w_c$  after saturation and consolidation of the samples there is a discontinuity in the relation between water content and shear strength. So, the initial water content at which the samples are dried have an important effect on the shear strength of the samples. The effect of desiccation of the samples on the compaction of the samples (decrease of the void ratio) seem to be a permanent effect.

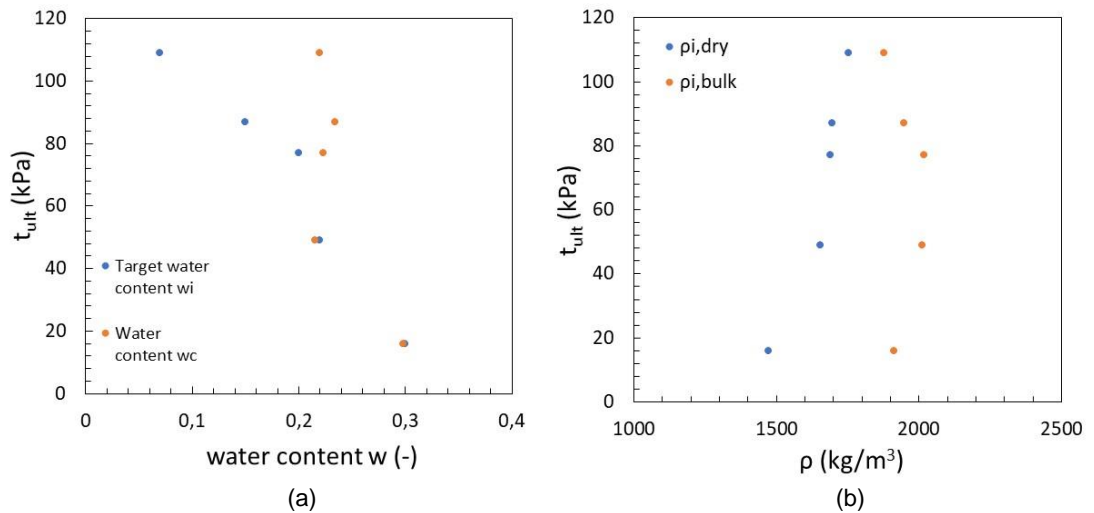


Figure 4.40 Shear strength  $t$  versus (a) water content  $w$  and (b) unit weight  $\rho_i$ .

## 4.8 Resistivity Cone Penetration Tests (RCPT)

In this project a GeoPoint resistivity cone of Wiertsema & Partners is tested in the laboratory of Deltares and in the field at Westervoort and Oijen. To get a first idea about the validity of the electrical conductivity and volumetric water content measurements some simple tests are performed in the laboratory:

- Tests to verify the volume which is measured by the cone in horizontal and vertical direction.
- Measurements in dry sand and water with increasing salt content.
- Measurements in sand with various water contents.
- Measurements in clay samples with decreasing water content.

Some of the most important findings from these tests are:

- There seems to be an offset of 10% water content.
- The measured water content in sand seems to be plausible.
- For clays the measured water content can deviate from the real water content. Therefore, calibration is required based on the soil to be tested.
- The measured temperature by the cone seems to be incorrect. The electrical conductivity depends on temperature.

The results of the tests in the laboratory are reported in Deltares (2019d). The findings as summarized above are discussed with Wiertsema & Partners and GeoPoint. After that the resistivity cone is tested at Oijen and Westervoort to compare the measurements with the results of the volumetric water content sensors.

The results of the tests in the field are presented in Figure 4.41. At each site two RCPTs with measurement of the electrical conductivity and dielectric constant are performed at two testing moments to get insight in the variability of the electrical conductivity and dielectric constant. The RCPTs are performed at September 30, 2020 and at September 30, 2021. The results of the dielectric constant measurements are compared with the volumetric water content measurements from the sensors at the timespan when the RCPTs are conducted (red points in the figures). To get a good comparison between the dielectric constant from the CPTs with the volumetric water content from the sensors the dielectric constant is transformed with a linear relationship:  $y = ax + b$ , with  $x$  the dielectric constant and  $y$  the volumetric water content. The factors  $a$  and  $b$  are used as follows:

$a = 0.00645$  at Westervoort and  $0.00455$  at Oijen.

$b = 0.25$  at Westervoort and Oijen.

Note that these factors  $a$  and  $b$  will be dependent on the soil type (clay content and organic content) and temperature.

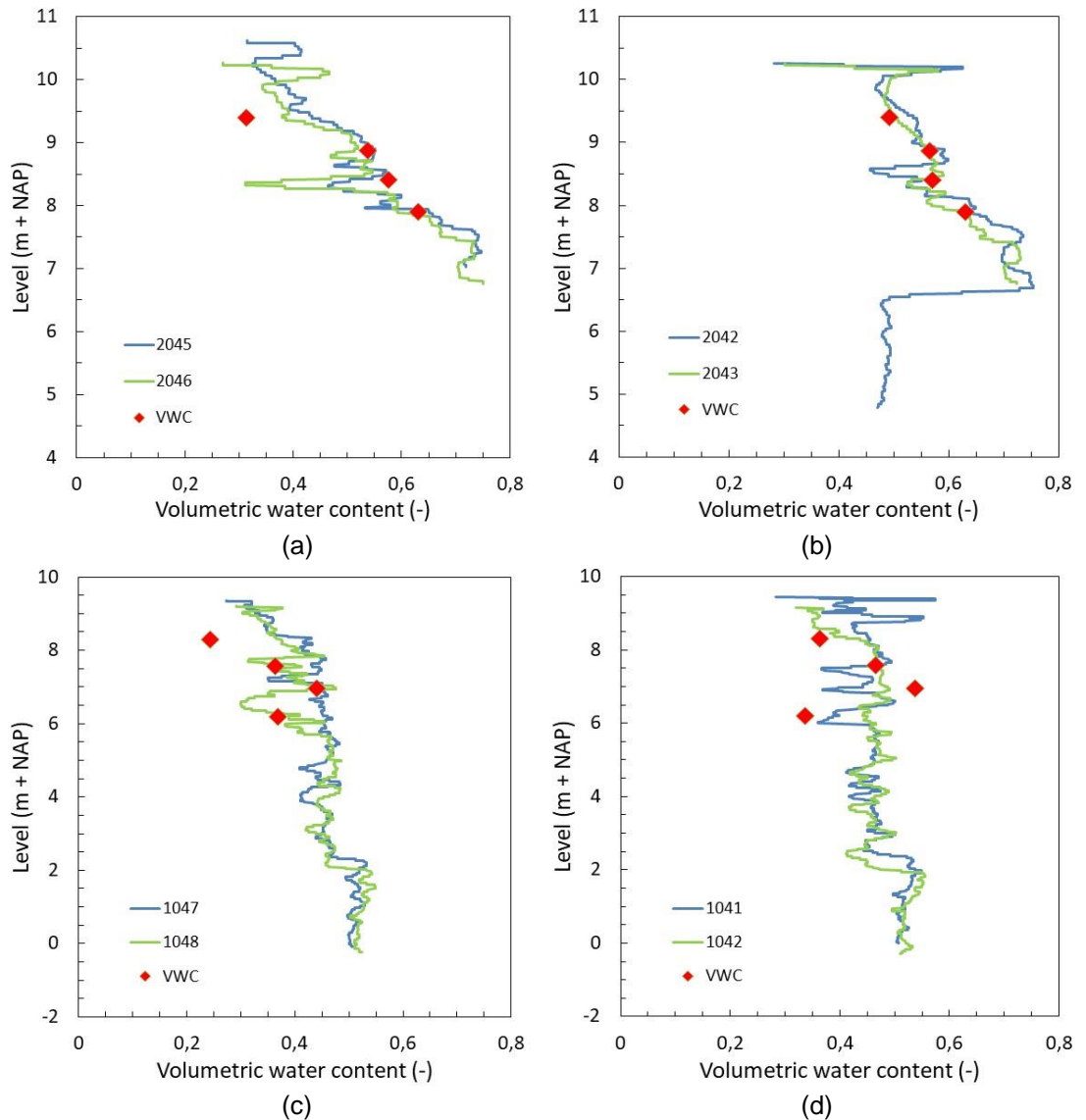


Figure 4.41 Comparison of the results of the dielectric constant measurements from the RCPT and volumetric water content measurements from the sensors at (a) Westervoort in 2020, (b) Westervoort in 2021, (c) Oijen in 2020 and (d) Oijen in 2021

# 5 Discussion

## 5.1 Introduction

In order to reach the objectives and to answer the key questions of this research a number of scientific questions are formulated (see Paragraph 1.2). The results of the field and laboratory tests as presented in the previous chapter are discussed in this chapter along the lines of the scientific questions. The scientific questions are:

1. What is the typical variation in water content of the cohesive soil in the dykes and the cover layers, if not constantly saturated?
2. For which hydraulic conditions and soil properties the soil becomes completely saturated during the wet season, when the precipitation and evaporation are given?
3. To what extent do the macro-pores in aggregated soil close at the saturated state, as a result of swelling of the aggregates? And which factors are of influence?
4. What are suitable criteria regarding texture, water content and aggregation to decide if the shear strength of saturated soil strength should be modelled drained or undrained, in case of stability analysis of primary flood defence dykes?
5. How does the water content and the coupled swelling and shrinkage behaviour affect the (drained or undrained) shear strength?
6. What is the relationship between the shear strength of the aggregates and the shear strength of the soil: to which extent can they be considered equal?

## 5.2 Variations in water content, suction and degree of saturation

The graphs of gravimetric water content, degree of saturation and suction show an interesting variation during the measurement period. In general the variations show a pattern which seem to be related to the yearly pattern of precipitation deficit. In summer period, when evaporation is generally more than precipitation, water content and degree of saturation decrease and suction increases. In winter period, when precipitation is generally more than evaporation, water content and degree of saturation increase and suction decreases.

Overall the derived data from the sensors seem to be consistent and reliable. Regarding the derived values it has to be noted that the sensors for the measurement of suction give absolute values. Uncertainties in the derived suction values can be caused by measurement errors of the sensors and possibly by installation effects of the sensors. Concerning the derived values of water content and degree of saturation there is some uncertainty caused by measurement errors of the sensors and by the uncertainty of the calibration factors. As described in Chapter 2 the calibration factors are slightly adapted from the calibration factors from the user manual of the sensors, such that the degree of saturation is 1.0 when the derived water content has the highest values and measured suction is zero or positive. Concerning the relation between water content, degree of saturation and suction it has to be noted that the different sensors to derive these parameters are installed at a distance of 0.5 m from each other. This gives some noise in this relation, because of the heterogeneity of the soil. Another source of uncertainty is the difference between the suction, which is measured at a small ceramic tip, and the water content, which is measured with 300 mm long probe rods. So, these measurements represent a big difference in volume of the soil.

The pattern and magnitude of the variations are the largest for the shallowest sensors at 1.0 m below surface level. The response in general decreases with depth. The magnitude of the response of the deeper sensors, which are at depths of 1.5 m and deeper below the surface level, is considerable smaller than the response of the shallowest sensors. At the Westervoort

site degree of saturation at the sensors at 1.5 m below surface level and deeper was in the complete measurement period higher than 0.9. For the Oijen site the variations of water content and degree of saturation were also much smaller for the sensors at 1.7 and 2.4 m below surface level, compared to the sensor at 1.0 m depth. For the Oijen site the deepest water content sensor at 3.1 m below surface level is an exception on this pattern. This sensor shows remarkable variations of water content and degree of saturation. Possibly these variations are caused by the influence of sandy layers on the hydrologic situation in the dyke. These sandy layers have been found in two bore holes. One of these sandy layers is found about 0.75 m below the sensor.

The descriptions of the bore holes show that the boundary between grey clay and brown oxidized clay is at about 2.0 m depth at Westervoort and at about 2.5 m depth at Oijen. At Westervoort this boundary is in the zone where the phreatic surface normally fluctuates. At Oijen this boundary lies about 2 m higher than the normal average phreatic surface. These observations of the color of the clay confirm that below these depths the degree of saturation is 1.0 or close to one and no air enters the pores. The sensors give degrees of variation around 0.95 and higher for the zone of the grey clay, except the lowest sensor at Oijen as mentioned before.

Regarding the yearly pattern of the precipitation deficit it is clear that this pattern shows a variation in successive years. The precipitation deficit in the summer of 2020 was, with a maximum deficit of about 250 mm in august 2020, much larger than the precipitation deficit in the summer of 2021, with the maximum deficit below 100 mm (KNMI, 2021). The precipitation deficit in 2019 was, with a maximum deficit of about 210 mm also relatively high. These precipitation deficit data are averaged values over 13 weather stations in The Netherlands. As a result the water content and degree of saturation was much higher and suction much lower in the summer of 2021 compared to the summer of 2020. For the shallowest sensor at Oijen a minimum degree of saturation of 0.58 is derived for 2020, while the lowest derived value for 2021 is 0.90. For Westervoort these values are 0.65 and 0.87 respectively. The magnitude of suction was in 2021 below 10 kPa at Oijen and Westervoort, while in 2020 the maximum suction was above 80 kPa for the shallowest sensors, as some of the sensors get outside their measurement range. Judging the water content and cone resistance and based on the water retention curves of the Staring series (Wösten et al., 2001) the maximum suction in 2021 at the shallowest sensors could have been more than 1000 kPa. For the deeper sensors the differences in water content, degree of saturation and suction due to the yearly seasonal pattern are negligible.

Probably due to the large precipitation deficit in the last part of the summer of 2019 the water content and degree of saturation were also relatively low at Oijen during a large part of the winter period 2019/20. Only at some days in March 2020 the degree of saturation was close to 1.0 and no suction was present in this short period. After this short period the degree of saturation decreased again and suction increased again due to the precipitation deficit in April 2020. At Westervoort degree of saturation was closer to 1.0 and suction closer to zero compared to Oijen. After the high precipitation deficit of summer 2020 the effects of this deficit on water content, degree of saturation and suction at Oijen was disappeared around the end of January 2021. For Westervoort this situation was reached already around the end of December 2020. But it can be seen that the summer conditions of precipitation and evaporation can determine water content, degree of saturation and suction in the winter period for several months.

The CPT cone with resistivity module (RCPT) gives the opportunity to measure a vertical profile of the water content of the soil. This RCPT could be a fast and useful tool for field investigations regarding the (initially) unsaturated zone. However, at the moment RCPT cones are not available in the (Dutch) market. Calibration of the measurement output of

RCPT measurements is required. Note that this calibration will be dependent on the soil type (clay content and organic content), water content and temperature. So, proper calibration is always required, however Figure 4.41 illustrates that the RCPT has the potential to be a useful tool to determine the water content and to be able to determine the influence of suction on the cone penetration resistance, as the water content can be used to estimate suction.

### 5.3 External factors and soil properties that affect the degree of saturation

As discussed in the previous paragraph there is a relation between precipitation, evaporation, water content, degree of saturation and suction. So, the weather conditions determine the water content in the upper part of the dyke and the subsoil. The importance of the weather conditions is such that a relatively dry summer period causes relatively low degrees of saturation and relatively high suction during several months of the winter period.

At the Westervoort site also the pore water pressures in the deeper part of the Holocene cover layer and the top of the aquifer are measured. During the measurement period some high water levels at the river IJssel occurred, with a substantial increase of the pore water pressures in the aquifer and the bottom part of the Holocene cover layer as a result. This increase in the pore water pressure however, had no clear effect on the water content, degree of saturation and suction in the upper part of the Holocene cover layer. The deepest water content sensor at 2.5 m below surface level and 0.6 m above the shallowest pore water pressure sensor gives a constant pattern of the water content and degree of saturation, with only small variations. It might be the case that the water content sensor at 2.0 m below surface level and 1.1 m above the shallowest pore water pressure sensor has more influence from the variations of the pore water pressure in the aquifer. Possibly this can be explained by the heterogeneity of the subsoil, as a sandy layer is found in one of the bore holes around 2.0 m below surface level.

Furthermore, the water content, degree of saturation and suction are affected by the distance to the phreatic surface. At Westervoort the sensors are installed at depths within the interval where the phreatic surface varies, as described in the description of the bore holes. At Oijen the deepest sensor is about 0.4 m higher than the upper limit of the interval where the phreatic surface varies, as described in the description of the bore holes. This position of the sensors relative to the phreatic surface does not seem to have much effect on the shallowest sensors, as the magnitude of the degree of saturation and suction are comparable for Westervoort and Oijen. For the shallowest sensors therefore, it is likely that the weather conditions are of the most importance, as discussed before. The position of the sensors relative to the phreatic level affects the gradients of water content, degree of saturation and suction between the shallowest sensors and the second sensors. These gradients are smaller when the phreatic surface is deeper compared to the level of the sensors.

As known from literature (Wösten et al., 2001) water content, degree of saturation and suction can also be affected by the texture of the soil. Water retention curves are different for clayey and sandy soil types. As the texture of the soil at Westervoort and Oijen is comparable no clear conclusions can be derived about the influence of texture of the soil from these measurement sites.

### 5.4 Swelling and shrinkage and their influence on dynamics of cracks and fissures

In this research up to now no specific measurements are performed to monitor the dynamics of cracks and fissures due to swelling and shrinkage of the soil. However, based on the derived degrees of saturation, suction and the observations of the boundaries between brown oxidized clay and grey clay as discussed in Paragraph 5.1 it is likely that no extensive pattern of cracks and fissures will be present below about 2.0 m depth at Westervoort and below about 2.5 m



depth at Oijen. Above these depths cracks and fissures will be present, at least in periods with low degree of saturation and high suction. The intensity and width of cracks and fissures will increase when the degree of saturation decreases and suction increases. These assumptions are in line with TAW (1996) in which is stated that in the upper decimetres below the surface the structure of the clay is well developed, with relatively small aggregates, with a size of millimetres or centimetres. According to TAW (1996) at larger depth it is more difficult to distinguish between aggregates and there is some cohesion between the aggregates. In this zone the aggregates have a size of about 10 centimetres or more. The International Levee Handbook (CIRIA, 2013) states that desiccation cracks generally are narrow and shallow and extent 0.3 to 0.5 m into an embankment. Blight (2013) observed cracks and fissures in soil profiles in the unsaturated zone and conclude that uninterrupted open vertical cracks usually are not deeper than 1.0 m. Cracks can usually be discerned to about 1.5 m, but these cracks are often not continuous to the surface.

As discussed in Paragraph 5.1 dry summers with high precipitation deficit will lead to low water content, low degree of saturation and relatively high suction during several months in winter period. Under such conditions cracks and fissures due to desiccation of the soil in summer period may endure in winter period for a long time.

## 5.5 Factors and soil properties that affect drainage conditions during shearing

For the Westervoort and Oijen sites it is already mentioned that below 2.0 m and 2.5 m respectively the degree of saturation is permanent above 0.95, based on the measurements. This is confirmed by the observations of the boundaries between the brown clay and grey clay in the bore holes. Suction is below 15 kPa in this zone. As discussed in Paragraph 5.3 in this zone no cracks and fissures are to be expected. Furthermore, the clay content at both sites is between 20 and 50%. Therefore, permeability of the soil will be relatively low. Due to these soil conditions it is likely that undrained shear behaviour will occur. This can also be inferred from the shear strength measurements from the in-situ tests and laboratory tests. The triaxial tests in the laboratory are performed undrained and the results of these tests compare well with the shear strength derived from the cone penetration tests and field vane tests. So, when performing these in situ tests the soil in situ behaves undrained for the encountered soil conditions. This is also inferred from the trends of shear strength against depth for both sites. Fitting the measured shear strength of the (initially) unsaturated zone of Westervoort (above NAP +8.0 m) and Oijen using the Mohr-Coulomb criterion with applying a cohesion and friction angle does not give a realistic agreement. The measured shear strength does not give an increase of the shear strength with depth according to the Mohr-Coulomb model. Miller et al. (2018) applied the Mohr-Coulomb failure criterion with a cohesion of 40 kPa to analyse their data of CPT tests in unsaturated soils (see Paragraph 3.9). However, for Westervoort and Oijen this does not give an accurate fit with the data. Preliminary results from analyses of CPT penetration in unsaturated clayey soil with the Material Point Method show that the generation of excess pore water pressures around the cone tip depends on the initial suction in the soil (Yerro et al., 2021). When suction increases the degree of saturation decreases and the magnitude of the excess pore water pressure around the cone tip decreases. For low suction, when the soil is saturated or nearly saturated, the magnitude of the excess pore water pressures suggests undrained shear behaviour.

The shear strength in the permanently saturated zone of the dyke at Oijen shows remarkable heterogeneity based on the CPT results. The upper bound of the shear strength is up to a factor four higher than the lower bound of the shear strength. This heterogeneity is remarkable, because the CPTs are performed in a relatively small area of 100 m<sup>2</sup>. This heterogeneity may be caused by the variability in the composition of the clay and by the effectiveness of the compaction of the clay at the construction of the dyke. For the Westervoort site the

heterogeneity is less noticeable, with the exception of the sandy layer between NAP +7.8 m and NAP +8.6 m.

In the upper 2.0 m of the Holocene cover layer at Westervoort and the upper 2.5 m of the dyke at Oijen water content, degree of saturation and suction vary throughout the year as has been discussed. These variations also affect swelling and shrinkage and development of cracks and fissures. Under these conditions the soil becomes oxidized, as has been confirmed by the bore holes. This zone of the brown clay therefore might be more permeable than the grey clay. Permeability will depend on water content, degree of saturation and suction. In wet conditions the water content and degree of saturation will increase, suction will decrease, and aggregates will swell, resulting in a decrease of permeability. Conducting cone penetration tests and field vane tests for these wet conditions resulted in shear strength values which are comparable with the shear strength values of the deeper zone of the grey clay. So, also for the shallow zone with the brown clay undrained shear behaviour occur when performing cone penetration tests or field vane tests under wet conditions. In dry conditions the aggregates will shrink, and cracks and fissures will become wider. Bulk permeability therefore will increase. Shear strength will also increase by the contribution of suction to the effective stress and shear strength. This is also observed with the cone penetration tests and field vane tests, which are performed in dry conditions. For these dry conditions the shear strength can be explained reasonably well assuming drained shear behaviour and considering the contribution of suction to the shear strength.

For the soil conditions of Westervoort and Oijen it is likely that for wet conditions the shearing behaviour in the performed in-situ tests and laboratory tests can be considered undrained while for more dry conditions a drained approach is more appropriate. Wet conditions and undrained shear behaviour occur when degree of saturation is above 0.90 to 0.95. Dry conditions with drained shear behaviour occur when degree of saturation is below 0.70 or 0.80. As clay content is an important parameter, for the water retention behaviour of soils from the Westervoort and Oijen sites, it can be deduced that the degrees of saturation as mentioned before are applicable for clay content between 20 and 50%. By performing measurements on other sites more insight can be gained in the relevant parameters and the range of the parameters for which drained or undrained conditions are to be expected. Potentially important measurement sites are situations with an old more heterogeneous dyke, a dyke with clay with lower clay content, a dyke with a lower degree of saturation and a dyke with a larger zone with brown oxidized clay.

Furthermore, it has to be noted here that undrained shear behaviour depends on strain rate at failure of the soil and dissipation of excess pore water pressures or permeability. So, when performing the cone penetration tests or field vane tests at a lower rate the soil may behave drained. Therefore, the drained or undrained behaviour found in in-situ testing might not be representative for a slope failure which might develop at a lower shearing rate. Further investigation of the dependency of the shear behaviour of partially unsaturated soil on strain rates and permeability is necessary. This could be performed in numerical simulations. Validation of the theoretical outcomes with in-situ measurements of permeability and by a failure test in the field is recommended.

## 5.6 Influence of water content and swelling and shrinkage behaviour on shear strength

Water content and degree of saturation are important parameters for partially saturated soils. These parameters are key parameters for the magnitude of suction, shrinkage and swelling behaviour of the aggregates and permeability. From this background these parameters are important for the choice to model shear behaviour of the soil drained or undrained in the assessment of slope stability. As discussed before undrained shear behaviour is relevant for a

higher degree of saturation and drained shear behaviour occurs for lower degree of saturation, for the soil conditions as encountered at Westervoort and Oijen.

For the undrained shear behaviour, which occurs in the grey clay, the state of the soil determines the undrained shear strength. The triaxial tests, which are conducted on reconstituted samples with different preparation methods, show that initial water content is important for the mobilized shear strength. For the samples which are dried out to a target water content and are saturated, consolidated and sheared thereafter, the initial water content is more important for the mobilized undrained shear strength than the water content after the consolidation stage. Due to desiccation the void ratio of the samples decreases. When the soil becomes saturated and swells, this decrease of void ratio is partly irreversible. Because of that desiccation affects the state of the soil. The same applies for the reconstituted samples, which are prepared at different water contents and are compacted with different amount of energy. This series of triaxial tests also shows that the initial conditions determine the shear strength much more than the water content of the soil after the consolidation stage. Also, in the field it will be the case that the mobilized undrained shear strength of the clay in the partially saturated zone is determined by the water content which occurs in desiccated conditions or the conditions during construction of the dyke. The shear strength values which are found in the triaxial tests on reconstituted samples agree with the shear strength values which are derived from the in-situ tests for the (initially) unsaturated zone. These triaxial tests also show that the undrained shear strength can be very high relative to the effective stress level. This high strength values can occur in undrained shearing conditions due to the dilative behaviour of the soil. This dilative behaviour is typical for transitional soils (Coop, 2015). As clayey soil in the partially saturated zone often may behave as a transitional soil an accurate determination of yield stress from compression tests is difficult and the relation between undrained shear strength and yield stress, according to the SHANSEP-model, is often unreliable. Therefore, it is difficult to follow an approach with derivation of the state of this type of soils. In case of transitional soils, an approach with direct determination of the mobilized undrained shear strength from in situ tests or laboratory tests is recommended.

Undrained shear behaviour also occurs in the brown clay zone during in-situ and laboratory testing when water content and degree of saturation are above a certain threshold. For Westervoort and Oijen undrained shear behaviour occurs when degree of saturation becomes above 0.8 and above 0.7 respectively. To be able to interpret shear strength data of the brown clay zone from field tests or laboratory tests a series of these tests at different water content is required. Based on this series of tests the relationship between effective stress, suction, undrained shear strength or drained shear strength can be derived and can be distinguished between drained shear behaviour or undrained shear behaviour.

When water content and degree of saturation are low and suction is high and drained soil behaviour is applied for the brown clay, water content, degree of saturation and suction determine the shear strength. In this study it is found that the applied shear strength model of Tarantino et al. (2013) works well for conditions with low water content and low degree of saturation. For the high suction range the analyses for Westervoort and Oijen showed uncertainty, because the high suction is outside the range of the water retention curves, which are performed in the laboratory and which cover the range up to 80 kPa. At the same time the tensiometers in the field, which were installed at shallow depths, get outside their measurement range in the dry summer of 2020. Therefore, the relation between water content and suction is based on the Staring series (Wösten et al., 2001), for the high suction range. This gives uncertainty about the suction that actually occurred in the field. It is therefore recommended to continue the measurements in the field to gain data for the conditions with high suction.

To account for the effect of swelling and shrinkage in the analysis of the shear strength insight in the relation between macro structural void ratio and micro structural void ratio for a wide

range of water contents is required. The degree of saturation of the macro pores determines the effect of suction on shear strength. The range of water contents for which micro structural void ratio is known is limited. Therefore, a constant micro structural void ratio is applied in the analyses, while in literature micro structural void ratio decreases with decreasing water content, until a residual value is reached. Furthermore, the micro structural void ratio as derived from the MIP tests is found to be a bit low compared to Romero et al. (2011). More insight in the micro structural void ratio is needed. It is recommended to perform additional MIP tests for a wider range of water contents and to perform cross checks based on derivation of the micro structural void ratio from retention curves, which cover the range to much higher suction values.

The shear strength values as derived from the field vane tests (FVT) is calculated applying the correction of Chandler (1988) and Larsson et al. (1987 and 2005). When applying the Larsson et al correction the  $N_k$  values for the correlation of the FVT and CPT results for Westervoort and Oijen are closer together compared to the Chandler correction. Therefore, the Larsson et al correction is preferred in this analysis. The  $N_k$  value as derived in this research gives a good fit for all FVT results, both for higher and lower suction values. Possibly for the highest suction values in the firm top layer another  $N_k$  value could be required. However, in this research the number of FVT results for very high suction values is too low to be able to draw the right conclusions. It has to be noted here, that no other studies are known from literature where FVTs are conducted in the unsaturated zone and where the empirical corrections are applied on the FVT measurements (see also Paragraph 3.11).

## 5.7 Relationship between shear strength of aggregates and bulk shear strength of the soil

The relationship between the shear strength of aggregates and the bulk shear strength of the soil is not yet considered in this research. To investigate this issue triaxial tests on large samples are provided in the research proposal (Deltares, 2019a). These tests have not yet been conducted.

As discussed before no well-developed pattern of cracks and aggregates are to be expected in grey clay. So, the strength as derived from the laboratory and in situ tests at Westervoort and Oijen will not be affected by cracks and fissures. However, cracks and aggregates are to be expected in brown oxidized clay. For the time being it must be assumed, on the basis of literature, that shallow shear surfaces can partly pass through cracks. See also the literature study (Deltares, 2019a), which is executed at the start of the research on the partially saturated soils. Because of the cracks and fissures the bulk shear strength of the soil can be lower than the shear strength of soils without cracks and fissures. Note that in fissures and cracks no suction will be active. The size of cracks and fissures is too large to develop capillary forces. To gain insight in the shear strength of soils with cracks and fissures it is recommended to conduct the triaxial tests on large samples.

## 5.8 Application in slope stability analyses

It is an important insight from this research that soil behaviour during CPT penetration and FVT testing changes from drained to undrained and vice versa, depending on degree of saturation. In literature the shear behaviour of the unsaturated zone is commonly described with the Mohr-Coulomb failure criterion (Deltares, 2019a). However, for clayey soils with high degree of saturation this approach does not give an accurate agreement with the data from Westervoort and Oijen as discussed before. Degree of saturation depends on soil type and hydrological conditions. When the soil has a substantial amount of clay, little or no cracks and fissures in the clay and degree of saturation is relatively high undrained shear behaviour is likely. At Westervoort and Oijen this is the case, while clay content is between 20% and 50%, the clay is not oxidized (grey clay) below about 2.0 m depth at Westervoort and below about 2.5 m

depth at Oijen and degree of saturation in the grey clay is around 0.94 or higher throughout the year. When the partially saturated zone consists of transitional soils, an approach with direct determination of the mobilized undrained shear strength from in situ tests or laboratory tests is recommended, as mentioned before.

In the upper part of dykes and the upper part of the Holocene cover layer degree of saturation varies considerable due to precipitation and evaporation. At Westervoort this concerns a depth of about 2.0 m and at Oijen this concerns a depth of about 2.5 m. In wet conditions, with high degree of saturation, these shallow layers of brown oxidized clay may behave undrained, but in dry conditions these shallow layers will behave drained. In these shallow layers also cracks and fissures will be present. The width of these cracks and fissures and their influence on permeability of the soil also will depend on the degree of saturation. The cracks and fissures might influence the shear strength as shallow slip surfaces may follow the existing pattern of the cracks and fissures (Deltares, 2019a). In dry conditions suction contributes to the shear strength of the aggregates. So, for the shallow zone drained shear behaviour with application of a friction angle, can be assumed for dry conditions. These dry conditions can last for several months during winter period depending on the weather conditions (precipitation deficit) in summer as observed at Westervoort and Oijen in 2019 and 2020. For wet conditions the undrained shear behaviour can be assumed, but caution is advised because of the presence of cracks and fissures, which will reduce the shear strength. As mentioned before cracks and fissures are most represented up to a depth of about 1.0 to 1.5 m. For large sliding planes this effect might be negligible.

## 6 Conclusions

Based on the collected data from the measurement sites Westervoort and Oijen the soil behaviour in the (initially) unsaturated soil is identified and quantified. Related to the project objectives it is important to remind that in practice the (initially) unsaturated zone is meant as the zone above the normal daily phreatic surface. In practice this zone is assumed to be (initially) unsaturated, as mentioned in Chapter 1.

### Three zones

In this research it is found that a substantial part of the soil above the normal daily phreatic surface can be permanently saturated. At Westervoort, where the measurements are conducted in the Holocene cover layer, this is not the case as the permanently saturated zone coincides with the zone where the normal daily phreatic surface fluctuates. However, at the Oijen site the permanently saturated zone is about two meters higher than the normal daily phreatic surface. On top of this permanently saturated zone lies a zone where degree of saturation and suction varies considerably. This zone reaches to a depth of about 2.0 m at Westervoort and about 2.5 m at Oijen. Because air can enter the pores in this zone the clay has a brown color due to oxidation processes in the soil. When precipitation deficit is low degree of saturation increases and suction decreases. When precipitation deficit is high degree of saturation decreases and suction increases. This dry condition can last over longer time in winter period when precipitation deficit is high at the end of summer period. The variations of degree of saturation and suction are the largest in the first 1.0 to 1.5 m below the surface level. In this shallow zone cracks and fissures may be present due to desiccation of the soil. High water conditions may also have influence on degree of saturation. However, at Oijen no influence of high water has been measured. At Westervoort a small influence of high water via the aquifer on degree of saturation is observed.

### Degree of saturation and shear strength

From the shear strength measurements at Westervoort and Oijen it can be determined that the soil behaves undrained in the permanently saturated zone. In the zone where degree of saturation and suction fluctuates the soil behaves undrained when degree of saturation is high enough and suction is low. The undrained shear strength can be very high relative to the effective stress level. This high strength is caused by the dilative behaviour of the soil in undrained conditions. Compaction of the soil due to desiccation and compaction during the construction of dykes can cause this dilative behaviour and high undrained shear strength. This dilative behaviour is also characteristic for clays with high soil unit weight in the Holocene clay layers, the so called 'transitional soils'. Drained soil behaviour occurs when degree of saturation is low and suction is high. The drained shear strength in this zone depends on suction and degree of saturation and varies therefore considerably. For Westervoort and Oijen undrained shear behaviour occurs when degree of saturation becomes above 0.8 and above 0.7 respectively. This soil behaviour is derived from the interpretation of cone penetration tests, field vane tests and triaxial tests. It is likely that these tests are representative for the soil behaviour during a slope failure. However, this is not fully sure, as strain rates and scale of the deformations are different for a slope failure and the mentioned field and laboratory tests. Further investigation of the dependency of the shear behaviour of partially unsaturated soil on strain rates and permeability is necessary. This could be performed in numerical simulations. Validation of the theoretical outcomes with in situ measurements of permeability and by a slope failure test in the field is recommended.

In the shallow 1.0 m to 1.5 m where cracks and fissures can occur, the mobilized shear strength can be reduced, when a slip surface can (partly) follow the pattern of the cracks and

fissures. In cracks and fissures suction will not contribute to the shear strength. In this research the effect of cracks and fissures on the shear strength is not investigated.

### **Schematization of the shear strength**

In summary, the zones above the normal daily phreatic surface and the recommended schematization of the shear strength in these zones are as follows:

1. Grey clay, where the degree of saturation is 1.0 throughout the year and suction varies relatively little. The soil behaves undrained.
2. Brown oxidized clay, where the degree of saturation and suction vary, depending on precipitation and evaporation. The soil behaves drained for low degree of saturation and high suction. The soil behaves undrained for high degree of saturation and low suction. The relatively dry conditions can also occur in winter period, when previous summer had a high precipitation deficit.
3. Brown oxidized clay at the upper 1.0 to 1.5 m below the surface, where cracks and fissures exist, of which the width varies in relation to water content and suction. The soil behaves drained for low degree of saturation and high suction. The soil behaves undrained for high degree of saturation and low suction. The mobilized shear strength of shallow slip surfaces can be reduced as a result of the cracks and fissures.

Dimensions of these three zones and magnitude of the shear strength within these zones depends on soil type and hydrological conditions at the site under consideration.

Based on the results of this research, a report is made (Deltares, 2021a; in Dutch) for water boards and engineering contractors, aimed at application of the acquired knowledge in engineering practice. This report provides insight into the steps in investigations in the field and the laboratory and analysis which can be taken to improve the assessment or design of dykes in which the shear strength of the unsaturated zone plays an important role on slope stability.

### **Impact of the research**

From the consequence analysis (Arcadis, 2020) it is known that differences in modelling of the shear strength of the dyke material can lead to differences in the probability of failure by a factor of 10 to 10,000. It also follows from this analysis that it can make the difference between the need of a stability berm or not or a difference in the required length of the stability berm of up to 20 m. The degree of optimization of the probability of failure will depend on the local soil conditions and hydrological conditions. The consequence analysis will be updated based on the results of this research.

## 7 Recommendations for further research and optimization

From the discussion of the results of this research there are a number of uncertainties and questions to be answered. Further research on these topics is recommended to gain insight in the behaviour of partially unsaturated soils and to reduce uncertainties in the analysis of the stability of slopes where partially unsaturated soils play a role.

Further investigation of the dependency of the shear behaviour of partially unsaturated soil on different strain rates and permeability is necessary. As a slope failure occurs much slower than failure during a cone penetration test or a field vane test the combination of strain rate, permeability and degree of saturation may cause drained shear behaviour under some circumstances to be determined. This could be performed in numerical simulations. Validation of the theoretical outcomes with in situ measurements of permeability and by an in-situ slope failure test is recommended as the knowledge about the behaviour of partially unsaturated soil is small in The Netherlands.

By performing measurements on other sites more insight can be gained in the relevant parameters and the range of the parameters for which drained or undrained conditions are to be expected. Potentially important measurement sites are situations with an old more heterogeneous dyke, a dyke with clay with lower clay content (<20%), a dyke with a lower average degree of saturation and a dyke with a larger zone with brown oxidized clay.

Up to now no high suction values are measured in the field, as some sensors failed in the dry summer of 2020. The sensors with higher measurement range, which are installed this year have not experienced high suction values. Therefore, the relation between water content and suction is based on the Staring series (Wösten et al., 2001), for the high suction range. This gives uncertainty about the suction that actually occurred in the field. It is therefore recommended to continue the measurements in the field to gain data for the conditions with high suction.

More insight in the micro structural void ratio is needed. It is recommended to perform additional Mercury Intrusion Porosimetry tests for a wider range of water contents and to perform cross checks based on derivation of the micro structural void ratio from retention curves, which cover the range to much higher suction values.

To gain insight in the shear strength of soils with cracks and fissures it is recommended to conduct triaxial tests on large samples, as recommended in the literature study (Deltares, 2019a).

Finally, it is recommended to investigate the availability of RCPT cones with resistivity module in the Dutch market or the possibility to make this RCPT cone available for the Dutch market. The RCPT could be a fast and useful tool for field investigations regarding the (initially) unsaturated zone of dykes.



## 8 References

- Akin, I. D., & Likos, W. J. (2014). Specific surface area of clay using water vapor and EGME sorption methods. *Geotechnical Testing Journal*, 37(6), 1016-1027.
- Alonso, E., Pereira, J.-M., Vaunat, J., & Olivella, S. (2010). A microstructurally based effective stress for unsaturated soils. *Géotechnique*, Volume 60 Issue 12, pp. 913-925.
- Alonso, E., Pinyol, N., & Gens, A. (2013). Compacted soil behaviour: initial state, structure and constitutive modelling. *Géotechnique* 63, No. 6, 463–478.
- Arnepalli, D. N., Shanthakumar, S., Rao, B. H., & Singh, D. N. (2008). Comparison of methods for determining specific-surface area of fine-grained soils. *Geotechnical and Geological Engineering*, 26(2), 121-132.
- Arcadis. (2020). Consequentieanalyse initieel niet verzadigde zone. Projectnummer c03011.000471. Referentie 084039777 0.1. 28 april 2020.
- ASTM D 698. (2000). Standard test method for laboratory compaction characteristics of soil using standard effort. Easton, PA: American Society for Testing and Materials.
- ASTM. D2573-01. (2008). Standard test method for field vane shear test in cohesive soil. ASTM West Conshohocken, PA.
- ASTM. D 3080. (1994). Standard test method for Direct Shear Test of soils under consolidated drained conditions. (Withdrawn 2020, no replacement). ASTM West Conshohocken, PA.
- ASTM D 4404-18. Standard Test Method for Determination of Pore Volume and Pore Volume Distribution of Soil and Rock by Mercury Intrusion Porosimetry.
- ASTM. D 6528. (2007). Standard Test Method for Consolidated Undrained Direct Simple Shear Testing of Cohesive Soils. ASTM West Conshohocken, PA.
- Azzouz, A. S., Baligh, M. M., & Ladd, C. C. (1983). Corrected field vane strength for embankment design. *Journal of Geotechnical Engineering*, 109(5), 730-734.
- Baker, R., & Frydman, S. (2009). Unsaturated soil mechanics: Critical review of physical foundations. *Engineering Geology*, Volume 106, Issues 1–2, Pages 26-39.
- Becker, D. E., Crooks, J. H., & Been, K. (1988). Interpretation of the Field Vane Test in Terms of In-Situ and Yield Stresses in Vane Shear Strength Testing in Soils. *Field and Laboratory Studies*, Richards, AF, Editor, ASTM, 71-87.
- Bishop, A. (1959). The principle of effective stress. *Tek. Ukebl.*, 859–863.
- Bjerrum, L. (1972). Embankments on Soft Ground, State-of-the-Art Report, presented at the June 11-14, ASCE Specialty Conference on Performance of Earth and Earth-Supported Structures, held at Lafayette, Ind., Vol. 2, pp. 1-54.
- Bjerrum, L. (1973). Problems of soil mechanics and construction on soft clays and structurally unstable soils. In *Proc. 8th ICSMFE* (Vol. 3, pp. 111-159).
- Blight, G. (2013). *Unsaturated Soil Mechanics in Geotechnical Practice*. Leiden, The Netherlands: CRC Press/Balkema.
- Boso, M. (2005). Shear strength behavior of a reconstituted partially saturated clayey silt, PhD thesis. University of Trento.
- Brunauer, S., Emmett, P. H., & Teller, E. (1938). Adsorption of gases in multimolecular layers. *Journal of the American chemical society*, 60(2), 309-319.
- Campbell. (2016). CS616 and CS625 Water Content Reflectometers. Instruction manual. Revision 2/16. Campbell Scientific, Inc.
- Chandler, R. J. (1988). The in-situ measurement of the undrained shear strength of clays using the field vane. In *Vane shear strength testing in soils: field and laboratory studies*. ASTM International.
- CIRIA. (2013). *The International Levee handbook*, C731, CIRIA 2013, RP957, ISBN: 978-0-86017-734-0.

- Coop, M. (2015). Limitations of a Critical State Framework Applied to the Behaviour of Natural and "Transitional" Soils. Deformation Characteristics of Geomaterials. V.A. Rinaldi et al. (Eds.). IOS Press, 2015. doi:10.3233/978-1-61499-601-9-115.
- Craig, R. (2004). Soil Mechanics, 7th Ed. Spon Press. Taylor & Francis Group.
- Deltares. (2016). Protocol laboratoriumproeven voor grondonderzoek aan waterkeringen. Deltares rapport 1230090-019-GEO-0002, Versie 03, 25 mei 2016, definitief.
- Deltares. (2019a). Shear Strength of Initially Unsaturated Soil - Literature Study and Research Proposal. Deltares report 11202560-020-GEO-0001, January 16, 2019.
- Deltares. (2019b). Plan van Aanpak KPP 2019 project - WK01 2019 - Kennis voor Keringen.
- Deltares. (2019c). Plan van aanpak onderzoek schuifsterkte (initieel) onverzadigde grond. 11204453-000-GEO-0001. 27 augustus 2019.
- Deltares. (2019d). Verkenning Diëlektrische Sondeer Conus GeoPoint.
- Deltares. (2021a). Handelingsperspectief schuifsterkte onverzadigde zone. 11207253-002-GEO-0002, 5 november 2021, draft.
- Deltares. (2021b). Shear Strength of Initially Unsaturated Soil – Factual report measurement sites Westervoort and Oijen. 11207253-002-GEO-0003, December 27, 2021.
- Durgunoglu, H.T., Mitchell, J.K. (1973). Static penetration resistance of soils. For NASA Grant NGR 05-003-406: Lunar Soil Properties and Soil Mechanics, Space Sciences Laboratory Series 14, Issue 24, UC Berkeley. 223 p.
- FprEN 22476-9:2010.3 (E) (CEN/TC 341 date: 2010-12): Ground investigation and testing - Field testing -Part 9: Field vane test.
- Fredlund, D. G., Rahardjo, H., & Fredlund, M. (2012). Unsaturated Soil Mechanics in Engineering Practice.
- Geokon. (2019). VW Piezometers & Pressure Transducers. 4500 Series.
- Goh, S. G., Rahardjo, H., & Leong, E. (2010). Shear Strength Equations for Unsaturated Soil under Drying and Wetting. Journal of Geotechnical and Geoenvironmental Engineering, 136(4).
- Grondmechanica Delft. (1996). Onderzoek stabiliteit Maasdijken, Vak D, Oijen Benedeneind – Zuiveringsinstal. HM 574 tot HM 595. Geotechnisch Profiel G-G'. Project CO-361580.
- Han, Z., & Vanapalli, S. (2016). Stiffness and shear strength of unsaturated soils in relation to soil-water characteristic curve. Géotechnique , Volume 66 Issue 8, pp. 627-647.
- I&M. (2021). Schematiseringshandleiding macrostabiliteit - WBI 2017. Versienummer 4.0. Datum 28 mei 2021. Status Definitief.
- Inpijn-Blokpoel. (2017). Grondonderzoek voor de 4e toetsronde - Resultaten geotechnisch onderzoek. Documentnummer 02P008040-RG-01. 1 augustus 2017.
- ISO 15901-1:2016. Evaluation of pore size distribution and porosity of solid materials by mercury porosimetry and gas adsorption – Part 1: Mercury porosimetry.
- ISO 17892-8:2018. Geotechnical investigation and testing — Laboratory testing of soil — Part 8: Unconsolidated undrained triaxial test.
- Jardine, R., Gens, A., Hight, D., & Coop, M. (2004). Developments in Understanding Soil Behaviour. Advances in Geotechnical Engineering: The Skempton Conference (pp. 103-206). London: Thomas Telford.
- KNMI (2021). Historisch verloop neerslagtekort. <https://www.knmi.nl/nederland-nu/klimatologie/geografische-overzichten/historisch-neerslagtekort>
- Koliji, A., Vulliet, L., & Laloui, L. (2010). Structural characterization of unsaturated aggregated soil. Canadian Geotechnical Journal, 47(3), 297-311.
- Konrad, J.-M., & Lebeau, M. (2015). Capillary-based effective stress formulation for predicting shear strength of unsaturated soils. Can. Geotech. J., 52: 2067–2076.
- Ladd, C.C. and Foott, R. (1974), New design procedure for stability of soft clays. J. Geotech. Eng. Div., 100(GT7), (1974) 763-786.
- Ladd, C.C. (1991). "Stability evaluation during staged construction (22nd Terzaghi Lecture)." J. of Geotech. Eng., 117(4), 540-615.

- Ladd, C. C., & DeGroot, D. J. (2004). Recommended practice for soft ground site characterization: Arthur Casagrande Lecture, 12th Panam. In Conf. on Soil Mechanics and Geotechnical Engineering.
- Larsson, R., Bergdahl, U., & Eriksson, L. (1987). Evaluation of shear strength in cohesive soils with special reference to Swedish practice and experience. *Geotechnical Testing Journal*, 10(3), 105-112.
- Larsson, R., & Åhnberg, H. (2005). On the evaluation of undrained shear strength and preconsolidation pressure from common field tests in clay. *Canadian geotechnical journal*, 42(4), 1221-1231.
- Liu, X., Buzzi, O., Yuan, S., Mendes, J., & Fityus, S. (2016). Multi-scale characterization of retention and shrinkage behaviour of four Australian clayey soils. *Canadian Geotechnical Journal*, 53(5), 854-870.
- Lu, Q., Randolph, M. F., Hu, Y. & Bugarski, I. C. (2004). A numerical study of cone penetration in clay. *Géotechnique* 54, No. 4, pp. 257–267.
- Mayne, P. (2007). *Cone Penetration Testing*. Washington: Transportation Research Board.
- Meter. (2018). T5/T5x Pressure Transducer Tensiometer - User Manual. METER Group AG München. Art. Nr. T5. Version 08/2018.
- Miller, G. A., Collins, R. W., Muraleetharan, K. K., Cerato, A. B., & Doumet, R. (2015). Interpretation of in situ tests as affected by soil suction, Report FHWA-OK-15-09. Oklahoma Department of Transportation.
- Miller, G. A., Tan, N. K., Collins, R. W., & Muraleetharan, K. K. (2018). Cone penetration testing in unsaturated soils. *Transportation Geotechnics*, 17, 85-99.
- Mitchell, J. K., & Soga, K. (2005). *Fundamentals of soil behavior* (Vol. 3). New York: John Wiley & Sons.
- NEN-EN-ISO 14688-2, Geotechnisch onderzoek en beproeving - Identificatie en classificatie van grond - Deel 2: Grondslagen voor een classificatie.
- NEN-EN-ISO 17892-1, Geotechnisch onderzoek en beproeving - Beproeving van grond in het laboratorium - Deel 1: Bepaling van het watergehalte.
- NEN-EN-ISO 17892-2, Geotechnisch onderzoek en beproeving - Beproeving van grond in het laboratorium - Deel 2: Bepaling van de dichtheid van fijn korrelige grond.
- NEN-EN-ISO 17892-3, Geotechnisch onderzoek en beproeving - Beproeving van grond in het laboratorium - Deel 3: Bepaling van de dichtheid van gronddeeltjes.
- NEN-EN-ISO 17892-4, Geotechnisch onderzoek en beproeving - Beproeving van grond in het laboratorium - Deel 4: Bepaling van de korrelgrootte verdeling.
- NEN-EN-ISO 17892-5:2017 en. Geotechnical investigation and testing - Laboratory testing of soil - Part 5: Incremental loading oedometer test.
- NEN-EN-ISO 17892-9:2018 en. Geotechnical investigation and testing - Laboratory testing of soil - Part 9: Consolidated triaxial compression tests on water saturated soils.
- NEN-EN-ISO 17892-12, Geotechnisch onderzoek en beproeving - Beproeving van grond in het laboratorium - Deel 12: Bepaling van de Atterbergse grenzen.
- NEN-EN-ISO 22475-1, Geotechnisch onderzoek en beproeving - Methodes voor monsterneming en grondwatermeting - Deel 1: Technische grondslagen voor de uitvoering.
- NEN-EN-ISO 22476-1. (2013). Geotechnisch onderzoek en beproeving – Veldproeven – Deel 1: Elektrische sondering. Nederlands Normalisatie Instituut.
- Pournaghiazar, M., Russell, A., & Khalili, N. (2013). The cone penetration test in unsaturated sands. *Géotechnique*, 63, No. 14, 1209–1220.
- Powell, J., & Quarterman, R. (1988). The interpretation of cone penetration tests in clays, with particular reference to rate effects. 1st Int. Symp. on Penetration Testing, (pp. 903-909). Orlando, USA.
- Romero, E., Della Vecchia, G., & Jommi, C. (2011). An insight into the water retention properties of compacted clayey soils. *Géotechnique* 61, No. 4. 313-328.
- Romero, E., & Simms, P. H. (2008). Microstructure investigation in unsaturated soils: a review with special attention to contribution of mercury intrusion porosimetry and

- environmental scanning electron microscopy. *Geotechnical and Geological engineering*, 26(6), 705-727.
- Romero, E., & Vaunat, J. (2000). Retention curves of deformable clays. *Proceedings of the International Workshop on Unsaturated Soils. Experimental Evidence and Theoretical Approaches in Unsaturated Soils*, (pp. 91–106).
- Santamarina, J. C., Klein, K. A., Wang, Y. H., & Prencke, E. (2002). Specific surface: determination and relevance. *Canadian Geotechnical Journal*, 39(1), 233-241.
- Schofield, A., & Wroth, P. (1968). *Critical State Soil Mechanics*. Maidenhead: McGraw Hill.
- Schnaid, F. (2009). *In Situ Testing in Geomechanics*. Oxon: Taylor & Francis.
- SIKB. (2018). Protocol 2101. Mechanisch boren. BRL SIKB 2100.
- Tarantino, A., Ridley, A., & Toll, D. (2008). Field Measurements of Suction, Water Content, and Water Permeability. *Geotech. Geol. Eng.*, 751-782.
- Tarantino, A., & El Mountassir, G. (2013). Making unsaturated soil mechanics accessible for engineers: preliminary hydraulic–mechanical characterisation & stability assessment. *Engineering Geology* 165, 89–104.
- Tarantino, A., & Tombolato, S. (2005). Coupling of hydraulic and mechanical behaviour in unsaturated compacted clay. *Geotechnique*, 55 (4), 307–317.
- TAW. (1996). Technisch rapport klei voor dijken. Delft.
- Teh, C. I. & Houlsby, G. T. (1988). Analysis of the cone penetration test by the strain path method. In: *Numerical Methods in Geomechanics*. Innsbruck. Swoboda (ed.). Balkema, Rotterdam.
- Teunissen, H. (2016). Wrijving in sterkteberekeningen. *Geotechniek*, Juli 2016.
- UGT. (2020). Full Range Tensiometer. Operating Manual. Version: 20/07/20.
- Vanapalli, S. (2010). Shear strength of unsaturated soils and its applications in geotechnical engineering practice. 4th Asia Pacific Conference on Unsaturated Soils, (pp. 579-598). Newcastle, Australia.
- Wösten, J., Veerman, G., de Groot, W., & Stolte, J. (2001). Waterretentie- en doorlatendheidskarakteristieken van boven- en ondergronden in Nederland: de Staringreeks. Alterra rapport 153. Wageningen: Alterra.
- Yerro, A., Girardi, V., Ceccato, F., & Martinelli, M. (2021). Modelling unsaturated soils with the Material Point Method. A discussion of the state-of-the-art. *Geomechanics for Energy and Environment*. May 31, 2021. Submitted.
- Zhou, A., Huang, R., & Sheng, D. (2016). Capillary water retention curve and shear strength of unsaturated soils. *Can. Geotech. J.*, 53: 974–987.

# A Bore holes

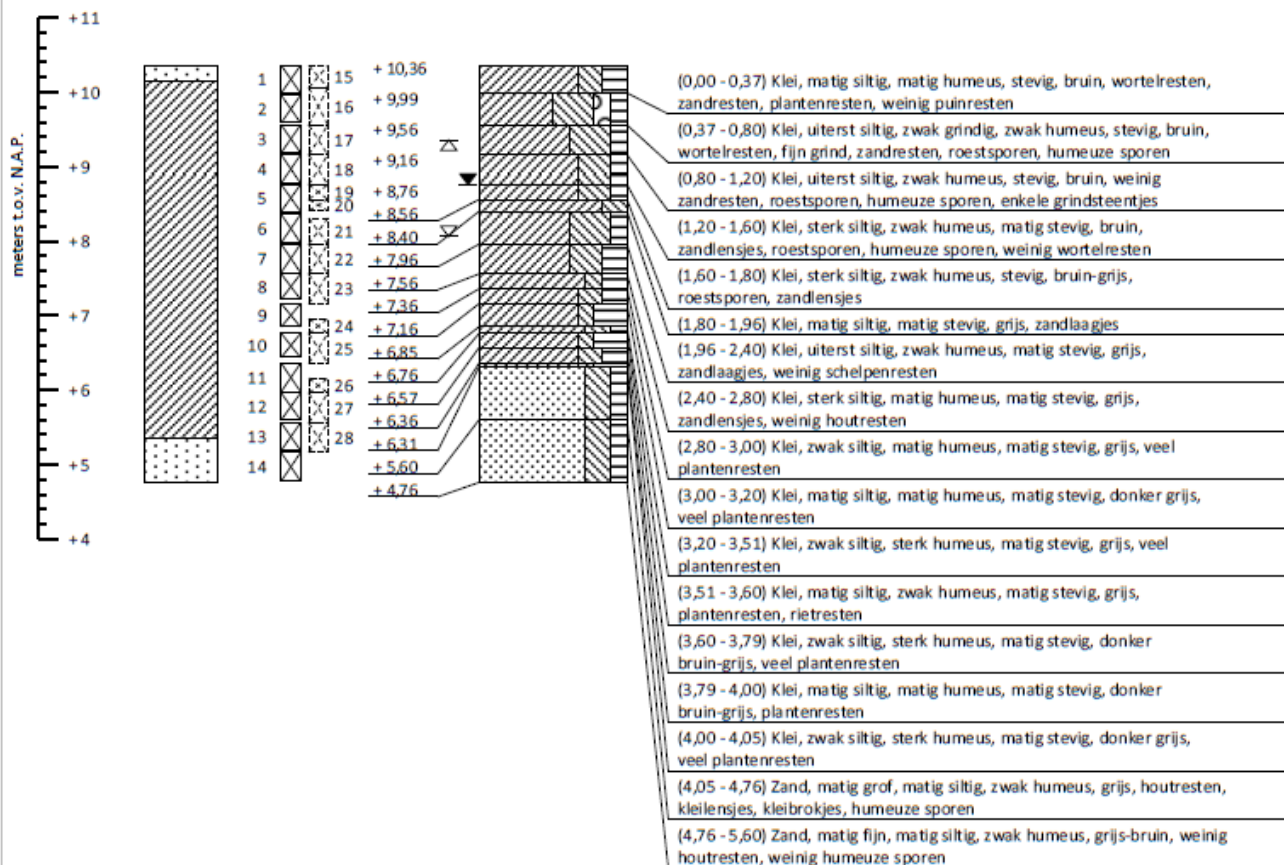
## A.1 Introduction

Six mechanical drillings are performed at Westervoort and Oijen. At both sites three mechanical drillings are performed. The descriptions and photos of the bore holes are given in this appendix.

## A.2 Westervoort


Maatvoering in meters t.o.v. N.A.P.  
 GWS d.d. (31-10-2019): N.A.P. + 8,76 m  
 G.H.G.: N.A.P. + 9,36 m  
 G.L.G.: N.A.P. + 8,06 m

Maatvoering in meters t.o.v. maaiveld



Boring conform NEN-EN-ISO 22475-1

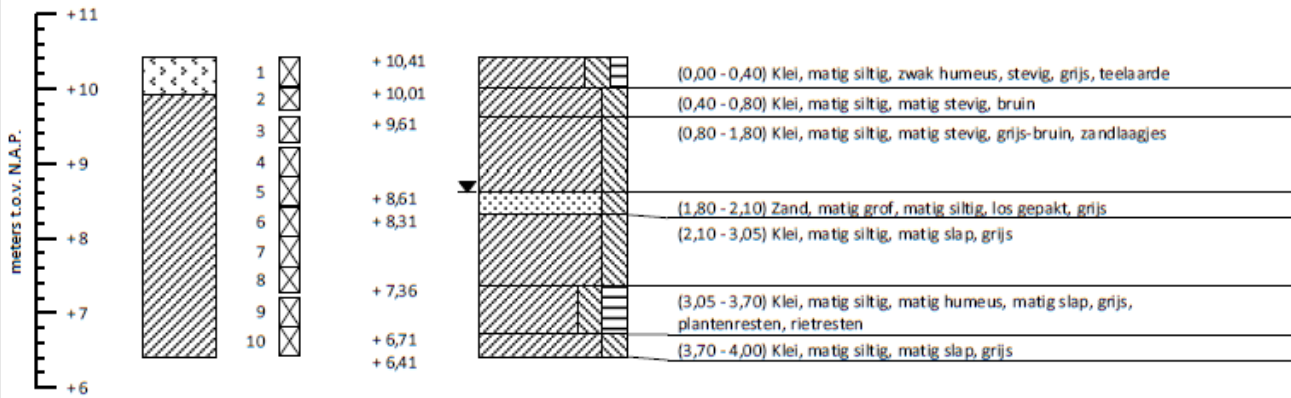
Boorstaat o.b.v. grondidentificatie in het veld incl. laboratoriumclassificatie monsters (NEN 5104)

Meetlocaties IJsseldijk te Westervoort	RD coördinatensysteem	Westervoort
Deltares	X = 194 453	Pulsboring (mechanisch)
 <b>Wiertsema &amp; Partners</b> RAADGEVEND INGENIEURS	Y = 442 127	Boormeester: Liekel Mellema
	Uitgevoerd: 31-10-2019	Opdrachtnr.: 74499
	Blad 1 van 1	Boomnummer: B201
		

WK-74499-2-201111 & 74499\_2011\_C01111

Maatvoering in meters t.o.v. N.A.P.  
GWS d.d. (11-8-2020): N.A.P. + 8,61 m

Maatvoering in meters t.o.v. maaiveld



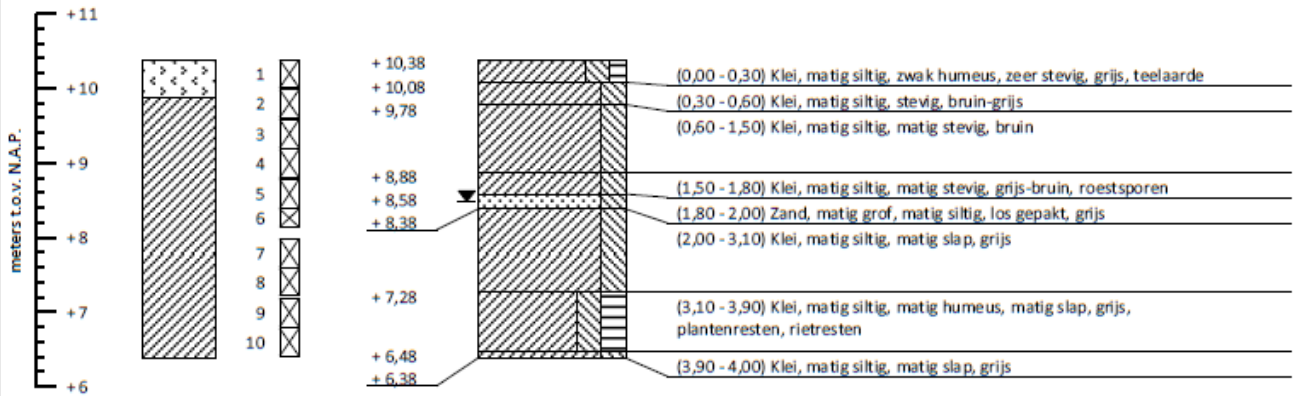
Boorstaat o.b.v. grondidentificatie in het veld (NEN 5104)

Boring conform NEN-EN-ISO 22475-1

Meetlocaties Maasdijk te Oijen	RD coördinatensysteem	Oijen
Deltares	X = 194 451	Edelmanboring
	Y = 442 125	Boormeester: Jan Berends
	Uitgevoerd: 11-8-2020	Opdrachtnr.: 74499
	Blad 1 van 1	Boomnummer: B202

Maatvoering in meters t.o.v. N.A.P.  
GWS d.d. (11-8-2020): N.A.P. + 8,48 m

Maatvoering in meters t.o.v. maaiveld



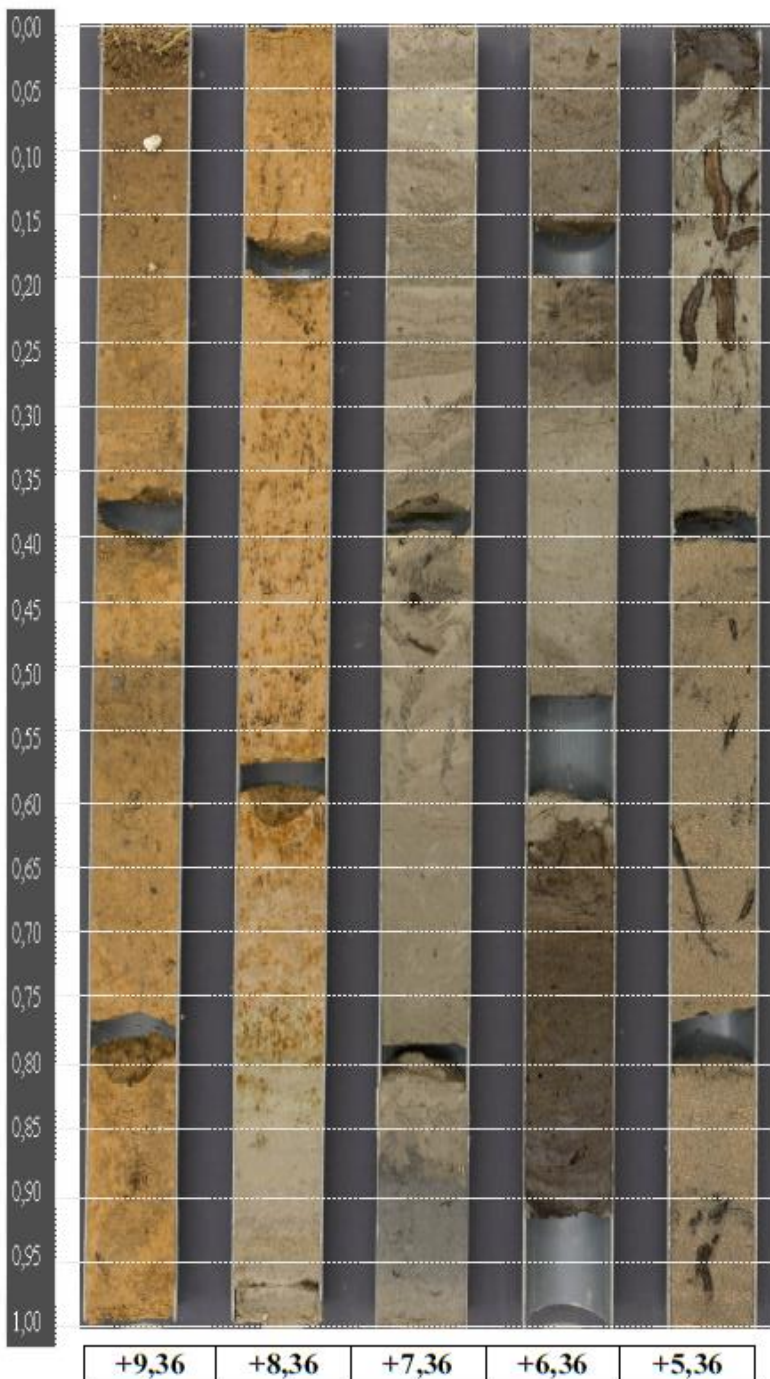
Boorstaat o.b.v. grondidentificatie in het veld (NEN 5104)

Boring conform NEN-EN-ISO 22475-1

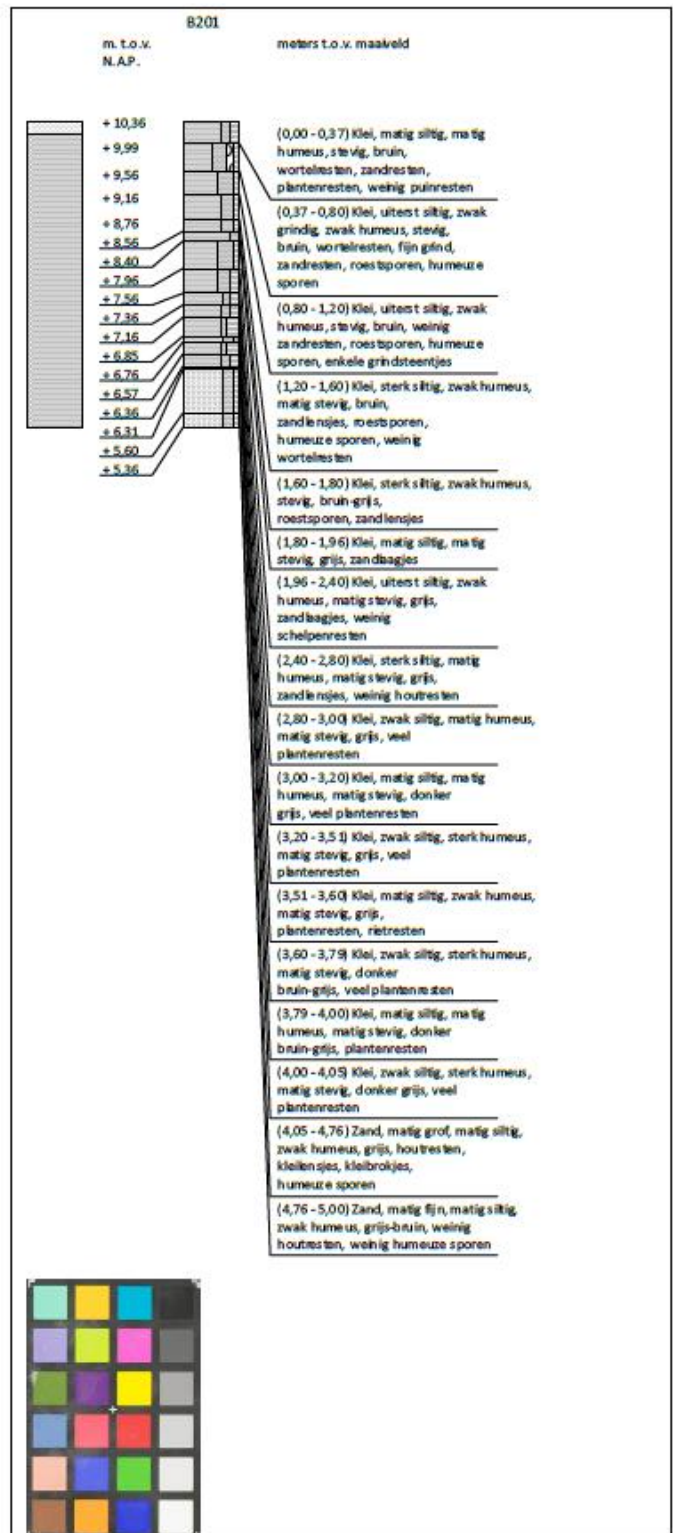
Meetlocaties Maasdijk te Oijen	RD coördinatensysteem	Oijen
Deltares	X = 194 450	Edelmanboring
	Y = 442 124	Boormeester: Jan Berends
	Uitgevoerd: 11-8-2020	Opdrachtnr.: 74499
	Blad 1 van 1	Boomnummer: B203

VN-74499-1-2020-110 8 74499\_2020\_01011111





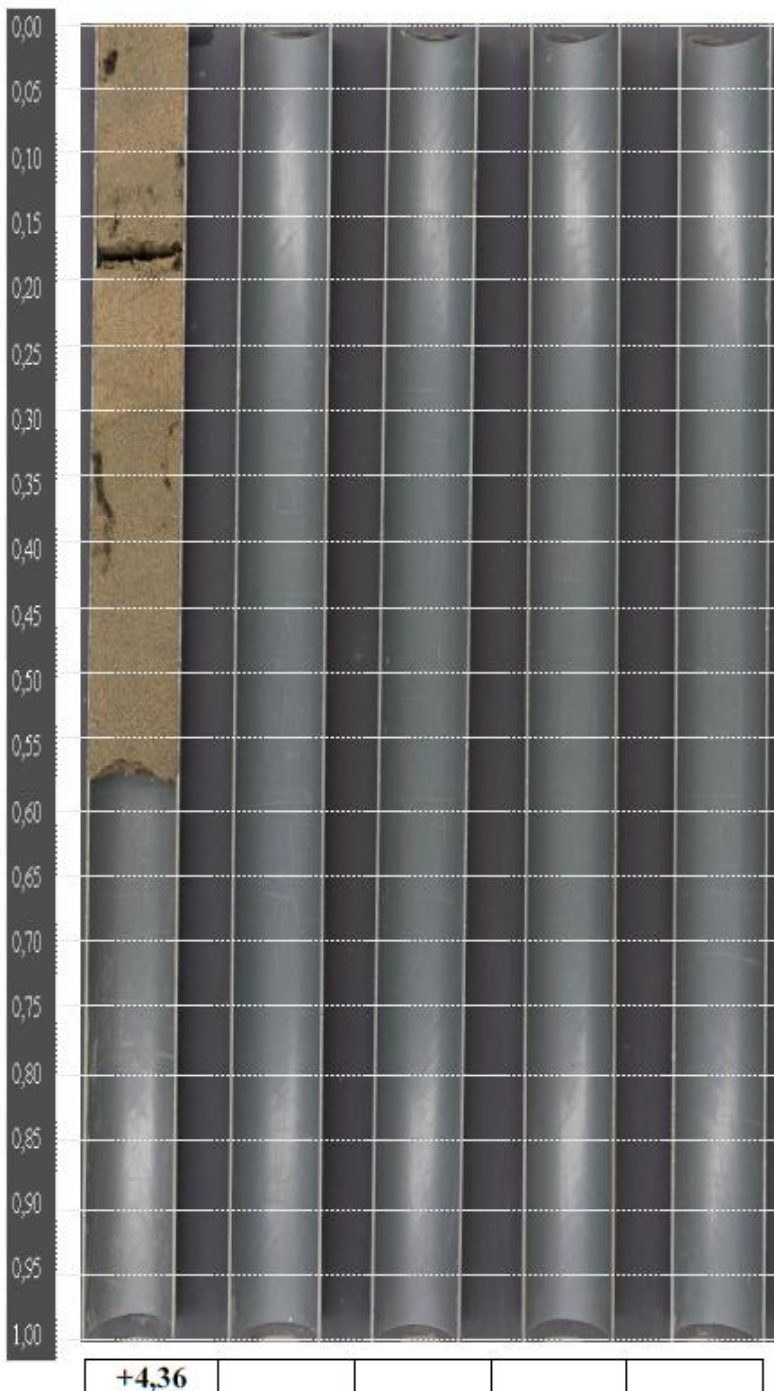
Hoogte in m t.o.v. NAP



Projectnummer	VN-74499-2
Plaats	Westervoort
Omschrijving	Meetlocaties IJsseldijk
Boring	B201
Hoogte maaiveld t.o.v. NAP	+10,36
Einddiepte boring t.o.v. NAP	+4,76
Boormethode	Pulsboring
Datum	-2019



**Wiertsema & Partners**  
 RAADGEVEND INGENIEURS



**B201**

m. t.o.v. N.A.P. meters t.o.v. maaiveld

+ 5,36

+ 4,76

(5,00 - 5,60) Zand, matig fijn, matig siltig, zwak humeus, grijs-bruin, weinig houtresten, weinig humeuze sporen

Hoogte in m t.o.v. NAP

Projectnummer	VN-74499-2
Plaats	Westervoort
Omschrijving	Meetlocaties IJsseldijk
Boring	B201
Hoogte maaiveld t.o.v. NAP	+10,36
Einddiepte boring t.o.v. NAP	+4,76
Boormethode	Pulsboring
Datum boring	31-10-2019



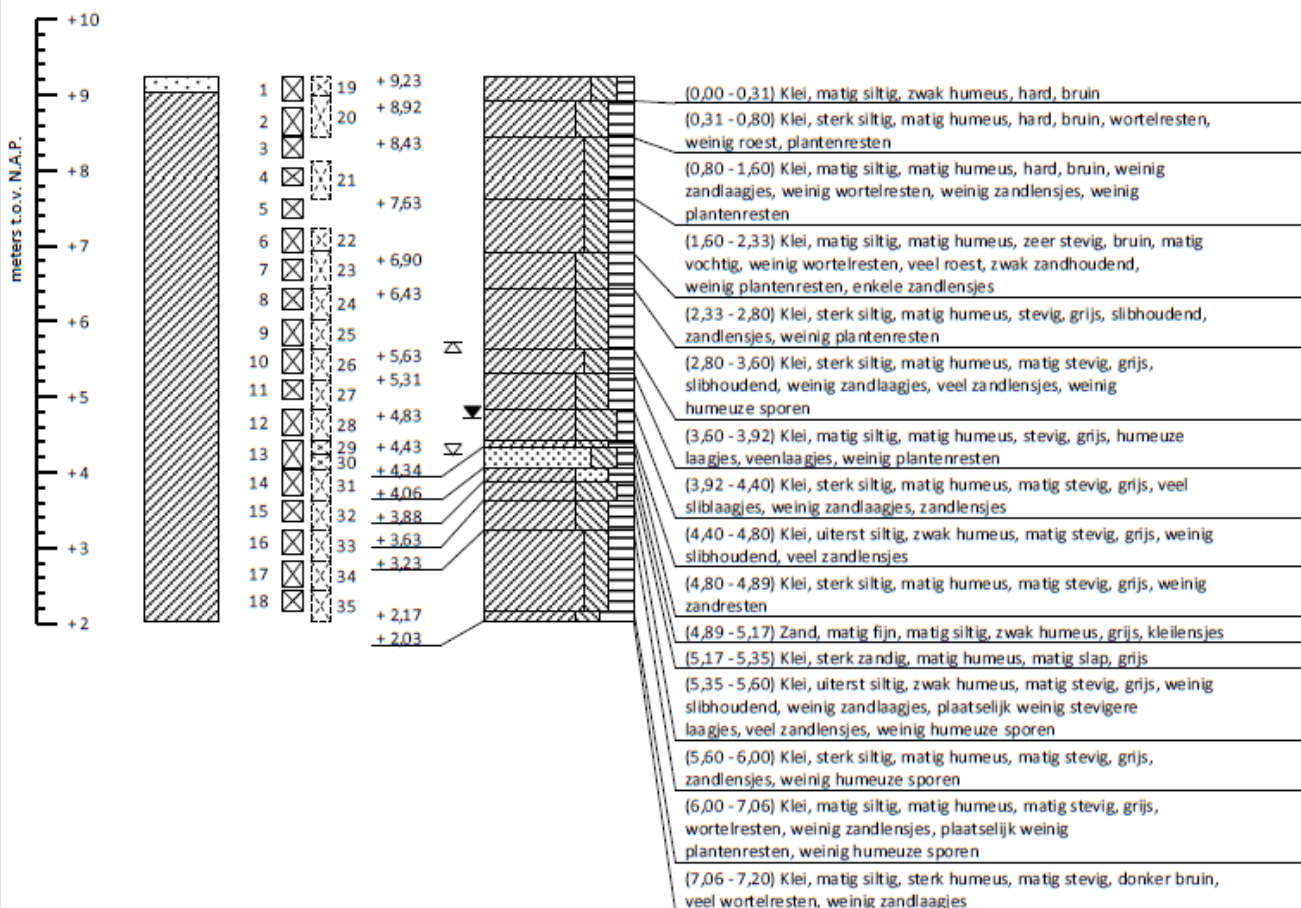
**Wiertsema & Partners**  
RAADGEVEND INGENIEURS





Maatvoering in meters t.o.v. N.A.P.  
 GWS d.d. (25-9-2019): N.A.P. + 4,73 m  
 G.H.G.: N.A.P. + 5,73 m  
 G.L.G.: N.A.P. + 4,23 m

Maatvoering in meters t.o.v. maaiveld



Boring conform NEN-EN-ISO 22475-1

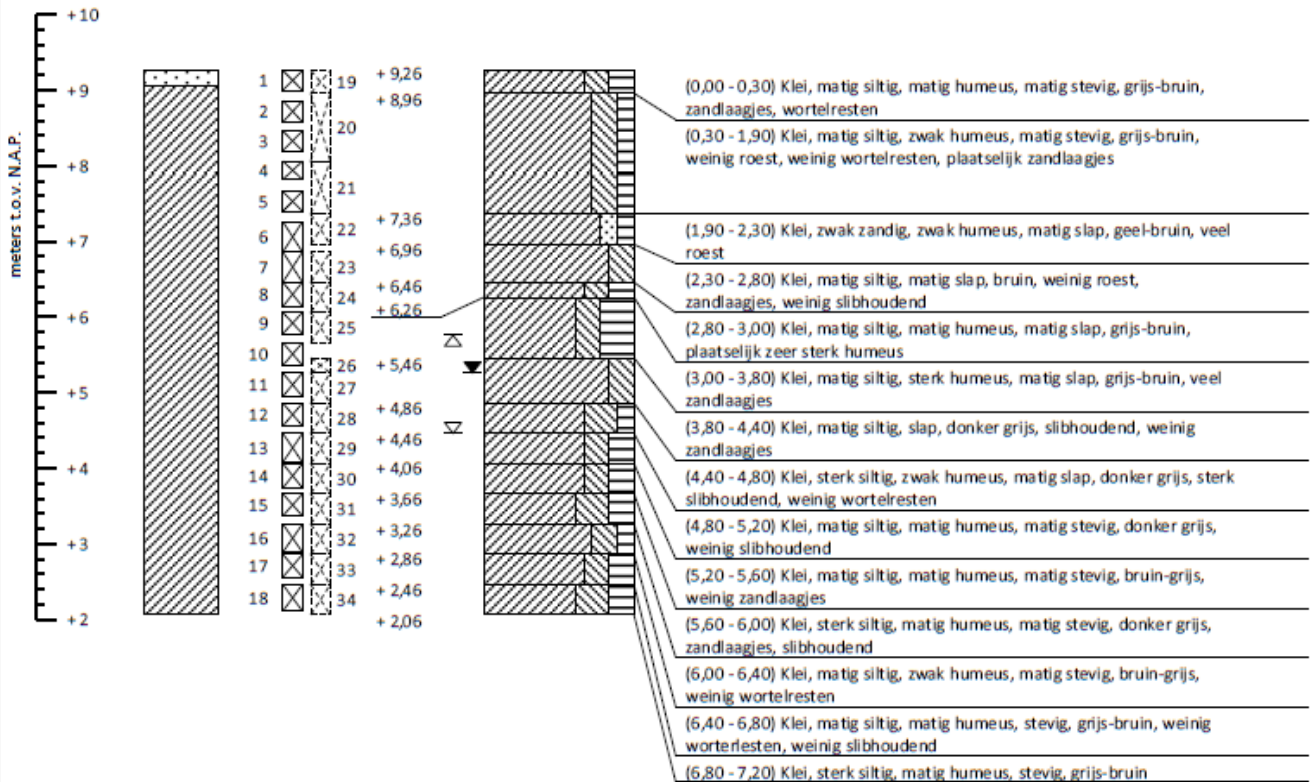
Boorstaat o.b.v. grondidentificatie in het veld incl. laboratoriumclassificatie monsters (NEN 5104)

Meetlocaties Maasdijk te Oijen	RD coördinatensysteem	Oijen
Deltares	X = 161 711	Pulsboring (mechanisch)
 <b>Wiertsema &amp; Partners</b> RAADGEVEND INGENIEURS	Y = 425 400	Boormeester: Liekel Mellema
	Uitgevoerd: 25-9-2019	Opdrachtnr.: 74499
	Blad 1 van 1	Boomnummer: B001
		

VN-74499-1-001.111 & 74499\_001\_C01.111

Maatvoering in meters t.o.v. N.A.P.  
 GWS d.d. (1-11-2019): N.A.P. + 5,26 m  
 G.H.G.: N.A.P. + 5,76 m  
 G.L.G.: N.A.P. + 4,46 m

Maatvoering in meters t.o.v. maaiveld

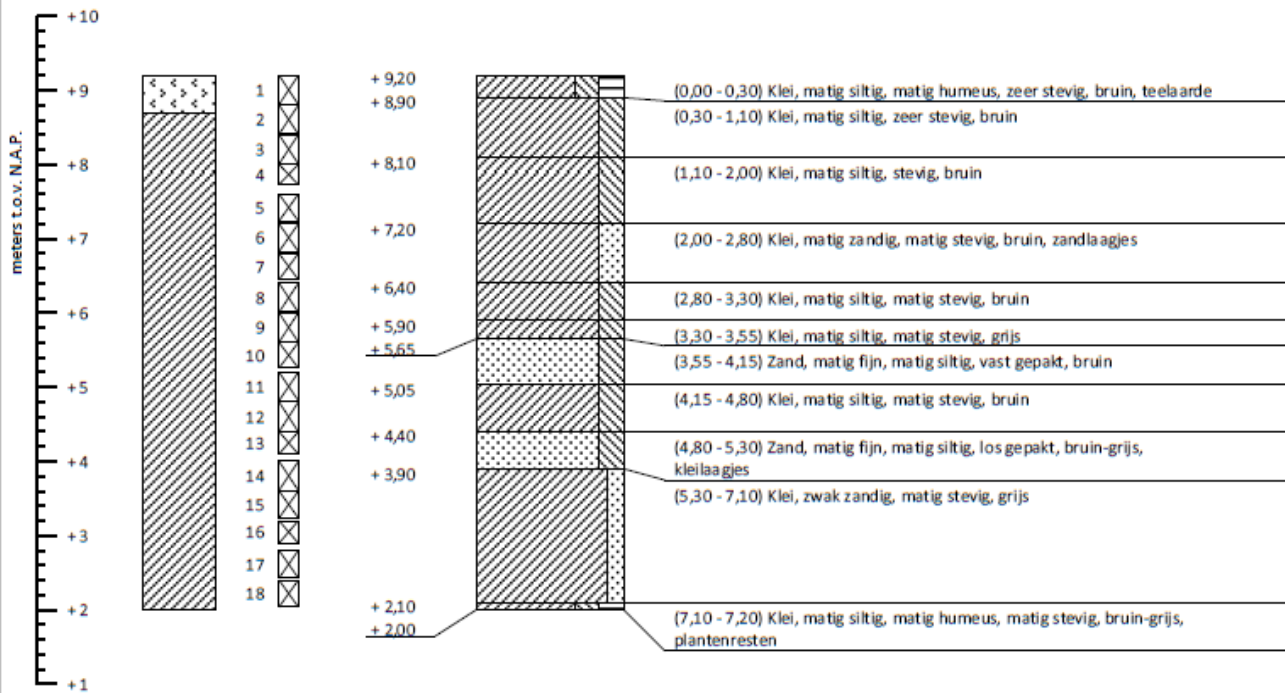


Boorstaat o.b.v. grondidentificatie in het veld (NEN 5104)

Boring conform NEN-EN-ISO 22475-1

Meetlocaties Maasdijk te Oijen	RD coördinatensysteem	Oijen
Deltares	X = 161 715,20	Pulsboring (mechanisch)
 <b>Wiertsema &amp; Partners</b> RAADGEVEND INGENIEURS	Y = 425 395,65	Boormeester: Liekel Mellema
	Uitgevoerd: 31-10-2019 t/m 1-11-2019	Opdrachtnr.: 74499
	Blad 1 van 1	Boomnummer: B002
		

VN-74499-1-0002.010 & 74499\_0002\_0105.010

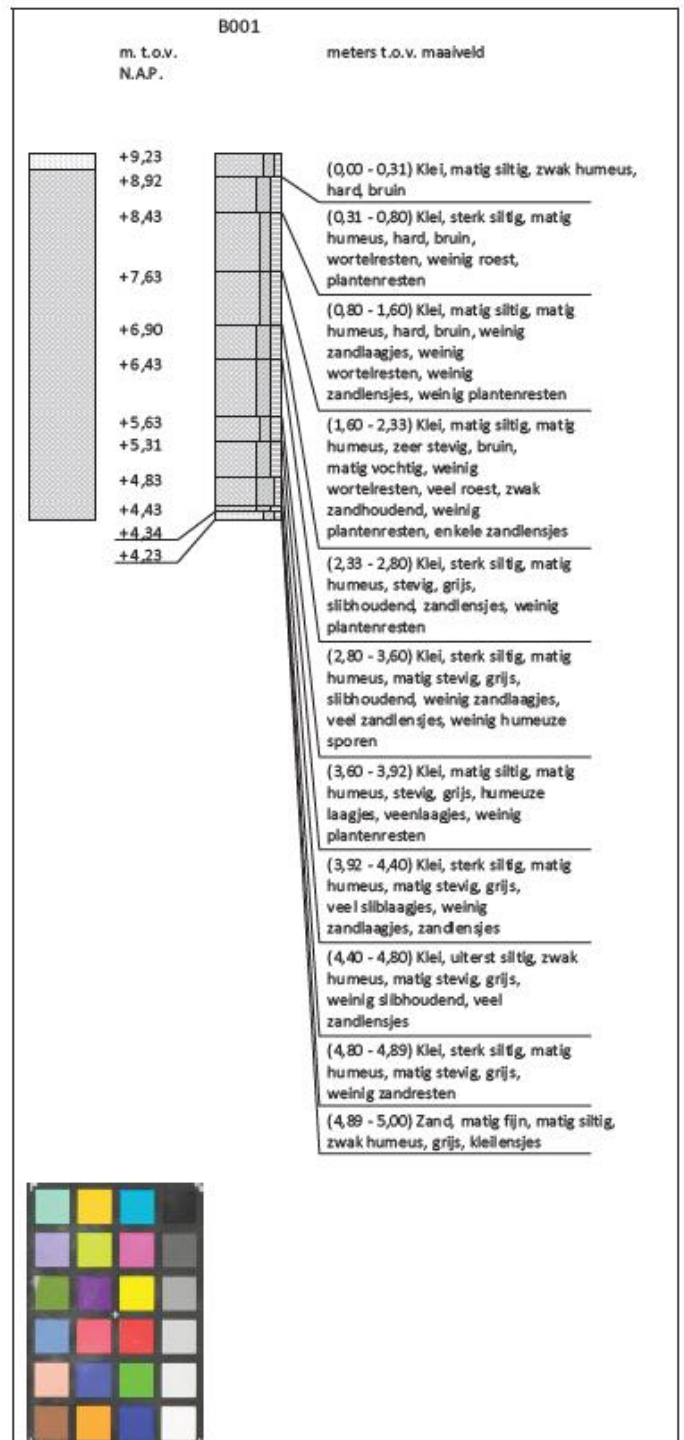
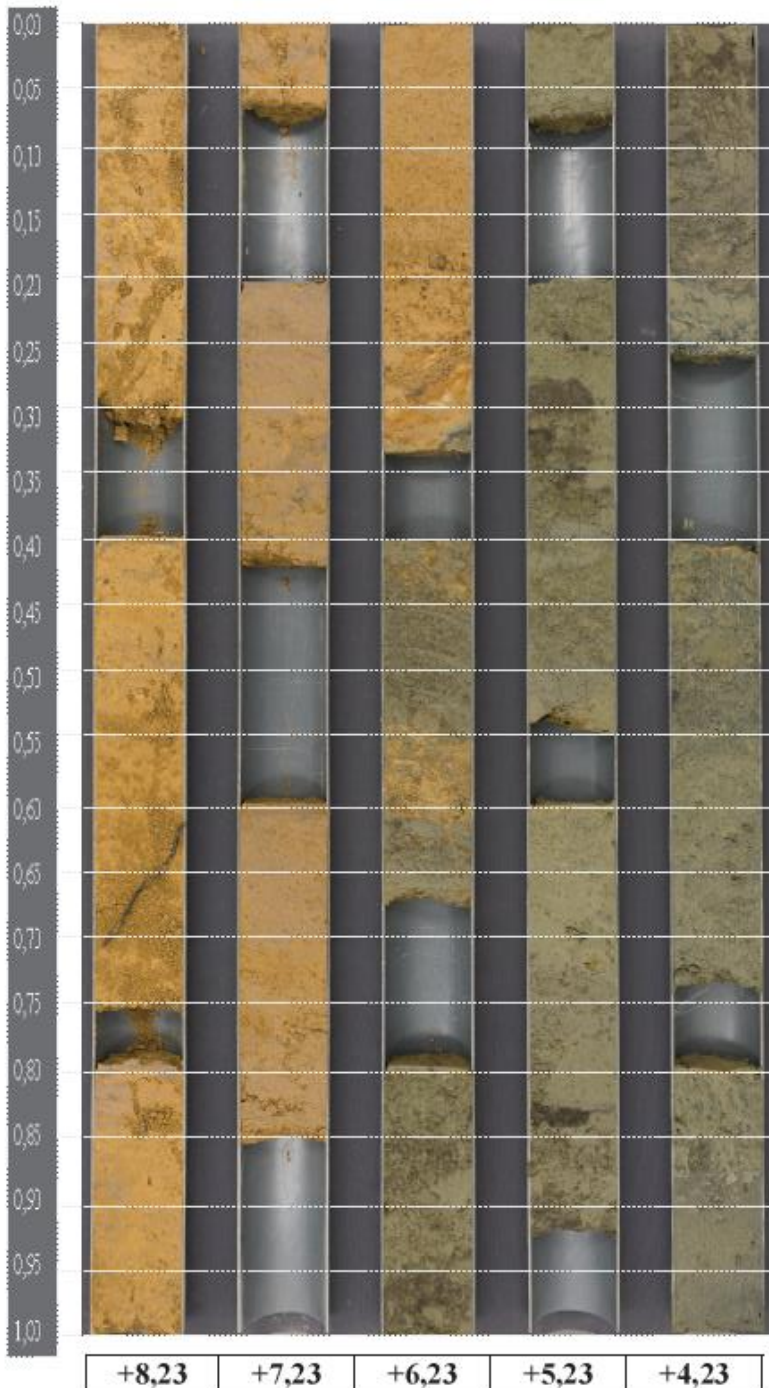


## Boorstaat o.b.v. grondidentificatie in het veld (NEN 5104)

Boring conform NEN-EN-ISO 22475-1

Meetlocaties Maasdijk te Oijen	RD coördinatensysteem	Oijen
Deltares	X = 161 716	Pulsboring (lichte stelling)
 <b>Wiertsema &amp; Partners</b> <small>RAADGEVEND INGENIEURS</small>	Y = 425 394	Boormeester: Jan Berends
	Uitgevoerd: 10-8-2020	Opdrachtnr.: 74499
	Blad 1 van 1	Boomnummer: B003
		

WV-74499-1-0003.010 &amp; 74499\_B003\_0103.010



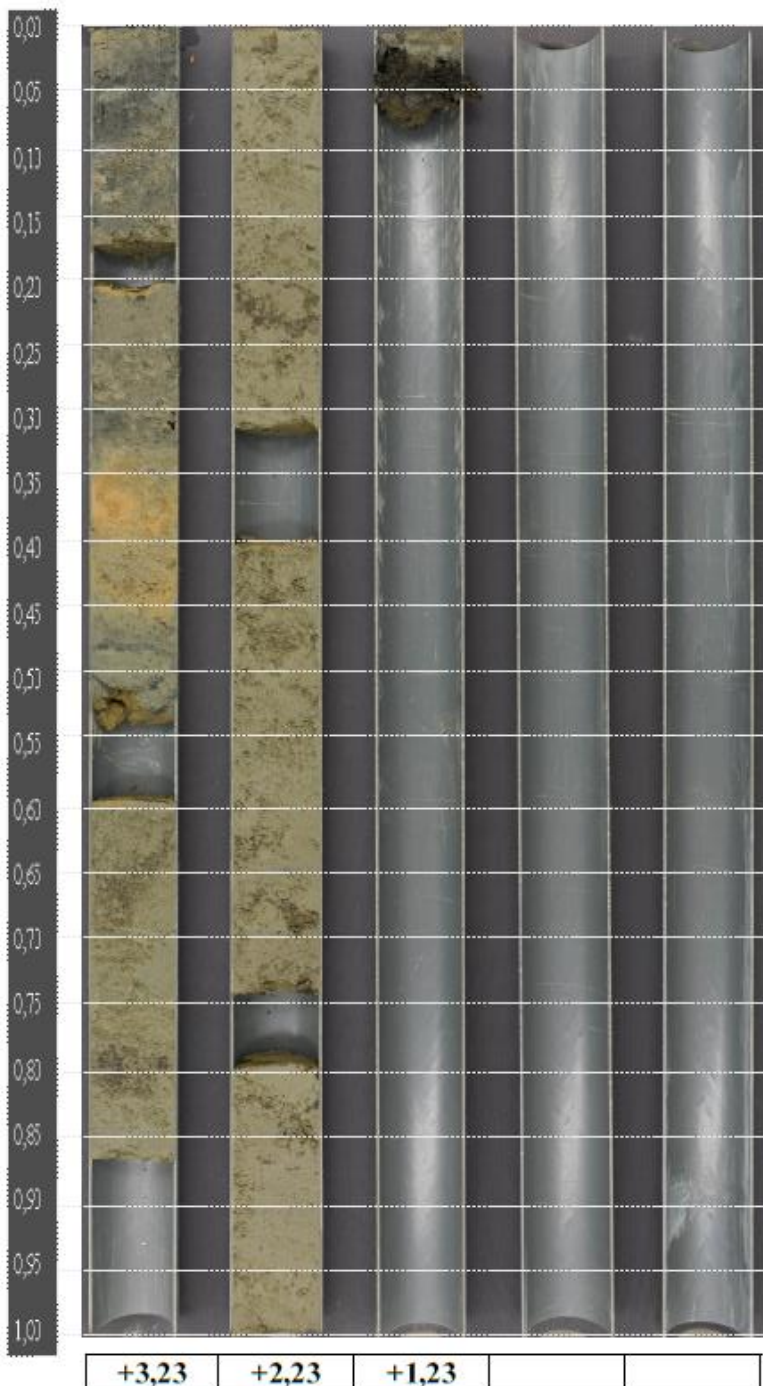
Hoogte in m t.o.v. NAP

Projectnummer	VN-74499-1
Plaats	Oijen
Omschrijving	Meetlocaties Maasdijk
Boring	B001
Hoogte maaiveld t.o.v. NAP	+9,23
Einddiepte boring t.o.v. NAP	+2,03
Boormethode	Pulsboring
Datum boring	25-9-2019

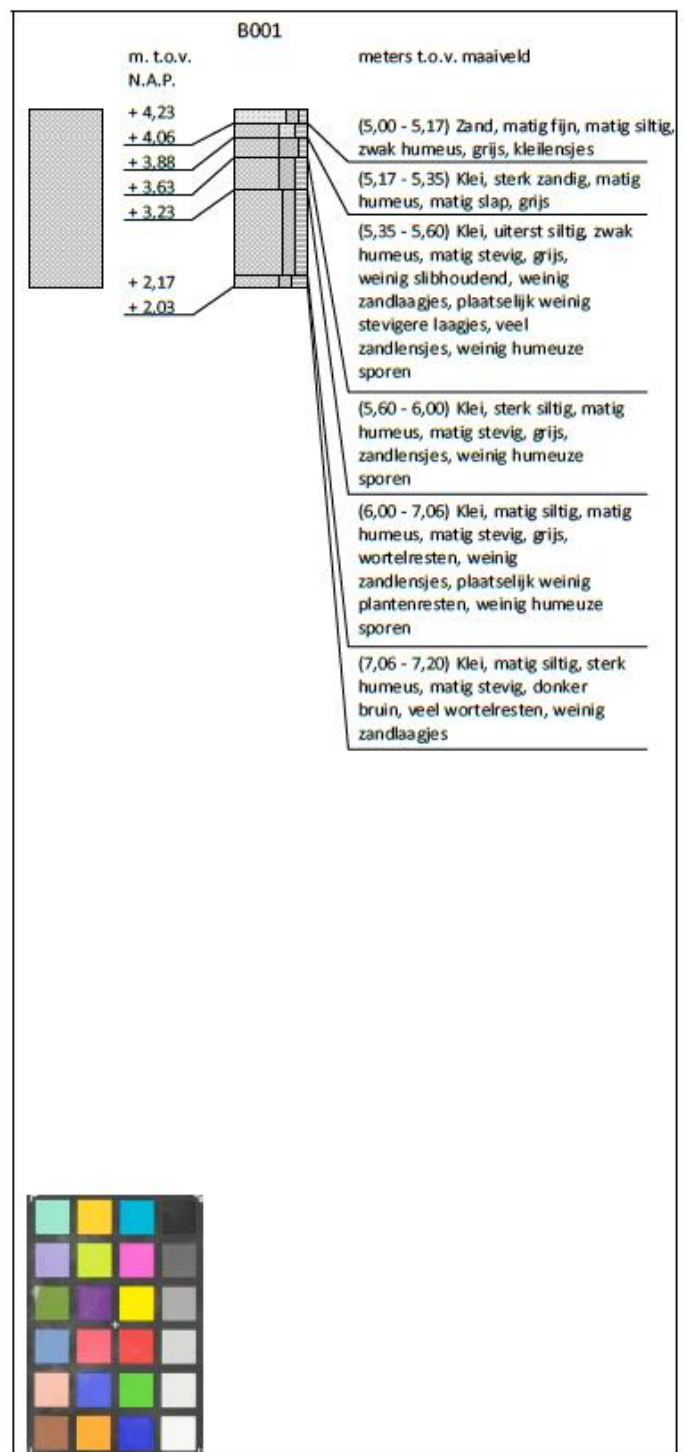


**Wiertsema & Partners**  
RAADGEVEND INGENIEURS





Hoogte in m t.o.v. NAP



Projectnummer	VN-74499-1
Plaats	Oijen
Omschrijving	Meetlocaties Maasdijk
Boring	B001
Hoogte maaiveld t.o.v. NAP	+9,23
Einddiepte boring t.o.v. NAP	+2,03
Boormethode	Pulsboring
Datum boring	25-09-2019



**Wiertsema & Partners**  
RAADGEVEND INGENIEURS





## B Soil water retention curves

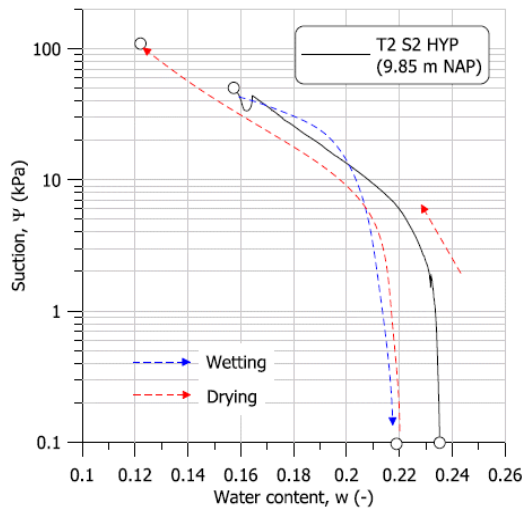
### B.1 Introduction

For this project eight soil water retention curves are determined; see Paragraph 3.16. For both sites four water retention curves are determined. The results of these tests are given in the factual report (Deltares, 2021b). In this appendix the graphs of the soil water retention curves are given (Paragraph B.2 and B.3).

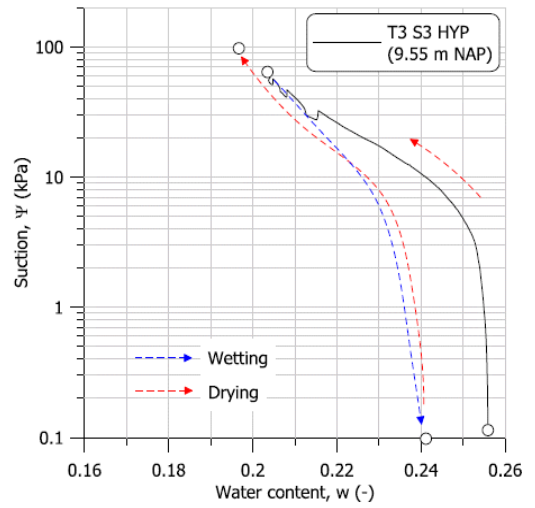
For low values of water content no information about suction was available from the sensors (tensiometers), as some of these sensors failed in the dry summer of 2020 and sometimes water content is so low that suction in the field becomes higher than the measurement range of the tensiometers. In that case soil water retention curves are used to estimate suction, based on measured water content. In case the measured water content is outside of the range of the soil water retention curves of this project water retention curves from the Staring series (Wösten et al., 2001) are used to estimate suction (Paragraph B.4).

### B.2 Westervoort

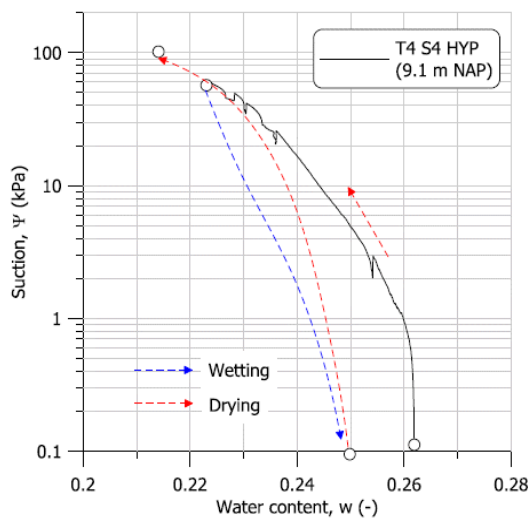
The soil water retention curves which are determined for the Westervoort site are given in Figure B.1.



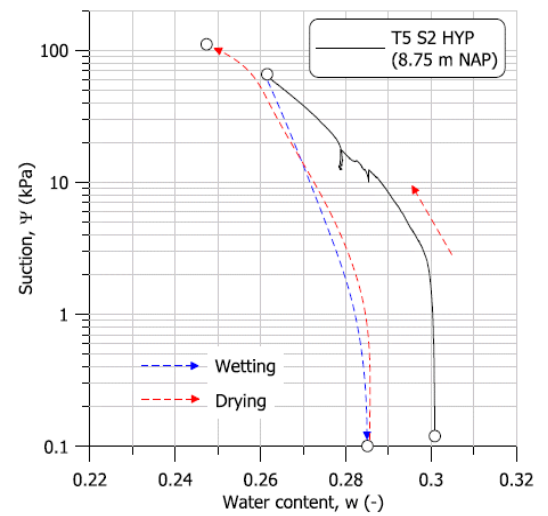
(a)



(b)



(c)



(d)

Figure B.1 Soil water retention curves which are determined for the Westervoort site.

### B.3 Oijen

The soil water retention curves which are determined for the Oijen site are given in Figure B.2.

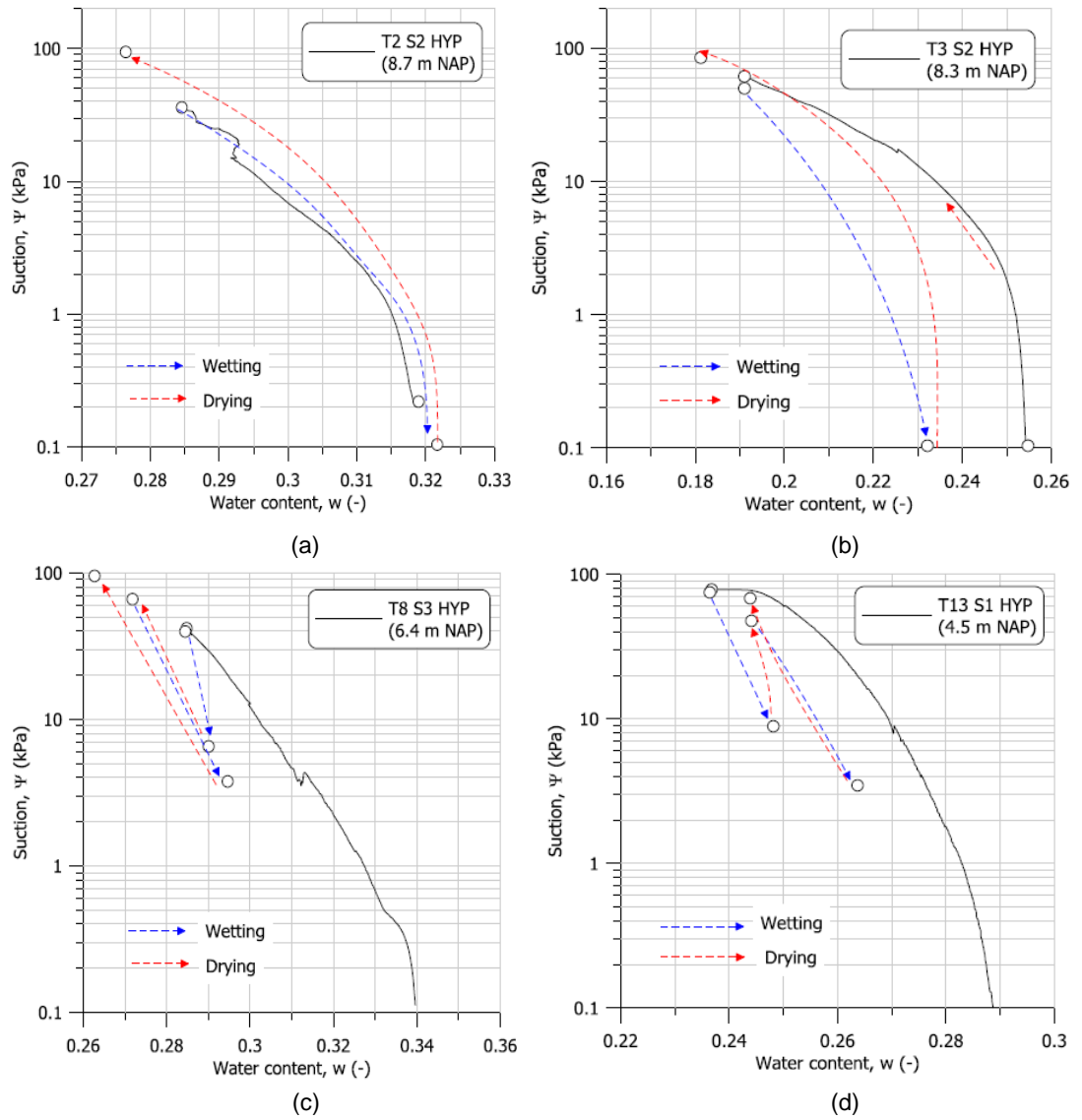


Figure B.2 Soil water retention curves which are determined for the Oijen site.

## B.4 Staring series

The soil water retention curves of the Staring series (Wösten et al., 2001), which are used in this project, are given in Figure B.3.

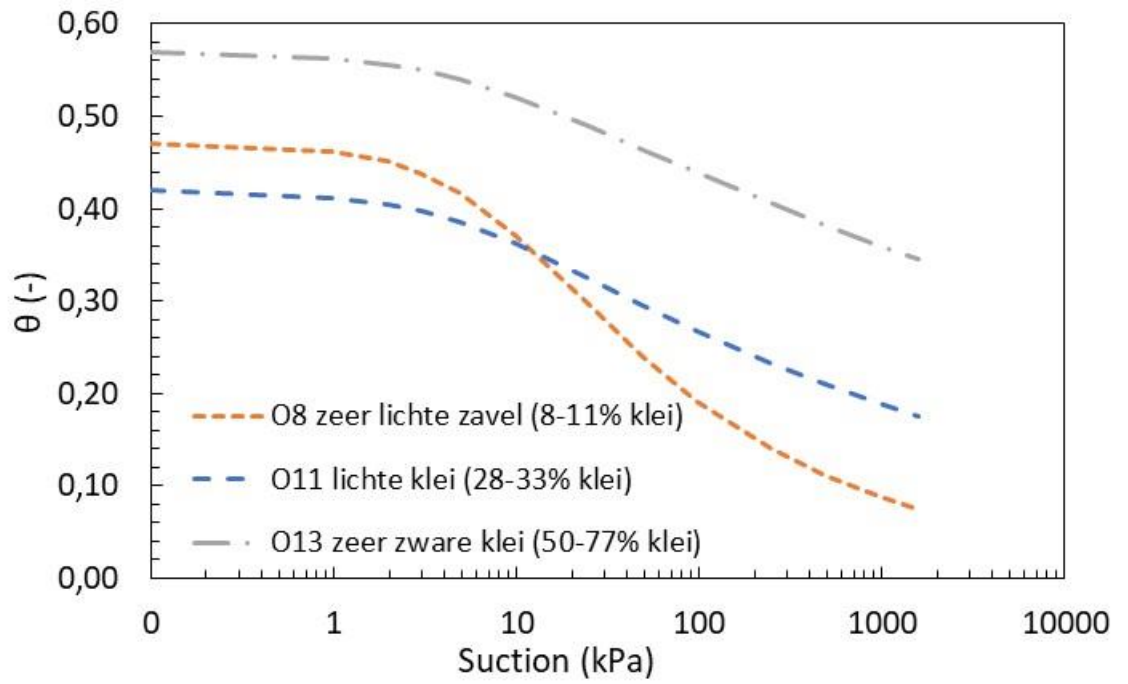


Figure B.3 Soil water retention curves of the Staring series (Wösten et al., 2001), which are used in this project.

Deltares is an independent institute for applied research in the field of water and subsurface. Throughout the world, we work on smart solutions for people, environment and society.

**Deltares**

[www.deltares.nl](http://www.deltares.nl)